

2015

Modeling economies and ecosystems in general equilibrium

<https://hdl.handle.net/2144/16349>

Downloaded from DSpace Repository, DSpace Institution's institutional repository

BOSTON UNIVERSITY
GRADUATE SCHOOL OF ARTS & SCIENCES

Dissertation

**MODELING ECONOMIES AND ECOSYSTEMS IN
GENERAL EQUILIBRIUM**

by

JARED WOOLLACOTT

B.S., Bentley University, 2004
M.P.P., Duke University, 2011
M.E.M., Duke University, 2011

Submitted in partial fulfillment of the
requirements for the degree of
Doctor of Philosophy

2015

© Copyright by
Jared Woollacott
2015

Approved by

First Reader

Ian J. Sue Wing, PhD
Associate Professor of Earth & Environment

Second Reader

Dana M. Bauer, PhD
Assistant Professor of Earth & Environment

Third Reader

Mark A. Kon, PhD
Professor of Mathematics & Statistics

ACKNOWLEDGMENTS

I thank Professor Ian Sue Wing for his patient and dedicated guidance and his willingness to advise an unconventional dissertation. Working with him has permanently changed the way I think about problems for the better. I entered my program with vague but inspiring ideas about how biological and technological systems behave and no clear angle on how to pursue them. I am leaving with a set of well-honed tools and a clear path forward to pursuing the research I find most compelling. Thank you Professor Sue Wing.

I also thank my committee members. Professor Dana Bauer generously offered many hours of friendly and helpful guidance, particularly on how best to work across disciplines. Professor Mark Kon offered great teaching and encouragement on the more challenging mathematical topics I faced. Professor Les Kaufman offered invaluable perspective on the biology literature and community.

I thank my partner, Jamie Crockett, for her extraordinary support. Our doctoral programs kept us living apart for four semesters. Difficult as it was, we are stronger for having faced the challenge and I am ever more confident that spending our lives together is the best idea we have ever had. Jamie has continually helped me identify the intellectual and emotional challenges needed for further growth, offering an abundance of love, support, and inspiration to see those challenges through. I am, across all aspects of my life, uniformly better off for our relationship. Thank you Jamie.

I thank my parents, Al and Jill. Their love, care, and emphasis on a strong and independent work ethic provided the necessary conditions for my reaching this milestone. I am uniquely grateful for their roles in my life. It is a good and essential norm that children's debts to their parents are forgiven - I am quite certain mine could never be repaid. Thank you Mom and Dad.

MODELING ECONOMIES AND ECOSYSTEMS IN GENERAL EQUILIBRIUM

(Order No.)

JARED WOOLLACOTT

Boston University, Graduate School of Arts & Sciences, 2015

Major Professor: Ian J. Sue Wing, PhD,
Department of Earth & Environment

ABSTRACT

This work exploits the general equilibrium modeling framework to simulate complex systems, an economy and an ecosystem. In an economic application, this work leverages a novel data revision scheme to integrate technological detail on electricity generation and pollution abatement into national accounts data in a traditional economic computed general equilibrium (CGE) model. This integration provides a rich characterization of generation and abatement for multiple fuel sources and pollutants across 72 different generation-abatement technology configurations. Results reveal that the benefits of reductions in oxides of nitrogen and sulfur from a carbon policy in the US electric sector are on the order of \$10bn., which rival the policy's welfare costs and make 12 – 13% carbon abatement economically justifiable without considering any climate benefits.

For ecosystem applications, this work demonstrates how the structure of economic CGE modeling can be adapted to construct a Biological General Equilibrium (BGE) model grounded in the theoretical biology literature. The BGE model contributes a novel synthesis of micro-behavioral, bioenergetic features with macroscopic ecosys-

tem outcomes and empirical food web data. Species respond to prevailing ecosystem scarcity conditions that impinge on their energy budgets driving population outcomes within and across model periods. This adaptive capacity is a critical advance over the commonly-taken phenomenological or first-order parametric approaches. The distinctive design of the BGE model enables numerical examination of how changes in scarcity drives biomass production and consumption in a complex food web. Moreover, the BGE model design can exploit empirical datasets used by extant ecosystem models to offer this level of insight for a wide cast of ecosystems.

Monte carlo simulations demonstrate that the BGE framework can produce stable results for the ecosystem robust to a variety of shocks and parameterizations. The BGE model's validity is supported in tests against real-world phenomena within the Aleutian ecosystem - both an invasive species and a harvesting-induced trophic cascade - by mimicking key features of these phenomena. The BGE model's micro-founded dynamics, the stability and robustness of its results, and its validity against real-world phenomena offer a unique and valuable contribution to ecosystem modeling and a way forward for the integrated assessment of human-ecosystem interactions.

CONTENTS

1	Introduction	1
1.1	Complex Adaptive Systems	1
1.2	Motivation for modeling complex systems	2
1.3	General equilibrium modeling	3
2	Greenhouse Gas Policy in the Electric Sector – Measuring the Costs and Ancillary Benefits	5
2.1	Introduction	5
2.2	Literature	7
2.3	Data Construction and Reconciliation	11
2.3.1	Bottom-up Technology Data	11
2.3.2	Bottom-up – Top-down Reconciliation	13
2.4	Model Structure	19
2.4.1	General Structure	19
2.4.2	Consumption	21
2.4.3	Resource-Intensive Sectors	21
2.4.4	Policy Design	25
2.5	Policy Experiments Results	26
2.5.1	Baseline Results	26
2.6	Conclusion	34
3	Modeling Ecological Dynamics – A General Equilibrium Approach	38
3.1	Introduction	38
3.2	Literature review	40
3.2.1	Optimal bioenergetic input	41
3.2.2	Optimal bioenergetic output	48

3.2.3	Ecosystem dynamics	51
3.3	Biological General Equilibrium Model	65
3.3.1	Overview	65
3.3.2	Stylized Model Example	71
3.4	Model Structure – Intra-Temporal Dynamics	74
3.4.1	General Structure	74
3.4.2	Behavior	78
3.4.3	Optimization & Duality	81
3.4.4	System Conditions & Equilibria	87
3.4.5	Model closure	92
3.5	Conclusion	93
4	Testing the Biological General Equilibrium Model	95
4.1	Introduction	95
4.2	Calibration – GEEM	95
4.2.1	Costs	96
4.2.2	Benefits	101
4.3	Calibration - Ecosim	103
4.3.1	Accounting identities	105
4.3.2	Data revision	107
4.4	Model structure	111
4.5	Results	115
4.5.1	Overview	115
4.5.2	Baseline diagnostics	116
4.5.3	Benchmark counter-factual scenarios	123
4.5.4	Monte carlo counter-factual scenarios	129
4.5.5	Summary	139

4.6	Conclusion	141
5	Applying the Bioenergetic General Equilibrium Model	143
5.1	Introduction	143
5.2	Invasive species	143
5.3	Trophic cascade	147
5.4	Conclusion	152
6	Conclusion	154
6.1	Summary	154
6.2	Future work	155
7	Appendices	157
7.1	Data Construction	157
7.1.1	The PAGE Dataset	157
7.1.2	Social Accounting Matrix	160
7.2	Model Elasticities	161
7.3	Model Technologies	162
	References	165
	Curriculum Vitae	177

LIST OF TABLES

2.1	Pollution abatement technologies by pollutant	12
2.2	Electric generation technologies costs & quantities (2010)	13
2.3	Summary of costs & quantities for four model technologies	14
2.4	Example technology-by-input unit-cost matrix	16
2.5	Summary of SAM sectors	20
3.1	Conservation conditions for an economy and an ecosystem	88
3.2a	BGE Model Equations	91
3.2b	BGE Model Equations – Definitions	91
4.1	Balanced mass Biological Accounting Matrix (BAM) based on GEEM mass data (Finnoff & Tschirhart, 2003)	98
4.2	Balanced energy Biological Accounting Matrix (BAM) based on GEEM energy data (Finnoff & Tschirhart, 2003)	99
4.3	Calibration of marginal cost of foraging prey	101
4.4	Environment energy budget allocation	102
4.5	BGE model species with Ecosim species count	104
4.6	Ecosim original & est. values for BGE calibration	108
4.7	Energy Biological Accounting Matrix (eBAM) for Ecosim data	110
4.8	Given & revised values for initial & boundary conditions	112
4.9	Ecosystem metrics for model datasets	117
4.10	GEEM species growth rates for growth scenarios	118
4.11	Ecosim species growth rates for growth scenarios	118
4.12	Mapping of Ecosim species to small species set	119
4.13	Distribution of elasticities for Monte Carlo simulations	130

4.14	Monte carlo mean squared errors for STS scenario	132
4.15	Monte carlo mean squared errors for SSH scenario	133
4.16	Monte carlo mean squared errors for SPS scenario	137
4.17	Monte carlo mean squared errors for EXT scenario	139
5.1	Species of interest and their harvested prey	148
5.2	Harvesting quantities and rates	149

LIST OF FIGURES

2.1	Production Structures	22
2.2	Generation, transmission, & distribution production structure	23
2.3	Primary-resource sectors production structures	25
2.4	Percent reduction in emissions for CO ₂ & other pollutants	27
2.5	Total & fuel-specific electric output under CO ₂ policy	29
2.6	Gross & net welfare cost of CO ₂ policy (\$2010 bn.)	30
2.7	Marginal ancillary benefit and welfare cost (\$2010)	31
2.8	Gross & net welfare costs, “stranded” capital (\$2010 bn.)	33
2.9	Marginal ancillary benefit & welfare costs, “stranded” capital (\$2010)	34
2.10	Electric output, “stranded” capital	35
2.11	Unit-cost by generation scatter for all technologies	36
2.12	Permit & electricity prices, “stranded” capital (\$2010)	37
3.1	Holling functional response types	42
3.2	Inverse Holling functional response types	46
3.3	Stylized input-output ecosystem accounting matrices	71
3.4	Biological Accounting Matrix of input-output data	74
4.1	Biomass accounting matrices for Ecosim data	105
4.2	Production structures for Orca whales	113
4.3	Ensemble of modeled ecosystem’s production structures	115
4.4	Model 1 (GEEM) growth scenarios’ population outcomes	120
4.5	Model 3 (EwE-Sm) growth scenarios’ population outcomes	121
4.6	Population outcomes for Model 2 (EwE) growth scenarios	122
4.7	Population outcomes for STS scenario - Model 2 (EwE)	124

4.8	Population outcomes for STS scenario	125
4.9	Population outcomes for SSH scenario - Model 2 (EwE)	125
4.10	Population outcomes for SSH scenario	126
4.11	Population outcomes for SPS scenario - Model 2 (EwE)	127
4.12	Population outcomes for SPS scenario	128
4.13	Population outcomes for EXT scenario - Model 2 (EwE)	129
4.14	Population outcomes for EXT scenario	130
4.15	Population distributions for STS scenario	134
4.16	Population distributions for SSH scenario	136
4.17	Population distributions for SPS scenario	138
4.18	Population distributions for EXT scenario	140
5.1	Baseline growth population outcomes	145
5.2	Population levels following invasive Norway rat	146
5.3	Relative population levels for perturbed species	150
5.4	Relative population levels for perturbed species	151
7.1	Elasticities used in CGE model	161
7.2	Legend of fuel & technology codes	162
7.3	Full list of model technologies	164

LIST OF ABBREVIATIONS

BAM	Biological Accounting Matrix
BGE	Biological General Equilibrium
CES	Constant Elasticity of Substitution
CGE	Computed General Equilibrium
EIA	Energy Information Administration
EPA	Environmental Protection Agency
EXT	Extinction scenario
GDP	Gross Domestic Product
GEEM	General Equilibrium Ecosystem Model J. T. Tschirhart (2000)
GHGe	Greenhouse Gas equivalent
HAP	Hazardous Air Pollutant
IPM	Integrated Planning Model
IVS	Invasive Species scenario
MACT	Maximum Achievable Control Technology
NERC	North American Electric Reliability Corporation
NMFS	National Marine Fisheries Service
NOAA	National Oceanic and Atmospheric Administration
PAGE	Pollution, Abatement, and Generation of Electricity
SAM	Social Accounting Matrix
SPS	Stochastically Perturbed System scenario
SSH	Stochastic Species Harvest scenario
STS	Starve The System scenario

CHAPTER 1: INTRODUCTION

1.1 Complex Adaptive Systems

Complex adaptive systems have multiple interacting parts. In these systems, the macroscopic outcomes need not be an immediate consequence of any individual part or sum of individual actions. Macroscopic outcomes instead emerge from the complex interactions of the system's many parts. The inter-connectedness of the different parts of the system means that activity in one part of the system can be transmitted in complex patterns throughout the system. For some activity and systems, these interconnections can lead to chaotic outcomes. If the constituent parts of the system are adaptive - their behavior changes in response to prevailing conditions in the system - the transmission of activity throughout the network may be damped. That is, as initial activity ripples out from one part of the system, adaptive behavior can dissipate its effects, attenuating the tendency toward chaos.

Ecosystems and economies are complex adaptive systems. Aggregate outcomes like population levels or GDP are the result of the complex interaction of many individuals and are not predictable by the simple sum of individual actions. Changes in the amount of primary resources or capital for example may have far-reaching effects for the various species in an ecosystem or industries in an economy. The ability of individual species members in an ecosystem or households and firms in an economy to change their behavior in response to changes in their system can help to mitigate negative and take advantage of positive changes.

From an economic perspective, decisions are driven by individuals' assessments of the costs and benefits of different actions. If the value gained from taking an action is greater than the value sacrificed, it is worth taking. This kernel of economic logic has been widely employed in economics and in ecology under the heading optimal

foraging. Critically, these “decisions” may be entirely passive requiring no cognitive effort. For example, if in searching for certain prey a species encounters fewer of them, that species is likely to consume less of that prey. In this case, the *scarcity* of the prey has increased the effort required to secure the prey. If the first bite of prey is more “valuable” than say the tenth, higher search costs will tend to reduce consumption of it. The principle works the same in economics, where scarce resources carry higher prices inducing firms and individuals to use less than they might otherwise.

Whether species are producing biomass or a firm is producing goods or services, a set of inputs must be combined to generate the desired output. The combination of inputs may vary - a large fish may eat mostly small fish this week and mostly invertebrates the next - and different inputs will produce more or less output per unit. It is the benefits produced and costs imposed by securing the different inputs that drives decisions about their use. By identifying different types of biomass or economic goods we can characterize different production “technologies” for combining inputs into a given output. This ensemble of model technologies constitute the different types of activities that will interact in each system by using each other’s outputs as inputs, making substitutions as certain outputs become more or less scarce.

1.2 Motivation for modeling complex systems

The complexity of ecosystems and economies means that the consequences of changes within the system cannot be directly traced from their source to a nearby outcome. Outcomes in complex systems can be difficult to trace and often counter intuition. Constructing a theoretically and mathematically consistent framework for simulating the system’s complexity is necessary to assess the consequences of different actions or events. Modeling the system from the perspective of its decision-making participants provides a conceptually clear way to relate the key dynamics at play in the model to

their real-world counterparts.

Economists have for several decades drawn on economy-wide modeling for policy analysis. This method of analysis helps elucidate important interactions and assess the aggregate impacts of different interventions. In the same way, ecosystem modeling is an important tool for understanding our influence on species that we may value economically or otherwise. Fisheries policy is a prime example of the need for powerful ecosystem simulations. Fishery policies require understanding sustainable harvesting practices both to ensure the persistent supply of economically valuable fish and to safeguard the ecosystem services or existence value provided by impacted species.

1.3 General equilibrium modeling

This work exploits the abstract features common to ecosystems and economies to simulate their behavior within a single framework known as general equilibrium modeling. The foundation of a general equilibrium model is an initial observation of the input-output relationships in the system. In an ecosystem, who is eating whom and in what quantity. In an economy, which industries and households require what goods and in what quantity. A balance of inputs and outputs is a key feature of this structure. Arranging all of the system's inputs and outputs in a common set of accounting matrices ensures that no biological or economic value is spontaneously created or destroyed within the model. All changes in value are the result of the modeled behavior of the system's participants: the ambient environment, species, households, firms, governments, or otherwise.

Drawing on the observed flow of inputs and outputs, each model participant can be characterized by a certain technology to describe how it combines inputs to generate its output. In the model, this technology is a mathematical function that can be analyzed to dictate how inputs should be combined to generate its output given

the prevailing scarcities in the system. The model structure is a highly-developed expression of constrained optimization from mathematics. The model's task is to identify an optimum for the system. This method imposes a certain determinism on the system, but in so doing it also guarantees an internal consistency to the results and a means to perform controlled simulation experiments. There are ways to relax the determinism, but more importantly, the optimum identifies the state toward which the system participants are competing. There are infinitely many sub-optimal outcomes the model could identify, but only a small number of optima, from which modelers are free to parameterize exactly how the system may deviate.

CHAPTER 2: GREENHOUSE GAS POLICY IN THE ELECTRIC SECTOR – MEASURING THE COSTS AND ANCILLARY BENEFITS

2.1 Introduction

The policy imperative for well-specified estimates of pollution abatement costs has driven economic modelers to incorporate increasing degrees of technical realism into their work. A top-down – bottom-up distinction is often offered at first approximation, though this distinction has become less stark with increasing emphasis on various hybrid approaches. Top-down, general-equilibrium models offer a richer measure of economy-wide costs but lack the engineering detail of bottom-up models. Methodological differences between the approaches and the dimensionality of bottom-up models can preclude full integration of the two, resulting in hybrid models that constrain one model type with the output of the other, sometimes in an iterative fashion (Böhringer & Rutherford, 2008, 2009).¹

This work implements a novel scheme for integrating bottom-up technological detail in the benchmark specification of a static national CGE model. Leveraging a specially-constructed dataset on the US electric sector, I capture much of the technical detail commonly omitted from CGE models without imposing external constraints from an independent bottom-up model. I take clean-air policy in the United States electricity sector as the object of analysis with a focus on carbon dioxide, though the construction is sufficiently general that it could be expanded to other sectors, pollution media, and regional aggregations provided adequate bottom-up cost and environmental data are available. The current iteration of the model includes CO₂ (N₂O and CH₄ can also be modeled), three criteria pollutants (NO_x, SO₂, and PM),

¹Examples include: the ADAGE model (Ross, 2008), a top-down approach constrained by bottom-up energy data; EPA’s IPM (ICF Resources, LLC, 2010), a bottom-up model constrained by macro forecasts; the NewERA model (*The NewERA Model*, 2013), a top-down model that iterates with a bottom-up electric sector model.

and one hazardous pollutant (Hg).

The primary challenge in building a model of this type lies in disaggregating input-output data summarized in macroeconomic accounts to a level of technical, sub-sectoral detail sufficient to reliably represent existing generation and abatement activity. Prior work (cf. Dellink, Hofkes, van Ierland, and Verbruggen (2004); Gerlagh, Dellink, Hofkes, and Verbruggen (2002); Kiuila and Rutherford (2013); Nestor and Pasurka (1995)) has abstracted a generic abatement sector with an independently estimated marginal abatement cost (supply) curve. Yet not all technologies can avail themselves of the same supply of abatement alternatives and, no matter how well articulated the abatement supply costs, this approach will likely impose a profile of abatement alternatives that is less sensitive to the general equilibrium effects of the model.

The solution proposed here is to identify and specify extant abatement technologies such that their cost profiles and output levels move with alternative equilibria. This requires “bottom-up” data for unit costs of generation and abatement and a means for reconciling these data with costs given by national accounts. Bottom-up data are available from the Energy Information Administration (EIA; Forms EIA-860 (*Form EIA-860*, 2010) and EIA-923 (*Form EIA-923*, 2010)), which form a partial basis for the Environmental Protection Agency’s (EPA) Integrated Planning Model (IPM), and from EPA (IPM cost assumptions (ICF Resources, LLC, 2010)). EPA also provide fuel and technology specific emissions factors for the included pollutants (the AP-42 compilation (*AP 42, Fifth Edition, Compilation of Air Pollutant Emission Factors, Vol. 1*, 1995)). I use a cross-entropy approach (cf. Robinson, Cattaneo, and El-said (2001)) to reconcile these bottom-up data with national macroeconomic accounts data from BLS and BEA.²

²This process could just as well be done with state-level data (e.g. IMPLAN *State-Level U.S. Data for 2010* (2012)) as the bottom-up data can be fully disaggregated to the level of the generating unit.

Once having disaggregated data into a social accounting matrix (SAM) split to the appropriate resolution of production-abatement technologies, I construct a static CGE model that imposes constraints on the ability to substitute across electric technologies (i.e. to capture grid-level generation load “preferences”). Finally, I leverage the CGE model to examine the cost associated with implementing a carbon dioxide policy akin to that recently outlined by EPA (EPA, 2014). Total welfare costs are considered alongside the benefits of ancillary abatement of two of the three modeled criteria pollutants (NO_x and SO_2). This model is ideal for assessing the near-term cost of imposing new clean air policies on the existing electric grid based on a rich characterization of the current menu of electric generation and abatement technologies.

Section two provides a brief overview of the relevant literature on this topic. Section three describes the data construction and reconciliation process. Section four outlines the model structure and specification of abatement trade-offs. Section five examines the welfare impacts of policy experiments, including an application to EPA’s Clean Power Plan, and section six concludes.

2.2 Literature

The two primary contributions of this work are the modeling approach and the assessment of ancillary benefits of greenhouse gas policy. On the former, prior work by Böhringer and Rutherford (Böhringer & Rutherford, 2008, 2009) gives a robust specification of how to link CGE models with models of the electricity sector. Using a top-down CGE model of the economy and a quadratic program to solve the bottom-up energy supply portion of the economy, Böhringer and Rutherford demonstrate how macro and sector-specific models can be iterated on prices and quantities toward a common solution. Doing so obviates the need for fully integrating the energy

sectors' complementarity relations for prices and quantities, which can frustrate solution algorithms, particularly to the extent exogenous bounds are imposed on these variables.

Böhringer and Rutherford offer a typology of linkages as either “soft linked,” where the “consistency and convergence of iterative solution algorithms” may be problematic, “reduced form,” where a highly simplified version of one of the models is employed, or a direct linkage, where the models are combined explicitly through complementarity relations on solution variables. The model developed in this work is closest to the third category, though the electric sector is modeled as an integrated part of the CGE model. Toward that end, Sue Wing (Sue Wing, 2008) outlines a method for integrating bottom-up technology data into an existing, top-down social accounting matrix to provide a direct complementarity representation of energy sectors. The work here uses a more general technique to render high technology resolution in the data.

On ancillary benefits of greenhouse gas policy, Burtraw and co-authors (Burtraw et al., 2003) take a detailed look at power generators' pollution control options using the Resources for the Future (RFF) Haiku Electricity Market Model (Paul & Burtraw, 2002). They find ancillary benefits of \$10/ton of CO₂ abated under a \$33 carbon tax, which does not affect SO₂ abatement levels. The authors also argue that ancillary benefits may arise from avoided future investments in abatement equipment, which increases ancillary benefits to \$16 – 18 per ton of CO₂ abated as compared with an estimated \$16 efficiency cost per ton of the tax.³ This is in line with the value of ancillary NO_x abatement estimated here of \$16 – 18/ton for 0 – 5% CO₂ abatement, declining thereafter by assumption. Ancillary benefits do not rise at higher carbon tax and abatement levels in their model. Similar to this study, the authors focus

³Dollar figures have been converted from Burtraw et al.'s \$1997 to \$2010 using a GDP implicit price deflator of 1.3 (*Gross domestic product: Implicit price deflator (GDPDEF)*, 2015).

on avoided health costs associated with NO_x as a precursor to particulate matter only. They give nuanced treatment to the spatial heterogeneity of pollutants using an atmospheric transport model.

Nam and co-authors (Nam, Waugh, Paltsev, Reilly, & Karplus, 2014) examine the extent of ancillary abatement in both the United States and China, estimating “cross-elasticities of control.” They rely on the MIT Emissions Prediction and Policy Analysis (EPPA5) model (Paltsev et al., 2005), a global recursive-dynamic CGE model, to assess co-benefits. In their analysis, Nam et al. consider both the impact of CO_2 reduction on NO_x and SO_2 and vice versa, whereas this study assesses only the former. They find that ancillary abatement of CO_2 is comparable for targeted reductions in SO_2 and NO_x (slightly higher for NO_x), with a higher median and a much wider range in China than the US. In the reverse direction, they find significant ancillary abatement of NO_x and SO_2 that is stronger in the US and stronger than the reverse relationships (i.e. carbon abatement under a NO_x and/or SO_2 policy). The average ancillary NO_x and SO_2 abatement is higher than for the reverse relationship with tighter ranges in both countries. Here China’s range of ancillary abatement is tighter than the US range.

In support of ancillary abatement as a real phenomenon, rather than just a modeled one, Holland finds empirical evidence that ancillary abatement does arise from reductions in output, though not from changes in actual emissions rates (Holland, 2010). That is, he finds evidence for output effects but not substitution effects. This could be an artifact of the empirical methods employed. Holland uses NO_x attainment status to proxy for NO_x prices. If a generator is fluctuating in and out of attainment, it may be more likely to make marginal adjustments to meet its attainment target (e.g. reducing output) as opposed to a generator that is persistently out of attainment, who may be more likely to make capital investments to substantially alter their

emissions rate. If these ‘marginal attainment’ generating units are frequently switching attainment status and manage their attainment through output, this could bias the attainment coefficient toward identifying output but not substitution effects in a way that might not generalize to carbon policy scenarios. Moreover, given that the period of study is well beyond the policy implementation, it is likely that the decision window for generators to make the capital investments to change their emissions rate had passed; i.e., it is only the generators who decided it best to manage their attainment through output that remain to drive the variation in attainment. Holland highlights important change-in-process considerations that the model developed here does not address. He gives the example of a higher burn temperature for natural gas fired plants as a way to reduce CO₂ emissions at the expense of higher NO_x emissions.

Nemet et al. (Nemet, Holloway, & Meier, 2010) summarize 48 estimates of co-benefits from a meta-analysis of 37 studies finding a median of \$31 of co-benefit per ton of CO₂ abatement in higher-income countries with higher estimates for lower-income countries (median of \$43/ton). The studies surveyed employ a variety of methods, which is reflected in the wide range of estimates produced (\$2 – 196/ton). The authors find that consideration of ancillary benefits is not common among the major integrated assessment models.

As Nemet et al.’s work highlights, there is considerable interest in ancillary benefits from carbon policy. They also emphasize that ancillary abatement value is under-represented in integrated assessments of carbon policies. This is despite early efforts to establish best research practices and broad-based policy support to “integrate the quantification and consideration of ancillary effects of climate policies more clearly into the national and international policy process” (OECD, 2000, p. 7).

2.3 Data Construction and Reconciliation

2.3.1 Bottom-up Technology Data

Data in national accounts present an aggregated electric generation, transmission and distribution sector. Capturing the heterogeneity of production and abatement alternatives requires a finer-grain representation, disaggregated along several dimensions to the level of production-abatement technology types. To achieve this, I integrate Forms EIA-923 and EIA-860 data (*Form EIA-860*, 2010; *Form EIA-923*, 2010), IPM generation and abatement cost estimates, and EPA emission factors to provide a comprehensive dataset covering 96% of electric generation, pollution, and abatement activity on the US grid: the Pollution, Abatement, and Generation of Electricity (PAGE) dataset (detailed in Appendix 7.1). All data are for the year 2010 where applicable.

Abatement technologies are for four pollutants: oxides of nitrogen and sulfur, particulate matter, and mercury. Emissions rates depend on the generation technology, fuel type, and installed abatement equipment. Mercury emissions depend on installed mercury technologies as well as nitrogen, sulfur, and PM abatement technologies, which provide mercury reduction co-benefits. Both end-of-pipe and change-in-process technologies are included. Table 2.1 summarizes the abatement technologies represented in the model. As no independently viable installations yet exist, no CO₂ abatement technologies are specified. The model could incorporate “backstop” specification of these technologies if desired, but the current iteration requires carbon abatement to come from adjustments to the level and mix of extant technologies.

Generation-abatement technology aggregates are further identified by prime mover and fuel type. For each aggregate, the PAGE data provide annualized cost estimates for the use of capital, labor, fuel, and electricity for the distinct generation and

Bottom-up Abatement Activity			
	Fraction of Net		Fraction of Net
Model technology	Generation	Model technology	Generation
<i>NOx Controls</i>		<i>Particulate Controls</i>	
Low NOx burner	20.44%	Cold side	30.15%
Catalytic reduction	19.68%	Fabric filter	7.19%
Overfire air	4.57%	Hot side	4.41%
Noncatalytic reduction	2.75%	Other methods	<u>1.51%</u>
Other change in process	1.73%	Total	43.26%
Fuel reburning	<u>0.00%</u>		
Total	49.18%		
<i>SOx Controls</i>		<i>Mercury Controls</i>	
Wet scrubber	65.47%	Activated carbon injection	5.40%
Dry scrubber	3.64%		
Total	69.11%		

Sources: PAGE dataset: Forms EIA-860 and EIA-923.

Notes: Model technologies aggregate EIA technologies.

A significant amount of mercury abatement occurs as a co-benefit of abating other pollutants.

Table 2.1: Pollution abatement technologies by pollutant

abatement equipment comprising the technology aggregate. Abatement equipment electric and fuel requirement costs are based on nameplate and heat rate penalties, respectively. Quantity data are provided for electric output, abatement and emissions for the four abated pollutants and three greenhouse gases (CO₂, CH₄, and N₂O). Table 2.2 summarizes relevant costs and quantities at the level of fuel type and reports an aggregate greenhouse-gas equivalent (GHGe) measure of the three greenhouse gases based on global warming potential. Table 2.3 summarizes four technologies at the technology resolution used in the model.

In all, generation-abatement technologies are specified on five characteristics: fuel type and controls for particulate matter, sulfur, nitrogen, and mercury. The PAGE data are generated at the plant-technology level allowing for geographic identification

Bottom-up Electric Sector Data										
	No.	Generation				PM			GHGe	
		Q (GWh)	K	L	E	Q (MMT)	K	L	Q (MMT)	
<i>Coal</i>	58	1,739,600	\$ 21,720	\$ 8,026	\$ 35,160	0.022	\$ 11,602	\$ 1,553	2,427	
Bituminous	23	890,000	\$ 6,420	\$ 3,600	\$ 22,100	0.007	\$ 6,520	\$ 861	1,140	
Sub-bitum.	29	769,000	14,800	4,100	11,700	0.014	4,510	629	1,130	
Lignite	6	80,600	500	326	1,360	0.001	572	63	157	
<i>Gas</i>	6	973,000	\$ 9,790	\$ 2,800	\$ 35,400	0.007	\$ 133	\$ 5	476	
<i>Nuclear</i>	1	807,000	\$ 18,800	\$ 1,320	\$ 2,080	0.000	\$ 0	\$ 0	0	
<i>Oil</i>	2	17,600	\$ 2,460	\$ 113	\$ 2,210	0.015	\$ 476	\$ 1	353	
<i>Renewables</i>	<u>1</u>	<u>413,000</u>	<u>\$ 12,200</u>	<u>\$ 1,160</u>	<u>\$ 1,350</u>	<u>0.000</u>	<u>\$ 0</u>	<u>\$ 0</u>	<u>0</u>	
Total Grid	68	3,950,200	\$ 64,970	\$ 13,419	\$ 76,200	0.045	\$ 12,211	\$ 1,559	3,256	

	No.	SOx				NOx			
		Q (MMT)	K	L	E	Q (MMT)	K	L	E
<i>Coal</i>	58	3.0	\$ 290	\$ 18,839	\$ 16,877	3.3	\$ 2,632	\$ 881	\$ 2,481
Bituminous	23	1.6	163	10,200	9,360	1.6	1,750	621	1,936
Sub-bitum.	29	1.2	115	7,760	6,740	1.6	818	228	516
Lignite	6	0.3	12	879	777	0.2	64	32	29
<i>Gas</i>	6	0.0	\$ 546	\$ 27,000	\$ 12,500	0.3	\$ 1,350	\$ 150	\$ 425
<i>Nuclear</i>	1	0.0	\$ 0	\$ 0	\$ 0	0.0	\$ 0	\$ 0	\$ 0
<i>Oil</i>	2	0.6	\$ 85	\$ 3,670	\$ 537	0.0	\$ 83	\$ 1	\$ 1
<i>Renewables</i>	<u>1</u>	<u>0.0</u>	<u>\$ 0</u>	<u>\$ 0</u>	<u>\$ 0</u>	<u>0.0</u>	<u>\$ 0</u>	<u>\$ 0</u>	<u>\$ 0</u>
Total Grid	68	3.6	\$ 921	\$ 49,509	\$ 29,914	3.6	\$ 4,065	\$ 1,033	\$ 2,907

Sources: PAGE dataset: Forms EIA-860 and EIA-923, Annual Energy Outlook (generation costs); EPA IPM V.4.10 (abatement costs); EPA AP-42 emissions factors.

Table 2.2: Electric generation technologies costs & quantities (2010)

for different regional aggregations. For the purposes of the national model presented here, the data are aggregated to the level of generation-abatement technology. A full summary of the data construction process is provided in Appendix 7.1.

2.3.2 Bottom-up – Top-down Reconciliation

Macroeconomic input-output data come from national accounts compiled by the Bureau of Labor Statistics (BLS) and Bureau of Economic Analysis (BEA) (Bureau of Economic Analysis, 2012; Bureau of Labor Statistics, 2012). Benchmark data are

Bottom-up -- Top-down Reconciled Model Technologies				
	Fuel: Sub-Bituminous Coal		Fuel: Lignite Coal	
	PM: Fabric filter		NOx: Low-NOx boiler	
	SOx: Dry scrubbed		PM: Cold-side ESP	
	Hg: None		SOx: Wet scrubbed	
	NOx: Non-Cat	Catalytic	Hg: None	Carbon Inject.
Quantities				
Net Generation (GWh)	3,956	7,411	27,600	12,600
Emissions (KTons)				
SOx	30.7	12.5	91.4	45.2
NOx	12.0	14.3	58.5	26.2
GHGe	9,050	10,800	53,800	24,100
Costs (\$2010 MM)	\$ 133.1	\$ 438.0	\$ 1568.4	\$ 771.2
Generation	\$ 52.4	\$ 253.9	\$ 767.0	\$ 378.0
Capital	\$ 3.8	\$ 117.0	\$ 180.0	\$ 83.4
Labor (O&M)	20.9	39.1	111.0	50.6
Fuel (HR Pen.)	27.7	97.8	476.0	244.0
SOx Controls	\$ 62.7	\$ 120.4	\$ 542.7	\$ 264.2
Capital	\$ 0.5	\$ 0.9	\$ 3.7	\$ 1.5
Labor (O&M)	37.1	69.1	274.0	126.0
Fuel (HR Pen.)	3.8	14.4	86.0	49.3
Electricity (Cap. Pen.)	21.3	36.0	179.0	87.4
NOx Controls	\$ 10.5	\$ 49.7	\$ 19.7	\$ 8.7
Capital	\$ 1.7	\$ 19.9	\$ 17.3	\$ 7.6
Labor (O&M)	7.7	7.0	2.4	1.1
Fuel (HR Pen.)	0.2	6.5	0.0	0.0
Electricity (Cap. Pen.)	0.9	16.3	0.0	0.0
Sources: PAGE dataset: Forms EIA-860 and EIA-923, Annual Energy Outlook (generation costs); EPA IPM V.4.10 (abatement costs); EPA AP-42 emissions factors. BLS 2010 input-output data and BEA value-add data.				

Table 2.3: Summary of costs & quantities for four model technologies

taken for the year 2010 in the form of “make” and “use” tables with a 195-industry resolution and transformed into a social accounting matrix (SAM) at a lower resolution. Even at the higher resolution, only a single “electric power generation, transmission, and distribution” aggregate (NAICS 2211) is presented. These data form the basis of the CGE model and must be reconciled with the bottom-up engineering data discussed in the previous section.

The technologies from the bottom-up data are assumed to employ a portion of the capital, labor, and electricity, all of the fuel, and none of the materials from the generation-transmission-distribution (GTD) aggregate of the national accounts. All of the materials and the remainder of the capital, labor, and electricity are then employed by a transmission and distribution sub-sector. Bottom-up cost estimates are incommensurate with values provided in the macro data and must be reconciled. This is particularly problematic for the technologies’ fuel uses, where bottom-up data yield totals for the various fuel types that differ markedly in absolute and relative magnitude from the top-down national accounts data.⁴

Drawing on the bottom-up data, I produce a technology-by-input unit-cost matrix of grid generation and minimally revise the matrix entries such that they reconcile with the relative fuel-use values given by macro accounts. I then scale the unit matrix by the fuel use totals from the macro data and remainder a minimum quantity of labor and capital (along with all materials) to the transmission and distribution sub-sector. An example unit cost matrix with technologies defined only on fuel type is presented in Table 2.4. The actual unit cost matrix used for the model represents approximately 70 technologies (defined on fuel type and abatement technologies). All model technologies are listed in Appendix 7.3.

The unit cost matrix sums to one by construction and all values are positive,

⁴This is partly a result of differences in data survey methods across the agencies, but a full account of the discrepancies is unknown. Correspondence with the agencies did not yield any new information.

Total Value:	\$ 173.9 Bn						
Bottom-up, Macro-inconsistent							
	Fuel Type						
Cost	BIT	SUB	LIG	GAS	NUC	OIL	RNW
K _{GEN}	0.027	0.062	0.002	0.041	0.079	0.010	0.051
K _{PM}	0.027	0.019	0.002	0.001	0.000	0.002	0.000
K _{SOX}	0.001	0.000	0.000	0.002	0.000	0.000	0.000
K _{NOX}	0.007	0.003	0.000	0.006	0.000	0.000	0.000
L _{GEN}	0.015	0.017	0.001	0.012	0.006	0.000	0.005
L _{PM}	0.004	0.003	0.000	0.000	0.000	0.000	0.000
L _{SOX}	0.043	0.033	0.004	0.114	0.000	0.015	0.000
L _{NOX}	0.003	0.001	0.000	0.001	0.000	0.000	0.000
E _{GEN}	0.093	0.049	0.006	0.149	0.009	0.009	0.006
E _{SOX}	0.016	0.009	0.001	0.027	0.000	0.002	0.000
E _{NOX}	0.003	0.001	0.000	0.000	0.000	0.000	0.000
Total	0.239	0.197	0.017	0.351	0.093	0.040	0.062
Sources: PAGE dataset: Forms EIA-860 and EIA-923, Annual Energy Outlook (generation costs); EPA IPM V.4.10 (abatement costs).							

Table 2.4: Example technology-by-input unit-cost matrix

hence it is a discrete probability distribution. To measure the extent to which I revise the bottom-up unit cost matrix, I use the Kullback-Leibler divergence, a standard information-theoretic pseudo-metric. I then minimize the divergence between the original and revised unit cost matrices subject to reconciling with the macro data. This is known as a cross-entropy method (cf. Robinson et al. (2001)). Both matrices must sum to one to ensure that the divergence measure is well-behaved and that the zero-profit condition on the Social Accounting Matrix (SAM) is met. All output of the generation-abatement technologies is purchased by the transmission and distribution (TD) sub-sector at a price equaling the value of inputs to ensure market clearance for the technologies and zero profit for the TD sub-sector. I first constrain the revised

matrix to sum to one unit of output, ensuring no economic profits are reaped. The supporting data preparation for this revision is analogous to that outlined by Sue Wing (Sue Wing, 2008).

I impose two additional constraints on the revised matrix. The first ensures that the total values of coal, gas, and oil implied by the revised unit-cost matrix match the values given by the macro data. The second ensures that the values of capital and labor implied by the revised matrix do not exceed what is available to the aggregate electric sector in the macro data, less a minimum amount of labor and capital for the transmission and distribution sub-sector. I base this minimum on ratios of capital and labor to materials inputs for a sample of RTOs and ISOs.⁵

The fuel value constraints are derived from the following identities.

$$\sum_{fc} \tilde{\sigma}_{cf} = F_c/\omega_G \quad (2.1a)$$

$$\sum_{fo} \tilde{\sigma}_{of} = F_o/\omega_G \quad (2.1b)$$

$$\sum_{fg} \tilde{\sigma}_{gf} = F_g/\omega_G \quad (2.1c)$$

where $\tilde{\sigma}$ is the revised unit cost matrix (σ the original, analogous to the values presented in Table 2.4), ω_G represents the total dollar value of generation output (e.g. \$174Bn in Table 2.4) on which the unit cost measures are based, the c , o , and g subscripts denote the subset of technologies (t) relying on coal, oil, and gas, respectively, and the f subscript represents the fuel-use input rows of the revised sigma matrix. Taking ratios of the equalities in eqn. (2.1) will constrain the shares by ratios of the

⁵Electric transmission and distribution entities that manage the electric grid: Regional Transmission Organizations and Independent System Operators.

known fuel values in the macro data (F_c, F_o, F_g). Specifically, I require that:

$$\sum_{fc} \tilde{\sigma}_{cf} / \sum_{fo} \tilde{\sigma}_{of} = F_c / F_o \quad (2.2a)$$

$$\sum_{fc} \tilde{\sigma}_{cf} / \sum_{fg} \tilde{\sigma}_{gf} = F_c / F_g. \quad (2.2b)$$

Both the benchmark and revised shares are defined positive. I then constrain the ratio of coal to the desired levels of total capital and labor for all technologies. For example, given a desired minimum value of capital in the transmission and distribution sub-sector, K_{TD} , and known value of coal, F_c , I require that:

$$\sum_{fc} \tilde{\sigma}_{cf} / \sum_{kt} \tilde{\sigma}_{tk} \geq \frac{F_c}{K_{ETD} - K_{TD}} \quad (2.3a)$$

$$\sum_{fc} \tilde{\sigma}_{cf} / \sum_{lt} \tilde{\sigma}_{tl} \geq \frac{F_c}{L_{ETD} - L_{TD}} \quad (2.3b)$$

where l (e.g. $L_{GEN} - L_{NOX}$ in Table 2.4) and k (e.g. $K_{GEN} - K_{NOX}$ in Table 2.4) are subsets of labor and capital inputs and L_{ETD} and K_{ETD} are the total amount of electricity-sector labor and capital given by the macro data. Finally, I require zero-profit in generation:

$$\sum_{ti} \tilde{\sigma}_{ti} = 1 \quad (2.4)$$

In sum, to derive the revised unit-cost matrix I minimize the Kullback-Leibler divergence of the original and revised unit-cost matrices (distributions):

$$D_{KL}(\sigma || \tilde{\sigma}) = \sum_{ti} \sigma_{ti} \ln(\sigma_{ti} / \tilde{\sigma}_{ti}) \quad (2.5)$$

subject to constraints 2.2, 2.3, and 2.4. All constraints bind. The algorithm is not permitted to revise original zero values at all and is infinitely penalized for revising original non-zero values to zero. The complete mathematical program is given as:

$$\begin{aligned}
\textbf{Given:} \quad & F_c, F_o, F_g, K_{ETD}, K_{TD}, L_{ETD}, L_{TD} \in \mathbb{R} \\
\textbf{Find:} \quad & \tilde{\sigma}_{ti} \quad \text{to minimize} \quad D_{KL}(\sigma || \tilde{\sigma}) = \sum_{ti} \sigma_{ti} \ln(\sigma_{ti} / \tilde{\sigma}_{ti}) \\
\textbf{Subject to:} \quad & \textit{Coal/Oil:} \quad F_c / F_o = \sum_{fc} \tilde{\sigma}_{cf} / \sum_{fo} \tilde{\sigma}_{of} \\
& \textit{Coal/Gas:} \quad F_c / F_g = \sum_{fc} \tilde{\sigma}_{cf} / \sum_{fg} \tilde{\sigma}_{gf} \\
& \textit{K-limit:} \quad \sum_{fc} \tilde{\sigma}_{cf} / \sum_{kt} \tilde{\sigma}_{tk} \geq F_c / (K_{ETD} - K_{TD}) \\
& \textit{L-limit:} \quad \sum_{fc} \tilde{\sigma}_{cf} / \sum_{lt} \tilde{\sigma}_{tl} \geq F_c / (L_{ETD} - L_{TD}) \\
& \textit{Zero profit} \quad \sum_{ti} \tilde{\sigma}_{ti} = 1
\end{aligned}$$

With the revised share matrix, $\tilde{\sigma}$, I can disaggregate the SAM's electric-sector aggregate. Drawing on the fuel-value identities (2.1), the original fuel input values divided by the sum of corresponding fuel input shares in the revised matrix gives the total value of generation, which can be used to scale the share matrix to a matrix of input dollar values consistent with macro data. A sample of four of the sixty-eight technologies produced by this method are summarized in Table 2.3.

2.4 Model Structure

2.4.1 General Structure

I construct a static model with one government and one household agent, a detailed electric sector, and fourteen other sectors, which are summarized in Table 2.5. A common production structure is shared by the non-resource sectors differing only in the degree of input substitution. Pollution is modeled only within the electric sector.

Producers demand intermediate goods from other sectors and fixed factors from households (i.e. labor and capital) and allocate an equal value (by zero profit) of output to other sectors and final demands (i.e. the household, government, and foreign markets) and investment. Outside the resource-intensive electric, fuel, and agriculture sectors, production technologies aggregate labor and capital, which is traded-off with an energy aggregate of electricity and fuel inputs. The energy-value-add aggregate then enters Leontief with materials (i.e. all other sectoral goods). Figure 2.1a di-

Sector Inputs (\$2010 Bn)						
Sectors	Value-add			Intermediate		Total
	Capital	Labor	Taxes	Energy	Materials	
Energy						
Natural gas distribution	87.5	11.0	1.9	294.2	32.3	427.0
Electric T&D (aggregate)	88.3	43.7	37.5	37.3	56.4	263.3
Petroleum and coal prod manuf.	87.4	25.2	23.6	21.8	52.1	210.1
Oil and gas extraction	22.8	11.3	9.7	57.8	17.8	119.4
Coal mining	<u>6.2</u>	<u>3.9</u>	<u>1.0</u>	<u>2.2</u>	<u>7.2</u>	<u>20.5</u>
Total	\$ 292	\$ 95	\$ 74	\$ 413	\$ 166	\$ 1,040
Energy Intensive						
Manufacturing	536.9	846.2	68.9	141.3	2,364.7	3,958.0
Municipal and Infrastructure	151.0	326.4	13.6	48.8	416.1	955.9
Transportation	104.4	197.7	19.6	76.9	263.2	661.7
Mining (non-fuel)	<u>25.5</u>	<u>29.8</u>	<u>3.4</u>	<u>6.7</u>	<u>51.0</u>	<u>116.4</u>
Total	\$ 818	\$ 1,400	\$ 106	\$ 274	\$ 3,095	\$ 5,692
Other						
Services	2,594.4	3,515.1	348.9	142.6	3,946.5	10,547.5
Trade	400.0	831.3	323.1	27.2	620.2	2,201.7
Special Industries	622.9	0.0	137.8	6.0	358.9	1,125.6
Agriculture	<u>79.6</u>	<u>35.0</u>	<u>-0.8</u>	<u>21.1</u>	<u>165.5</u>	<u>300.4</u>
Total	\$ 3,697	\$ 4,381	\$ 809	\$ 197	\$ 5,091	\$ 14,175
Government						
Public Government	235.9	1,293.7	0.0	37.7	567.9	2,135.3
Government Enterprises	<u>10.5</u>	<u>81.6</u>	<u>-6.0</u>	<u>7.2</u>	<u>35.2</u>	<u>128.4</u>
Total	<u>\$ 246</u>	<u>\$ 1,375</u>	<u>-\$ 6</u>	<u>\$ 45</u>	<u>\$ 603</u>	<u>\$ 2,264</u>
Grand Total	<u>\$ 5,053</u>	<u>\$ 7,252</u>	<u>\$ 982</u>	<u>\$ 929</u>	<u>\$ 8,955</u>	<u>\$ 23,171</u>

Sources: BLS 2010 input-output data and BEA value-add data.

Notes: The electric transmission & distribution sector is as presented in national accounts.

Table 2.5: Summary of SAM sectors

agrams the production structure for non-primary-resource sectors (primary-resource sectors are described further below). Imports and domestic production are combined as imperfect substitutes for the goods market via Armington aggregation “production” (Armington, 1969). Elasticity parameters are based on those in the MIT EPPA model (Paltsev et al., 2005) and are summarized in Appendix 7.2.

A representative household constructs welfare from consumption alone, which is funded by the value of endowments of labor, capital, and transfer payments. The entire labor endowment is marketed each period – no leisure value is specified. Benchmark fiscal and balance of payments deficits are endowed to the government agent who makes a lump-sum transfer to the household to cover private debts.

Tax payments accrue to the government agent to offset government expenditure on public goods. The representative household owns the pollution permits and uses their proceeds to offset consumption purchases. Permits have no value in the benchmark. A government public good is produced in a Leontief block and government enterprises carry a production structure similar to non-resource private sectors but with attenuated substitution elasticities.

2.4.2 Consumption

All welfare impacts are borne by the household. Real government purchases are held constant and the consequent deficits of policy-induced changes in government revenue and expenditure are funded by the household. All endowments are owned by the household (i.e. labor and all types of capital). Real investment and net exports are held constant. The household trades off transportation and all other consumption, which aggregates energy and non-energy goods. Energy goods aggregate fuels and electricity and other consumption aggregates materials and services separately. Figure 2.1b diagrams the “production” structure for the household consumption good.

2.4.3 Resource-Intensive Sectors

Electric Generation, Abatement, Transmission & Distribution

The electric sector is built from the bottom up. Its key feature is the micro-specified generation-abatement technologies. Each technology requires a particular mix of capital, labor, fuel, and electricity to operate its generation and abatement equipment (if

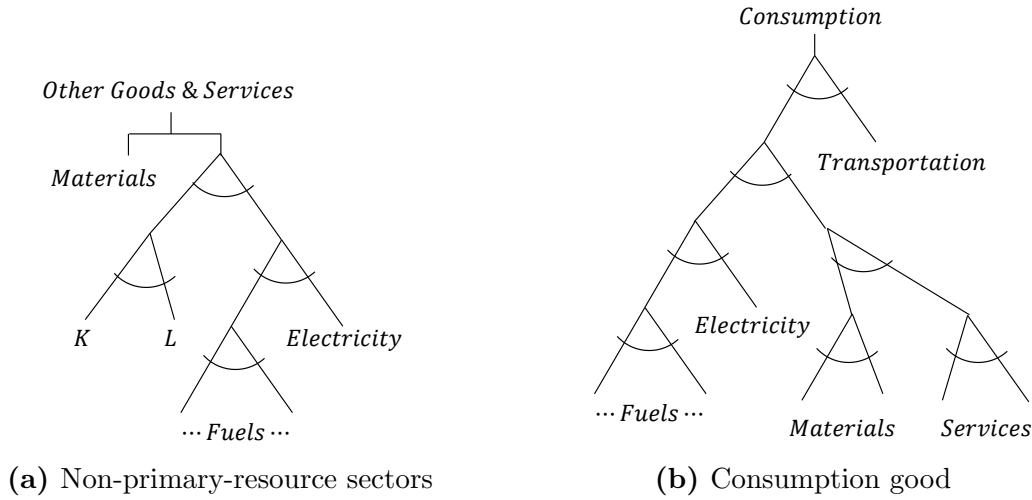


Figure 2-1: Production Structures

it runs any). Each technology produces outputs of electricity and unabated pollution. Pollution permits are required for the quantities of pollution that each technology's installed abatement equipment cannot abate. Pollution quantities are determined by the specific generation-abatement technology pair and are emitted in fixed relation to the technology's total electric output. This implies that the abatement technology is also run in fixed relation to total electric output. The upper-most nest of the CES production function for a given technology is then a Leontief aggregation of electric generation output, abatement services, and pollution permits (see below the first hashed line in Figure 2-2).

Given the fixed pollution-generation relationships of the individual technologies, the model's abatement-pollution substitution must occur across technologies, not within. As an example, consider mercury abatement in the context of the second two technologies summarized in Table 2.3. Here it is evident how the model's electric clearing house can choose between generation from a lignite-coal-fired generator with a low-NOx boiler, a cold-side electrostatic particulate precipitator, wet-scrubbed desulfurization, and no mercury technology and the same technology with an active-carbon injection mercury control device. The reality such model behavior represents

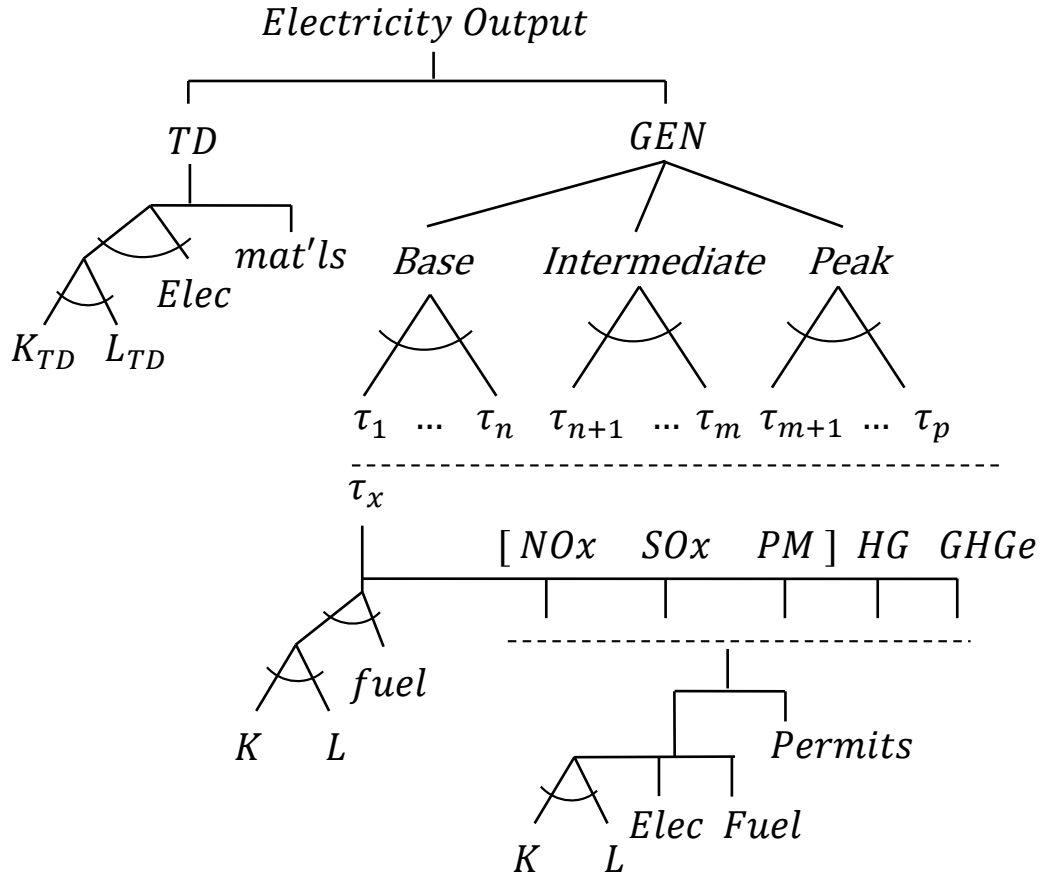


Figure 2-2: Generation, transmission, & distribution production structure

might be a retrofit or new construction, but this distinction is abstracted in the model – a mark of its top-down approach.

The model's electric clearing house then aggregates the output of the discrete generation-abatement technologies into a single electricity good for consumption by other sectors and agents. Substitution across technologies is limited by the load they serve and motivated by changes in relative prices of the labor, capital, environment, and energy inputs required to operate the technologies. The strength of this approach is that it requires full specification of the technology for each productive generation and abatement option, avoiding further abstraction to a generalized abatement ser-

vice sector. That is, if more abatement is to be done without simply reducing grid output, this approach forces the modeler to articulate specifically by what available technologies it might be achieved. Specifying discrete technologies in this way attenuates the oft-critiqued excessive “smoothness” of the top-down approach without compromising the overall method.

The electric clearing house aggregates these technologies first into base, mid, and peak load “nests.” This structure helps preserve the extant technological heterogeneity on the grid and limits the extent to which low-cost, base-load technologies can compete with peak-load technologies whose higher cost is justified by other services they provide to the grid (e.g. fast ramp times). Labor and capital for the TD sub-sector are aggregated with substitution and enter Leontief with materials and the electricity aggregate to produce final electricity output. Figure 2-2 diagrams the production structure. Hashed horizontal lines indicate that the structure below is repeated for all elements immediately above.

Individual technologies purchase permits from the household. (Permits enter Leontief with abatement in Figure 2-2, but are just as well considered Leontief to the technology’s electric output given the structure.) In this way, the relative costs on which the clearing house chooses its technology portfolio are driven by the technologies’ permit requirements, resulting in a higher marginal cost of electricity output. This generates both the substitution and total output effects necessary to reduce CO₂ emissions.

Primary-Resource Sectors

In models with constant returns to scale in production, rate limiting of economic growth is imposed primarily by the availability and productivity of fixed factors, the most basic of which are labor and capital. Fuel production is further limited by fixed quantities of raw fuel stocks and limited extraction capacities. Regardless of the

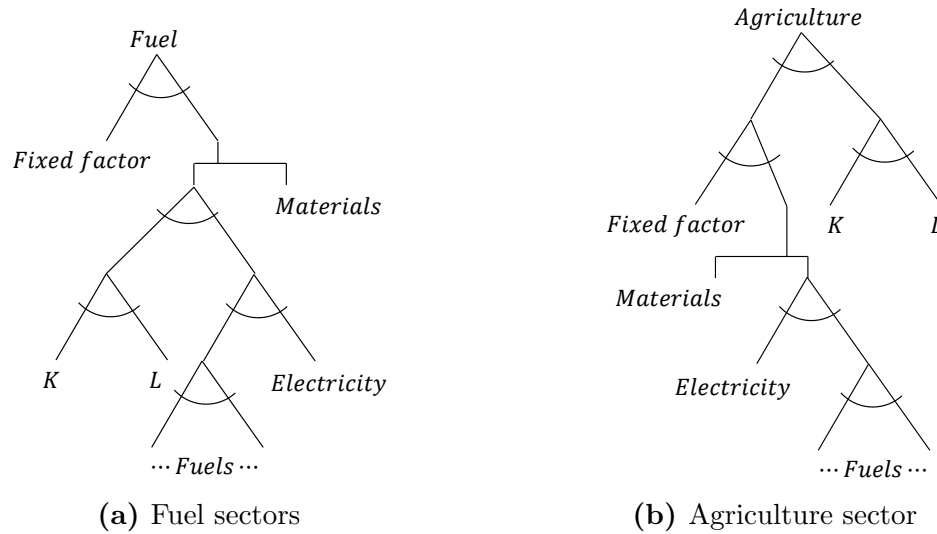


Figure 2.3: Primary-resource sectors production structures

output price, only a certain quantity of fuel can be produced in a given period. In a similar way, agricultural production is limited by a fixed quantity of arable land.

To implement this dynamic in the model, fuel producers must draw on a set endowment of technologically feasible fuel inputs and agricultural producers on a set endowment of land capital. The value of these sector-specific factors is deducted from the capital given in the macro data. A similar procedure is completed for renewable and nuclear generation technologies, whose fuel inputs are assumed to be paid in part to capital premia. This offers a mechanism for restricting certain technologies from expanding to levels that are known to be unrealistic in terms of physical or policy constraints not otherwise represented in the model. Figure 2.3 diagrams the fuel and agriculture sectors' production structures.

2.4.4 Policy Design

Pollution permits are the model mechanism for implementing clean-air policies in the modeled electric sector. Permits are only demanded, in a Leontief structure, by the generation technologies. Permits are endowed to the representative household in an

amount equal to that required to run the grid in the benchmark. Policies are implemented by reducing the quantity of endowed permits for the pollutant targeted by the policy. Benchmark permit prices are set to a *de minimus* value so that generation technologies' costs are not disturbed.

The pollution permits are primarily a modeling tool. In the abstract, they allow the modeler to identify the least expensive means for reaching a target level of emissions given extant technologies. This is an ideal formulation for criteria pollutants and greenhouse gases, for which standards are or would most likely be set according to ambient levels. By contrast, hazardous air pollutant (HAP) policies are typically implemented via a maximum achievable control technologies (MACT). So evaluating a HAP policy (e.g. a mercury rule) would warrant different treatment than criteria pollutants and could be easily accommodated within the model by modifying the various technologies cost structures and emissions factors with reliable cost and performance estimates for the MACT.

Real government expenditures are held fixed without substitution and resulting deficits are borne by the households. Deficits are generated by the interaction of changes in prices and tax revenues. Equivalent variation is then measured by the dollar-quantity change in the household consumption (cf. Pizer and Kopp (2003)).

2.5 Policy Experiments Results

2.5.1 Baseline Results

Abatement activity of any given pollutant may come with a suite of co-benefits from ancillary abatement of other pollutants. Abatement is achieved both by changing the composition of operating generation and abatement technologies and by reducing the total level of electric output. In both cases, levels of pollutants not targeted by the policy intervention are also subject to change. This ancillary abatement has

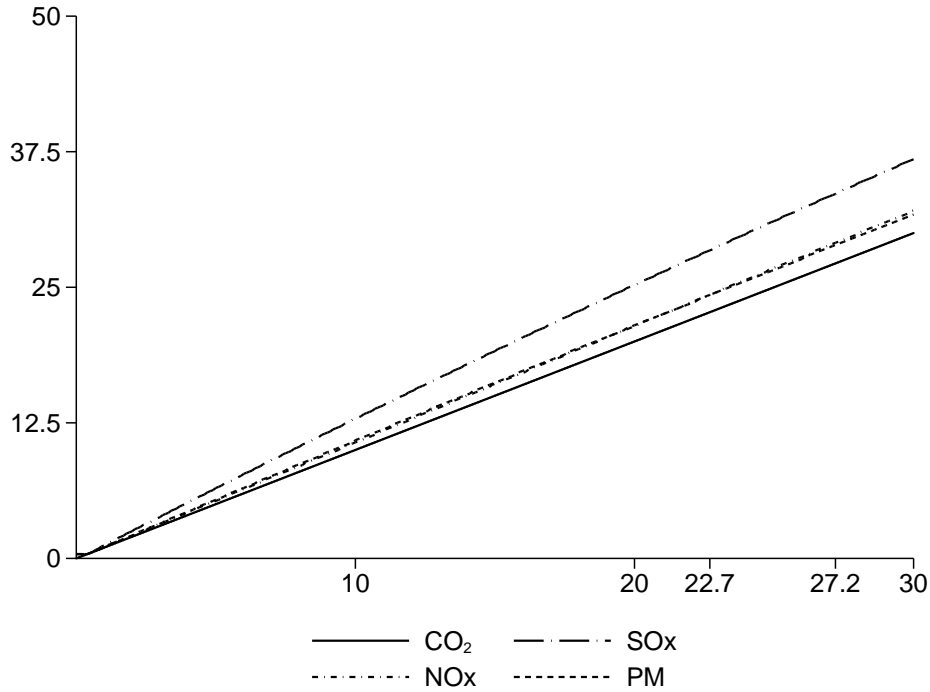


Figure 2-4: Percent reduction in emissions for CO₂ & other pollutants

value and, even absent reliable estimates on the value of abatement benefits for the targeted pollutant, is an important consideration in the cost-benefit assessment of clean-air policies. (The horizontal axis of all graphs in this section is percent CO₂ reduction unless otherwise noted.)

As an example of co-abatement under a greenhouse gas policy, consider the first two model technologies presented in Table 2.3. If greenhouse gas permits are expensive enough, the second technology will be favored to the first for its lower GHGe emissions factor (1,457 vs. 2,287 tons/GWh). The second technology also has a lower NO_x emissions factor (1.93 vs. 3.03 tons/GWh). So the greenhouse gas policy has also induced NO_x abatement and, in this case, actually led to an equivalent percent decline in NO_x and greenhouse gases (36.3%), *ceteris paribus*.

This simplified example has abstracted away from the explicit cost considerations

made by the electric clearing house in choosing technologies, but demonstrates how ancillary abatement is likely to come about. Figure 2-4 demonstrates how this dynamic unfolds in the model by plotting percent reductions in three pollutants (NO_x, SO₂, and PM) for a range of percent-reduction policies on greenhouse gases.⁶ Most notable here is that all non-targeted pollutants experience *larger* abatement percentages than the targeted CO₂.

Carbon dioxide has no available control technologies in this model so abatement must be achieved through a combination of technology substitution and reduced electric output. Figure 2-5 presents the changes in output for four technology categories (based on fuel type) and total electric output. Electric output begins its decline immediately with the implementation of any CO₂ policy driven by sharp declines in coal and oil and offset by larger nuclear, renewable, and gas technologies' output.

The final task is to consider what value some of the policies ancillary benefits might carry. Here I rely on benefit estimates by Fann, Fulcher, and Hubbell (Fann, Fulcher, & Hubbell, 2009) for NO_x and SO₂ as PM precursors. Fann et al. provide dollar estimates of the benefits associated with abating NO_x and SO₂ strictly as a function of their being precursors to particulate matter formation. These benefits arise primarily from reduced mortality and morbidity from a variety of types of illness (e.g. respiratory, cardiac). Fann et al. estimate national benefits for abatement from electric generating unit sources of \$15,000 per ton for NO_x and \$82,000 per ton for SO₂. Marginal benefits are assumed to be declining in the amount of abatement achieved with a demand elasticity of 5. That is, after 20% ancillary abatement of NO_x or SO₂, additional abatement is assumed to have no further economic benefit. Valuing this particular subset of benefits alongside the welfare costs provides a more comprehensive estimate of the net cost of the policy. Figure 2-6 presents the total

⁶The 22.7 and 27.2% reduction marks on the horizontal axis correspond to 25 and 30% below 2005 levels, the reference point for the Clean Power Plan.

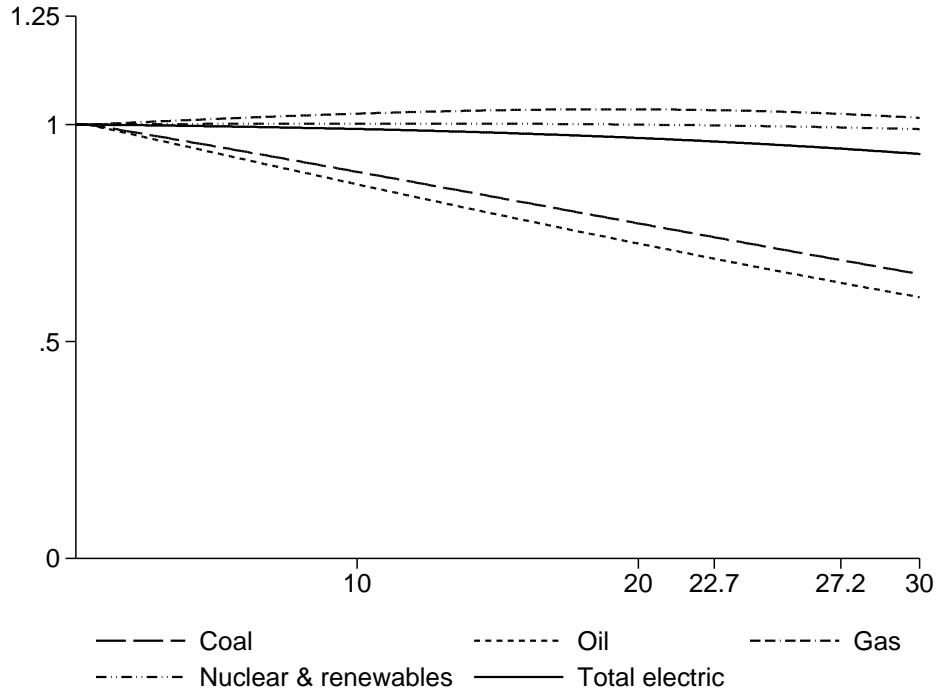


Figure 2·5: Total & fuel-specific electric output under CO₂ policy

and net-of-benefits welfare cost of a greenhouse gas policy.

Considering only the health benefits of NO_x and SO₂ as PM precursors, the net policy cost is negative through all 30% of CO₂ reductions, suggesting a possible “no regrets” policy window for CO₂ abatement in the electric sector. In order to assess the optimal “no regrets” policy we consider marginal costs and ancillary benefits of a carbon policy. The marginal ancillary benefit of abatement is \$14 – 18 for NO_x and \$110 – 155 for SO₂ for CO₂ abatement less than 5%. By assumption, these marginal benefits are declining, to approximately \$9 and \$58 by ten percent CO₂ abatement, respectively, and zero by 20% CO₂ abatement. Figure 2·7 presents the no-regrets optimum at the intersection of the marginal ancillary benefit and welfare cost curves. The no-regrets optimum for the policy is 13.3% CO₂ reduction at \$26/ton. Of course, this is a lower bound on the actual optimum given that carbon abatement also carries

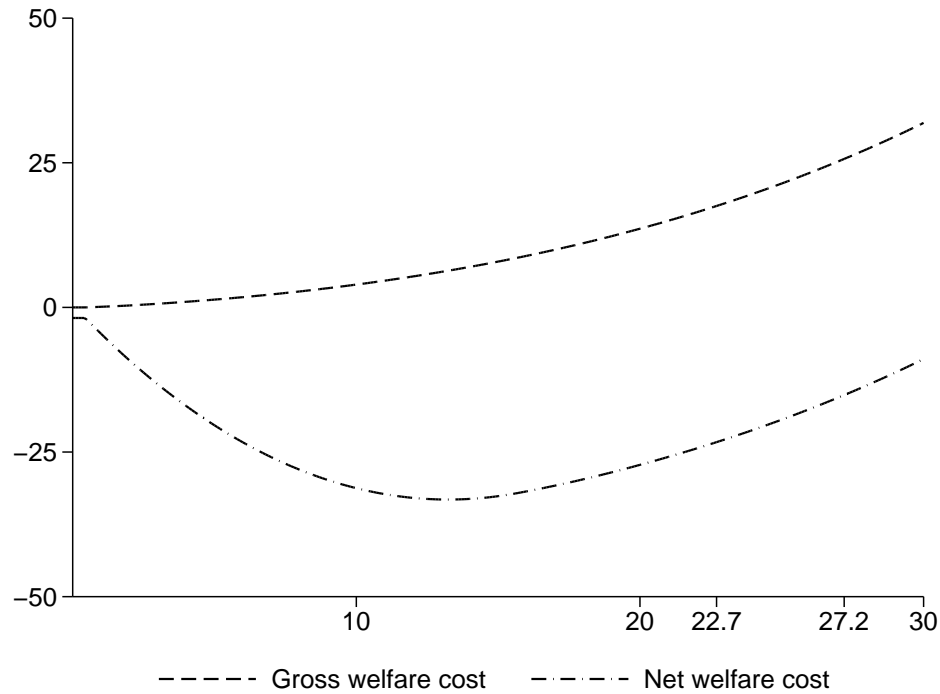


Figure 2.6: Gross & net welfare cost of CO₂ policy (\$2010 bn.)

marginal benefits.

Next I consider alternate modeling scenarios designed to represent plausible constraints on electric-sector compliance that might drive gross policy costs higher.

Alternate estimates

In the above estimates, electric generation technologies' capital is free to be reallocated to other purposes. In reality, reallocations are likely to leave some capital "stranded" in existing relatively "dirty" generating units. To model this behavior, I immobilize a certain fraction of generation and abatement capital by generating separate markets for them. Creating these markets has two primary effects, both of which will drive gross welfare costs higher. First, generation and abatement capital allocated to the new technology-specific markets is no longer free to be reallocated to other purposes. This restricts the supply of capital available to new installations

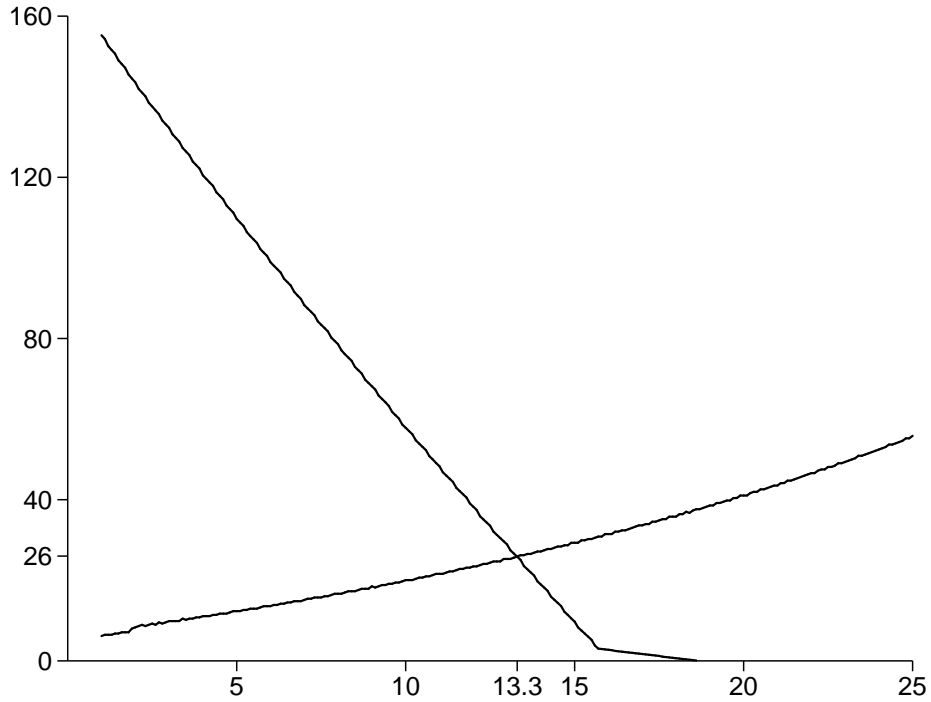


Figure 2-7: Marginal ancillary benefit and welfare cost (\$2010)

thereby increasing the cost of expanding cleaner generation. Second, as demand for “dirty” capital installations drops, with no alternate uses, the value of this capital falls and households incur losses.

Separate capital markets are created for fossil-fuel generation technologies and pollutant-specific abatement technologies (five new markets). All but a nominal amount (\$1,000) of capital used by the technologies is designated to its corresponding market. A capital production block aggregates the former amount with the nominal residual drawn from the general capital pool to produce the total quantity of capital used by the technologies. In this way, the initial quantity of capital used by the generation and abatement technologies (less a nominal amount) is left “stranded” within the technologies, though new capital can still be added. The capital production block aggregates technology-specific and general “jelly” capital with an elasticity of 5.

Figure 2·8 compares gross and net welfare costs associated with greenhouse gas abatement policies with the capital constraint. As expected, welfare costs are higher – 33% higher than without stranded capital at maximum. Welfare costs net of benefits still remain negative until 29.5% CO₂ abatement. In both scenarios, the NO_x and SO₂ ancillary benefits provide a substantial reduction of gross costs and are 10 – 20% higher with the capital constraint but converging for higher abatement levels. The marginal ancillary benefit of abatement is lower with fixed capital, \$12.5 – 14.5 for NO_x and \$98 – 158 for SO₂ for CO₂ abatement less than 5% declining, by assumption, to approximately \$10 and \$40 by ten percent CO₂ abatement, respectively, and zero by 20% CO₂ abatement. The no-regrets optimal abatement is also lower at 11.7% and \$33/ton. Figure 2·9 presents the no-regrets optimum at the intersection of the marginal welfare cost and marginal ancillary benefit curves. If the marginal benefits are given an elasticity of 1 (i.e. marginal benefits decline to zero only at 100% abatement instead of at 20%), the no-regrets optimum more than doubles to 29.2% abatement.

Figure 2·10 shows changes in total and fuel-specific electric output. The capital-constrained scenario has gas generation playing a larger role in absorbing reallocation and greater total generation than the unconstrained scenario. Gas generation with the capital constraint will be relatively cheaper in that fossil-fuel-generation capital is freed from the relatively dirty coal and oil generation with only gas generation to absorb the newly available supply. This dynamic is particularly evident at reductions beyond 15%. Future work would give more scrutiny to capital markets and the extent to which different capital stocks can be repurposed.

Figure 2·11 presents a scatter plot of the unit cost (dollars per kilowatt-hour) for all model technologies. The solid markers present the baseline data and the hollow markers present the post-policy outcomes for a 30% reduction in greenhouse gases

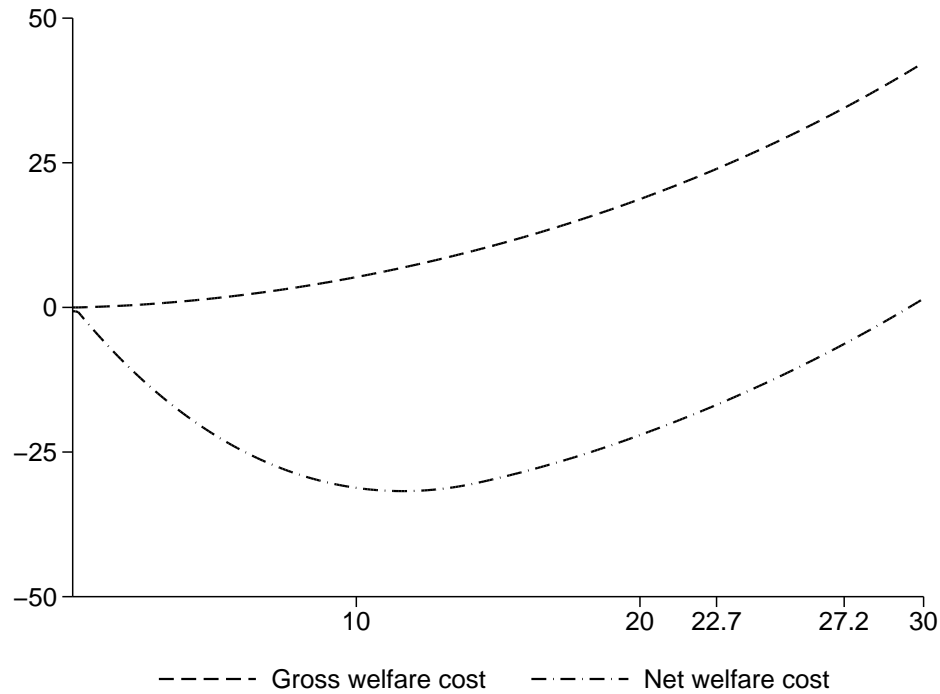


Figure 2-8: Gross & net welfare costs, “stranded” capital (\$2010 bn.)

with fixed capital and flexible substitution across technologies. A large price gap is evident for coal technologies whereas gas technologies move relatively more in the quantity dimension.

Last, CO₂ permit prices are higher in the capital-constrained scenario as expected. Prices reach a high of \$50–60 per ton and are comparable with and without stranded capital. Figure 2-12 shows permit prices for the range of CO₂ abatement levels. As Morris, Paltsev, and Reilly demonstrate, these marginal abatement cost (MAC) estimates “are, in general, not closely related to MWCs,” which were presented above to estimate the no-regrets abatement optimum (Morris, Paltsev, & Reilly, 2012, p. 325).

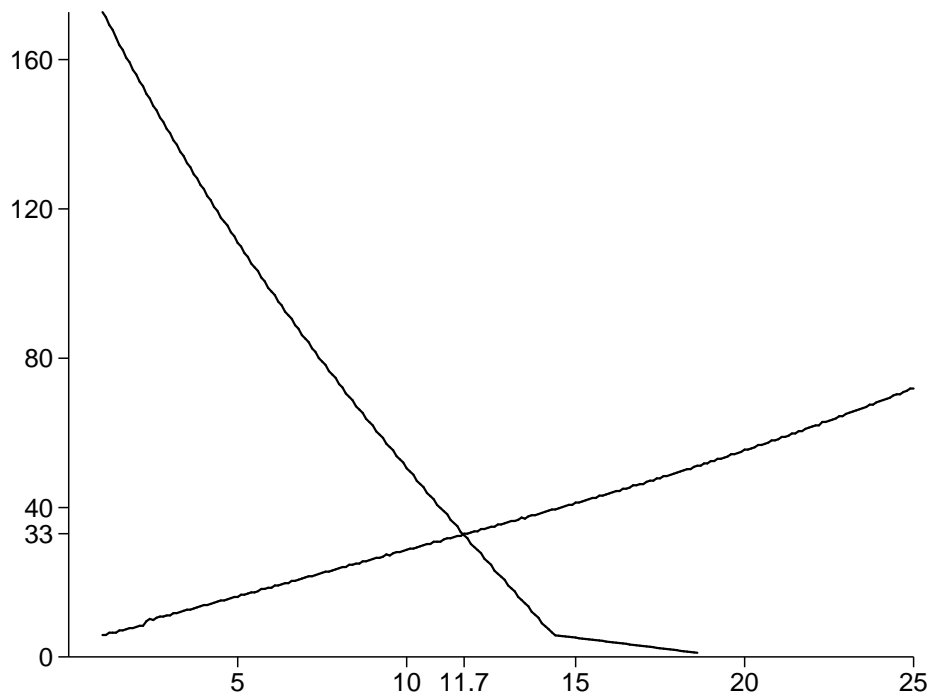


Figure 2-9: Marginal ancillary benefit & welfare costs, “stranded” capital (\$2010)

2.6 Conclusion

This work leveraged a uniquely detailed CGE model of the electric sector in the United States to estimate the costs and ancillary benefits of abating CO₂ pollution. In particular, I find that, given existing electric generation and abatement technologies, the welfare costs associated with CO₂ abatement are largely offset by the ancillary benefit of NO_x and SO₂ abatement. That is, without considering the direct benefits of CO₂ abatement, whose valuation can be challenging, net policy costs do not appear to pose an appreciable hurdle for these benefits to clear for modest levels of abatement. However, the no-regrets optimum is well shy of the percent reductions targeted by EPA’s clean power plan (approximately 25%). To justify that level of reduction, we would need marginal benefits of CO₂ abatement to roughly equal or exceed those of

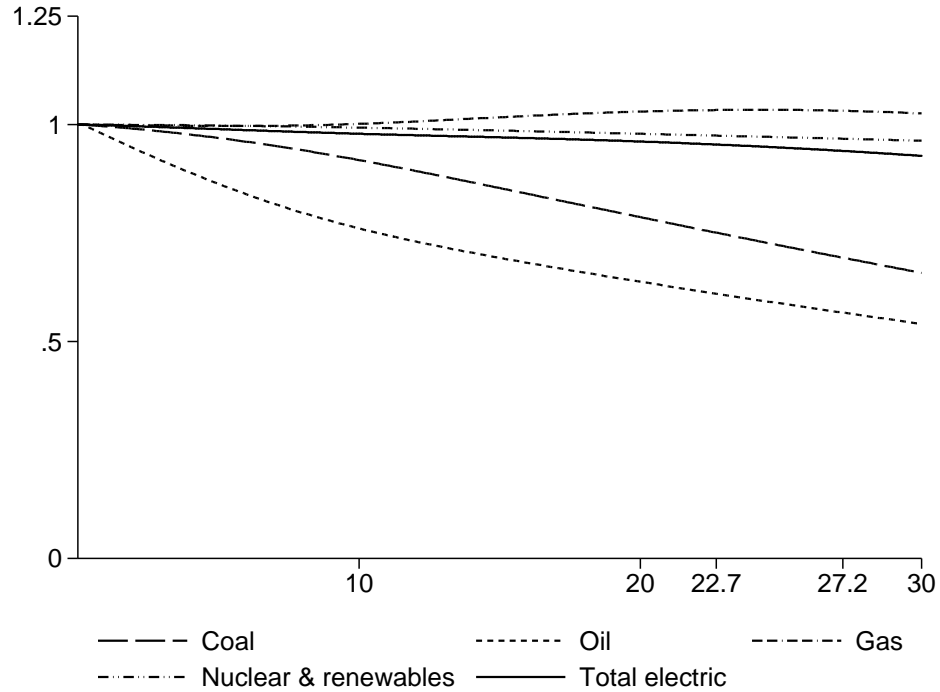


Figure 2-10: Electric output, "stranded" capital

NO_x and SO₂ as PM precursors. Whatever the benefits of CO₂ abatement, this study suggests that the cost hurdle they must clear to meet the broad goals of the Clean Power Plan is roughly halved by the ancillary benefits that arise from CO₂ policy in the electric sector.

These results give a preliminary indication that multi-pollutant linkages could play a significant role in mitigating, or potentially driving, environmental policy costs. This analysis has not considered what ancillary costs might obtain with a CO₂ policy. For example, natural gas generation grew in both scenarios considered. Recent opposition to the expansion of natural gas extraction has focused on potential environmental costs that could add to welfare losses from CO₂ policy. Moreover, I have not considered how the general equilibrium outcomes may influence pollution in other sectors. Again, losses in the natural gas extraction and distribution system

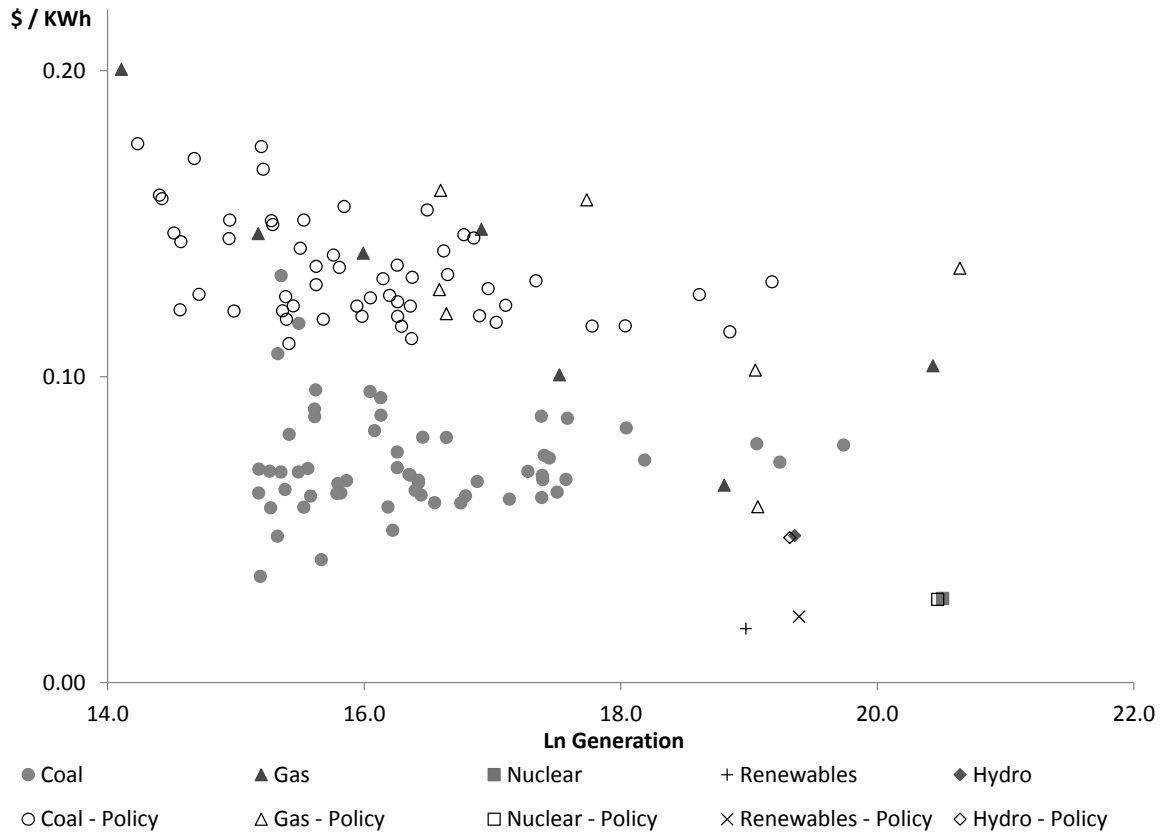


Figure 2-11: Unit-cost by generation scatter for all technologies

are a notable source of greenhouse gases, which could offset some gains achieved by a CO₂ policy.

Future work could improve the estimates here by adopting a regional or even state-level aggregation scheme, possibly with state-level policy implementation. A more nuanced approach to capital markets and the role of capital vintages in the model might also produce more accurate estimates. While these modifications will likely change the level estimates of policy costs and ancillary benefits, they are not likely to change the central message that multi-pollutant linkages through the technology structure of the electric sector, or other emitting sectors for that matter, are a critical consideration in cost-benefit analysis of clean-air policy.

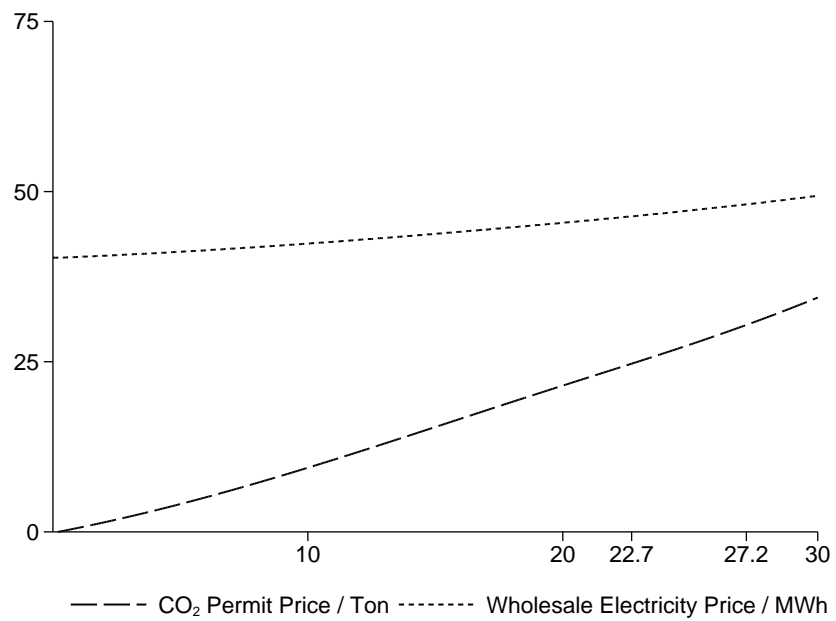


Figure 2.12: Permit & electricity prices, “stranded” capital (\$2010)

CHAPTER 3: MODELING ECOLOGICAL DYNAMICS – A GENERAL EQUILIBRIUM APPROACH

3.1 Introduction

This work constructs a general equilibrium model of multiple adaptive species in a generic ecosystem. The model is constructed from a “micro-founded” bioenergetic optimization perspective. The bioenergetic optimization of the species in the model motivates ecosystem dynamics. While a number of ecosystem models have incorporated adaptive responses, the responses to prey-densities tend to be uniform across prey (if multiple prey are modeled) and not clearly tied to the underlying bioenergetic trade-offs. Bioenergetically-optimal functional response generalizes species optimal (or adaptive) foraging behavior in a way that can be made sensitive to other environmental conditions not related to prey densities (e.g. temperature, ambient toxicity). This approach represents a novel synthesis of three veins of theoretical biology literature: optimal foraging, bioenergetic optimization, and food web dynamics. The coherence of this synthesis within a single model is supported by the theory of economic general equilibrium, which provides a method and framework for identifying feasible equilibria in conservative systems (i.e. systems that conserve an aggregate quantity such as energy or economic value). This approach makes a hard link between the micro bioenergetics and macro population-dynamics of ecosystems that remains underdeveloped in the literature.

The underlying bioenergetic optimization takes a measure of energetic surplus as the object of maximization (maximand), as is common in the theoretical biology literature. There is also clear intuitive support for a measure of this sort in as much as it proxies for robustness against evolutionary selection pressures.¹ That is, the more

¹There also exists tentative theoretical support for such a measure from a thermodynamic perspective (cf. Dewar (2010); Kleidon and Lorenz (2005); Lorenz (2002); Wissner-Gross and Freer

energetic surplus embodied within the species, the greater the selection pressure would be required to threaten its survival.

The optimization works on the premise that species produce available energy (exergy) from consumption of prey and allocate it to support their activities and propagate their genes. After sacrifices to predators and metabolic “debts” from rest processes and activity are accounted, any remaining energy surplus is allocated to ending biomass. Ending biomass might take the form of structural biomass, storage biomass (Giacomini & Shuter, 2013), or offspring, with selection pressure forcing species toward an optimal allocation among these to maximize genetic propagation. Selection pressure forces an optimum on varying timescales. Optimization occurs at the genetic level, not the individual (Dawkins, 1989), so that phenotypic and behavioral adaptations are made to maximize the energetic surplus of the genetic kin as a whole. The bioenergetic optimization can generate a functional response for species to a wide cast of environmental factors influencing the energetic costs and benefits to the species. (The term species will be used loosely here to connote a collection of individuals that are functionally equivalent with respect to the modeled ecosystem.)

The strength and novelty of the model lies in its capacity for endogenously modeling species adaptation to changing ecosystem dynamics and external forcings. The model is designed to be fit to simulated or empirical input–output data.² Bioenergetic functions can be tuned to generate, as an outcome of the optimization, common Holling response types (Holling, 1959) that drive the trophic links in the model. Feasible equilibria are those population (scarcity) vectors that can simultaneously satisfy

(2013)).

²Food web data are simulated in a variety of forms (e.g. random May (1972), cascade Cohen and Newman (1985), niche R. J. Williams and Martinez (2000)). An example of empirical data is that collected by the Northeast Fisheries Science Center’s (NEFSC) Food Web Dynamics Program (FWDP), a part of the National Oceanic and Atmospheric Administration (NOAA). The program collects data on stomach contents and population estimates.

bioenergetic input (consumption) and output (production) as an optimum while also conserving system aggregates.

In sum, this model adapts extant optimization-based, input-output modeling techniques common to economics to a biophysical setting where bioenergetic optimization drives individual species' behavior from whose interactions emerge macroscopic equilibrium outcomes in the ecosystem.

3.2 Literature review

Broadly speaking, this is a work of theoretical biology. Within theoretical biology there exist three main veins of research most relevant to constructing a “Biological General Equilibrium” (BGE) model:³ optimal foraging, bioenergetic optimization, and food web (or ecosystem) dynamics. A synthesis of these three veins will present a unique contribution to ecosystem modeling, one that may answer a direct call from Beckerman, Petchey, and Morin in a recent introduction to a special feature in the journal *Functional Ecology*: “after 40 years of [optimal foraging theory’s] development, there are precious few advances towards truly synthesizing the connections between individuals, populations and large interconnected food webs” (A. Beckerman, Petchey, & Morin, 2010, p. 1).

The coherent synthesis of these three veins will be enabled by the framework and (numerical) methods of the economic computed general equilibrium (CGE). Despite drawing on CGE theory to structure the model, the supporting literature is not reviewed as this work is not intended to make a novel contribution to CGE theory; however, a general overview of general equilibrium theory is given. Of course, certain aspects of the economic theory are not transferable to an ecosystem setting. Some of the simplifying assumptions used to ease algebra, and for lack of strong alternative

³This work is most similar to the “General Equilibrium Ecosystem Model” (GEEM) concept coined by Tschirhart in his 2000 *Journal of Theoretical Biology* paper (J. T. Tschirhart, 2000). Tschirhart’s model is covered in detail below.

convictions, in CGE theory are inappropriate in a biophysical setting. What’s more, biophysical properties such as allometry can offer helpful guidance not available to economic models for specifying bioenergetic dynamics. To best accommodate a biological setting and avail the well-understood biological dynamics, I look to abstract just the essential structure of CGE theory.

The basic structure of general equilibrium modeling is built on an input-output accounting framework owing to early work by Leontief and the (much) earlier “tableau economique” proposed by Quesnay. The input-output structure is helpful in that it lends itself nicely to conservation conditions requiring that the aggregate input quantities (e.g. of energy) equal their output counterparts. Imposing these conditions precludes “leaks” in the system’s accounting so that all value flows within and across the boundaries of the system are properly accounted. To assemble the requisite biological theory to support this structure, the literature review proceeds in parallel to the three veins of biology literature synthesized in the model. I look to the literature to inform first, how species choose their inputs, second, how they allocate their outputs, and third, how these choices drive ecosystem outcomes.

3.2.1 Optimal bioenergetic input

Functional response and switching

Optimal foraging theory, now nearly fifty years old (Emlen, 1966; MacArthur & Pianka, 1966), holds that competitive interactions within and among species forces survivors toward optimal behavior. In the framing of Stephens and Krebs (Stephens & Krebs, 1986), this is a process by which species face *decisions* to be made subject to certain *constraints*, the outcomes of which can be evaluated, through natural selection, by a *currency*. Constrained optimization, a mathematical method central to CGE models used to analyze measured objectives beset with constraints, is then well-suited to evaluating the evolution of biological systems as framed by Stephens

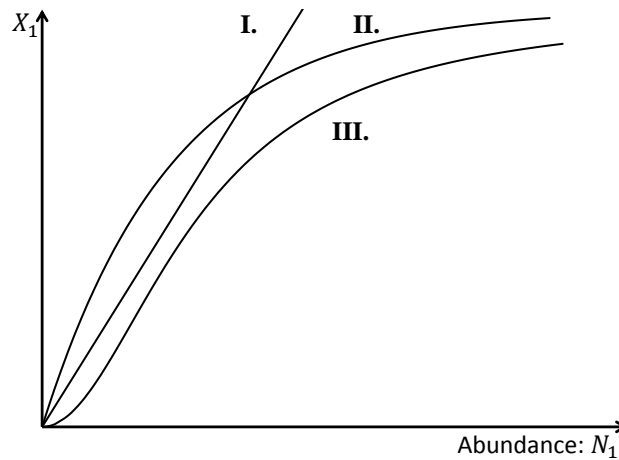


Figure 3-1: Holling functional response types

and Krebs. As they emphasize, “adaptation . . . is an integral part of evolutionary biology, and . . . optimality models . . . are part of a separate and necessary enterprise” (Stephens & Krebs, 1986, p. X).

Early work on foraging posited that predators might exhibit a density-dependence in their selection of prey (inputs) known as apostatic selection (Murdoch, 1969; Murdoch & Oaten, 1975). This arose from a three-part typology of functional responses offered early by Holling (Holling, 1959) based on the shape of consumption as a function of prey density: type I (linear), type II (asymptotic), and type III (logistic). This typology has survived well and is still used to characterize the behavior of species within contemporary models. Type II and Type III responses are most common. The next logical step, to relate *relative* densities and consumption of multiple prey, was given by Murdoch (Murdoch, 1969) and later generalized by Elton and Greenwood (Elton & Greenwood, 1970). The definition of switching in biology bears a direct relation to the definition of substitution in economics.

Figure 3-1 provides a stylized representation of the three response types. Note how both type II and III responses have an upper bound on the amount the predator consumes. As defined by Murdoch, functional response characterizes “[t]he way the

number of prey eaten per predator changes as a function of prey density” (Murdoch, 1969, p. 335). This is distinct from the *numerical* response, which Murdoch defines as “the way the number of predators changes” with respect to changes in prey densities (Murdoch, 1969, p. 336). Murdoch gave an early and impactful empirical investigation of functional responses by examining the lab-controlled feeding behavior of sea snails. Both when there was only a single prey species and when there were multiple prey species where the predator held a strong preference, Murdoch found evidence for Holling type II response (i.e. diminishing response to increases in density), likely reflective of predator satiation; however, Holling type II response fit the data for predators with weak preferences poorly in the presence of multiple prey and Murdoch found some evidence for Holling type III responses among switching predators.

Murdoch (Murdoch, 1969) also expanded upon the functional response model by considering it in a relative sense. In particular, he investigated the presence of “switching” behavior, a particular form of relative functional response. Murdoch defined switching as occurring when “the relative amount which ... [a prey] species forms ... [in a] predator’s diet increases disproportionately in comparison with the expected amount” given an increase in prey abundance (Murdoch, 1969, p. 337).

Interest in switching stemmed from its potential to offer a mechanism for population stability in addition to self-regulatory processes. That is, are observed stable population levels of various species the result of the species exhausting its prey, a self-limiting growth dynamic, or the adaptive response of its predators? Put in economic terms, are input costs rising with increased production, does production technology exhibit diminishing returns, or does increased production go disproportionately to intermediate uses? Focusing on the relative abundance of prey, Murdoch tested the null hypothesis of no switching defined by the relationship

$$p_1/p_2 = cN_1/N_2 \tag{3.1}$$

for two prey species (1 and 2) where p is the amount consumed, N the abundance, and c the relative preference. Elton and Greenwood (Elton & Greenwood, 1970) later generalized Murdoch's expression for switching to include a parameter for the 'degree of switching' between species instead of a fixed value of 1.

$$C_{ij} = C_{0,ij} \left(\frac{N_i}{N_j} \right)^{b-1}. \quad (3.2)$$

Here, C_{ij} is the consumption ratio of prey species i and j , C_0 the ratio at equal-density, N the population density of each prey species, and b the degree of switching parameter. I return to these expressions below in examining their relation to economic substitution.

Prey switching empirics & theory

While empirical field estimates of the degree of switching are available (e.g. Rindorf, Gislason, and Lewy (2006)), estimation strategies are complicated by the endogeneity of consumption and population levels. Elliott notes that prey switching "is difficult to demonstrate unambiguously in the field" (Elliott, 2004, p. 710). This difficulty may contribute to differences in field and laboratory estimates. Van Leeuwen, Jansen, and Bright (Van Leeuwen, Jansen, & Bright, 2007) summarize that field estimates are more likely to indicate Holling type II responses whereas laboratory estimates (e.g. Elliott (2004, 2006); Weale, Whitwell, Raison, Raymond, and Allen (2000)) are more likely to generate Holling type III responses. Last, Weale et al. (Weale et al., 2000) find that density-dependence is higher at lower overall densities, indicating that absolute abundance may also matter.

Certain factors are likely to limit the extent to which predators can respond to changes in prey densities. Predators may harbor strong preferences based on, for example, limits in their ability to assimilate a mixed diet, to perceive and identify

alternate prey, or to learn how to capture and handle them. Some of these limits may be genetic in origin. Predator phenotypes will influence how they are able to identify, attack, handle, and digest prey. For example, Agrawal (Agrawal, 2001) emphasizes the influence of phenotypic plasticity on species adaptation and evolution, particularly with respect to ecosystem patterns. Cognitive capacity may also limit the extent to which species can recognize beneficial tradeoffs (Bond, 2007; Dukas, 2002; Dukas & Kamil, 2001; Reader & Laland, 2003; Sol, Duncan, Blackburn, Cassey, & Lefebvre, 2005).

These factors will influence the relative consumption of species and the extent to which predators are able to make substitution in their prey consumption (input) choices. Limited capacity for substitution could lead predators to expend ever-higher energetic resources on securing an adequate amount of preferred prey whose increased scarcity drives search costs higher. This rigidity in preferences could lead to “counter-switching” behavior if securing a fixed amount of essential prey at higher cost crowds out the capacity to secure alternate prey. That is, counter-switching occurs when, in the presence of increased scarcity, a given prey comprises a *larger* share of the predator’s diet. For example, Kean-Howie et al. (Kean-Howie, Pearre, & Dickie, 1988) explain observed counter-switching among sticklebacks as a preference for preserving their alternative prey, zooplankton, which provide habitat for their larvae.

Relating economic concepts

Functional responses bear a direct relationship to economic demand curves. If I interpret prey-species’ abundance as the inverse of the species scarcity, or an economic “price,” I find a common demand curve shape as shown in Figure 3.2. That is, as scarcity rises consumption declines (nonlinearly) giving a common interpretation for both biological (Holling) functional response and economic demand. Note that, because of the abundance-scarcity inversion, this is both a rotation and a re-scaling

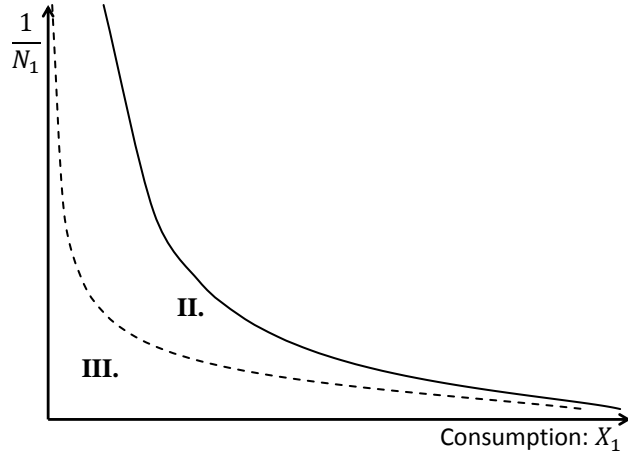


Figure 3.2: Inverse Holling functional response types

of the functional response graphs. Qualitatively, this gives type II and III functional responses that appear to exhibit the convexity properties one would require of a demand curve. The analytical reality here will depend on how one specifies the functional response.

Switching behavior also has a direct relation to an essential economic concept, substitution. To see this, I return to the null hypothesis of no switching tested by Murdoch, given by equation (3.1). If I again take inverse abundance as the “price,” $P_{x_1} = N_1^{-1}$, of the prey species, I can rewrite Murdoch’s equation (3.1) as

$$\frac{p_1}{p_2} = c \frac{N_1}{N_2} \quad \rightarrow \quad \frac{p_1}{p_2} = c \frac{P_{x_2}}{P_{x_1}} \quad (3.3a)$$

$$c = \frac{P_{x_1}/p_2}{P_{x_2}/p_1}, \quad (3.3b)$$

recalling that p_1 and p_2 are Murdoch’s diet shares. Economic substitution is measured by elasticities, which, in a relative consumption context, give the percentage change in relative consumption for a percentage change in relative prices. Calculating this derivative for Murdoch’s specification illustrates how his null hypothesis was

equivalent to a test of a unitary elasticity of substitution among prey.

$$\frac{P_{x_1}/P_{x_2}}{p_2/p_1} \frac{\partial(p_2/p_1)}{\partial(P_{x_1}/P_{x_2})} = c_c^1 = 1 . \quad (3.4)$$

Elton and Greenwood’s generalization from equation (3.2) makes explicit the elasticity parameter. In particular, taking the appropriate derivative reveals that the implied elasticity of their switching specification is $b - 1$. Given that b is the degree of switching, the direct relationship between switching and substitution is clear and I can exploit this link to parameterize the Biological General Equilibrium (BGE) model developed here. The parameterization can then rely on empirically-estimated degrees-of-switching (e.g. Elliott (2004); Van Leeuwen et al. (2007); Weale et al. (2000)).

Positive and negative switching discussed in the biology literature is akin to economic discussions of compensated elasticity of substitutions greater than and less than one, respectively. Murdoch’s elasticities are compensated because the snail species were observed in environments beyond their “saturation densities.” That is, for the switching experiments, Murdoch’s species were intentionally subjected to environments in which total abundance did not affect their overall consumption levels, meaning “income” effects were absent and Murdoch was measuring pure substitution.

On a more technical note, this fixed (compensated) “income” is somewhat different than that in the economic, Hicksian-demand sense of a compensated elasticity common to the dual-posing of CGE models. Rather than being an analytical abstraction as in economics, the fixed biological income here arises from the snails’ satiation. We might argue in this case that the satiation indicates that the marginal energetic benefit of consumption has fallen below the marginal cost of securing and digesting the prey.

3.2.2 Optimal bioenergetic output

Optimal foraging covers one half of the optimization scheme affected by competitive selection pressures. Once having optimally aggregated its prey into available resources for its disposal, an individual must optimally allocate those resources toward various ends that ensure the propagation of its genetic material. After satisfying activity and maintenance costs accrued within the period, individuals must allocate the surplus to one of three broad categories of stocks: structural biomass, reserve biomass, or offspring. In contrast with the foraging decisions and their attendant activity costs, biomass allocations bear on the future costs and benefits the individual will face. These differences make it helpful to further distinguish input and output dynamics by intra- and inter-temporal tradeoffs.

The primary unit of analysis for much of the literature on this topic is individual “energy budgets.” A vast literature has been populated under the heading “Dynamic Energy Budget Theory” (DEB), propagated by Kooijman and colleagues (cf. Kooijman (2000); Sousa, Domingos, Poggiale, and Kooijman (2010)). Others (e.g. Giacomini, Shuter, and Lester (2013); Quince, Abrams, Shuter, and Lester (2008)) have taken a similar tack, though not under the DEB heading. The DEB literature is broad and includes many aspects of foraging and much greater detail for individual energy budgeting than is considered in this work; however, its unit of analysis and essential method are consistent with the approach to inter-temporal allocation that a BGE model would take.

A common focal point for research on inter-temporal tradeoffs is the examination of why individuals’ growth might exhibit a maximum. The most common model to describe this behavior is given by a logistic expression credited to von Bertalanffy: $l_t = l_\infty(1 - e^{-k(t-t_0)})$, where l is a size parameter, l_∞ maximum size, t the time period, and k the growth rate. As Kozłowski and Teriokhin summarize (Kozłowski &

Teriokhin, 1999, p.424), Roff (Roff, 1983) suggested early that growth may be limited by reproductive demands later in life and, by introducing a seasonal environment (Kozłowski & Uchmański, 1987), finds that *indeterminate* growth is actually optimal, though outcomes still resemble the von Bertalanffy logistic model. These authors (Kozłowski & Teriokhin, 1999) propose a model in which species attempt to maximize their reproductive success.

$$R = \int_0^T u(t)f(w(t))L(t) dt \quad (3.5a)$$

$$w_t = [1 - u(t)]f(w(t)), \quad (3.5b)$$

where T is the maximal lifespan, $u(t)$ the optimal share of energy devoted to reproduction, $f(w(t))$ the energy produced from biomass $w(t)$, and $L(t)$ gives survivorship. The solution is given by the reproductive allocation, $u(t)$, that maximizes R , found by the Pontryagin Maximum Principle. Optimal switching between growth and reproduction in a seasonal environment exhibits a ‘saw-tooth’ pattern. This gives a more dynamic picture of the growth-reproduction tradeoff than was found earlier in aseasonal environments by Ziólko and Kozłowski (Ziólko & Kozłowski, 1983) and by Perrin, Sibly, and Nichols (Perrin, Sibly, & Nichols, 1993).

Expanding on earlier work, particularly Abrams and Ludwig (Abrams & Ludwig, 1995; Kirkwood, 1981), Teriokhin (Teriokhin, 1998) took a broader approach to this problem by allowing individuals to moderate their current and future mortality by the amount of energy they invest in survival and repair, respectively. In maximizing the reproductive rate, allocations are prioritized by reproduction, current survival, and then future survival.

Similar dynamic programming models have been used to interact reproductive strategies with prey size and size-number tradeoffs among offspring (Thygesen, Farnsworth,

Andersen, & Beyer, 2005). Semelparity and iteroparity have also been derived as optimal strategies in the presence of stochastic mortality (risk) following alternate optimization methods (Katsukawa, Katsukawa, & Matsuda, 2002). As part of a broader model seeking to explain foraging behavior, Giacomini, Shuter, and Lester (Giacomini et al., 2013) build from density- and size-dependent predation with activity costs to predict the optimal age at which a fish ceases growth. This latter decision determines the size spectrum and is determined in part by growth-reproduction tradeoffs.

Recent work by Ejsmond et al. (Ejsmond, Czarnoleski, Kapustka, & Kozłowski, 2010) expanded on the dynamic programming method interacting seasonal variability with offspring life-prospects to show wider variation in optimal breeding strategies. Here the authors discuss, but do not analyze, the role of “capital breeding” strategies (as opposed to “income breeding”), where individuals accumulate an energetic reserve (storage) before breeding. This introduces the second allocation problem: once having allocated energetic surplus across own-biomass and offspring, an individual must allocate within own-biomass to structure and storage.⁴

Giacomini and Shuter (Giacomini & Shuter, 2013) provide a nice synthesis of theory and empirics on the structure-storage tradeoff. Considering a seasonal bioenergetic model, they focus on the timing of structure and storage allocations finding that a dichotomous, “structure-first” allocation strategy is optimal in a wide cast of environments. Critically, the authors note that, of the previous life-history optimization models they reviewed, none has “explicitly included a detailed representation of the annual pattern of energy surplus and deficit that defines the seasonal growth pattern, and the constraints it imposes on growth and life history” (Giacomini & Shuter,

⁴In the biology literature reserves are the capital in capital breeding; however, both structure and reserve constitute capital in an economic sense. Much has been made of a similar distinction in the economics literature, particularly following the energy crises of the 1970s. In that case, reserve capital is called “putty capital” in that it is still malleable (or allocable), structural or installed capital is called “clay capital” reflecting the more fixed nature of its future costs and benefits (Phelps, 1963).

2013, p. 2). Giacomini and Shuter therefore make a novel and valuable contribution to structure–storage optimization and its implications for growth–reproduction trade-offs. Their work is also valuable in that it models an explicit temperature–dependence of the bioenergetic dynamics, an essential component for BGE applications involving climate forcing such as climate change or El Niño events.

3.2.3 Ecosystem dynamics

Though input and output dynamics are commonly considered in isolation by ecosystem models, the obvious next step of integrating their components into a coherent model of a system of species has been largely neglected or underdeveloped. Many ecosystem models take phenomenological approaches that do not explicitly consider the micro-dynamics of the ecosystem participants (e.g. (Stouffer, Camacho, Guimera, Ng, & Amaral, 2005)). Stouffer provides a helpful comparative assessment of phenomenological and population-level models (Stouffer, 2010). Here I consider two distinct types of approaches, each with an example. First, I examine the properties of the Ecosim fisheries population model. Of models taking approaches common to the biology literature, Ecosim is perhaps the most similar to the current work. Still, this model has critical limitations in its ability to represent the general outcomes of multi-species adaptation and interaction. As an example of modeling approaches common to the biology literature, it highlights how these approaches tend to be more static and low-order parametric than is desired here.

The second subsection details the closest example overall to the Biological General Equilibrium (BGE) approach developed here, the General Equilibrium Ecosystem Model (GEEM) of Tschirhart and collaborators (Finnoff & Tschirhart, 2003; J. T. Tschirhart, 2000, 2004). This model takes a micro-founded bioenergetic approach to drive system dynamics. Species abundances depend on their ability to secure energy over and above their metabolic requirements and demands by their

predators. GEEM’s strengths and weaknesses are covered within the second subsection.

Biology approaches & the Ecosim model

Multi-species ecosystem models attempt to capture the interaction of the populations of various species in a given ecosystem. These models tend to be highly parametric, most often relying on exogenous behavioral rules for functional responses (e.g. (Berryman, Michalski, Gutierrez, & Arditi, 1995; Drossel, 2001; Křivan & Diehl, 2005)). For example, a common approach to modeling predator–prey interactions is the generalized logistic response given by Berryman et al. (Berryman et al., 1995), who give the growth rate from the model for an arbitrary species i as

$$R_i = a_i - b_i X_i - \frac{X_i}{\sum_j c_{ji} X_j F_j^{r(i)}} - \frac{\sum_k d_{ik} X_k F_k^{c(i)}}{X_i}, \quad (3.6)$$

where $F_j^{r(i)}$ denotes the fraction of population j used as a resource by i , $F_k^{r(i)}$ is the fraction of population k that consumes i , X ’s are populations, b_i a coefficient of intra-specific competition, c_{ji} the impact of a lower-trophic species j on the growth rate of species i , and d_{ik} the impact of species i on the growth rate of species k (in a lower trophic level). In this example, species are required to maintain a diet “menu” in fixed proportions, which eliminates the possibility for adaptive substitutions by the model species. Markov chains of consumption probabilities are also a common, less parametric alternative (cf. Bélisle and Cresswell (1997); van Leeuwen, Brännström, Jansen, Dieckmann, and Rossberg (2013)), though they are an atheoretical approach.

The “Ecosim” model is a prominent example of a comprehensive input-output-style ecosystem model. As such, this model is worth exploring in detail as a point of contrast with the BGE model constructed here. Ecosim is an empirically-based model used for fisheries designed to accommodate field survey data that are mass-

balanced by the companion “Ecopath” utility. As Walters et al. summarize, “Ecopath provides a way to organize baseline . . . observations on abundances and trophic flows (feeding rates, diet compositions, and growth efficiencies) into an initial, static picture of ecosystem state” (Walters, Pauly, Christensen, & Kitchell, 2000, p. 71). This is an analogous task to the construction of a “social accounting matrix” in economic general equilibrium models.

The Ecopath mass-balancing routine is run on empirical data prior to calibrating the Ecosim model. Input data are minimally-revised by the Ecopath routine to satisfy the system of mass-balance equations (Christensen & Walters, 2004; Kavanagh, Newlands, Christensen, & Pauly, 2004)

$$P_i = Y_i + E_i + BA_i + M0_i \times B_i + M2_i \times B_i, \quad (3.7)$$

where Y_i gives harvesting, E_i net migration, BA_i biomass accumulation rate, B_i the biomass, $M0_i$ the catch-all ‘other mortality’ rate, and $M2_i$ the instantaneous predation rate. Empirical data can be balanced manually or through the automated Ecopath routine (outlined by Kavanagh et al. (Kavanagh et al., 2004)).

Fixing diet shares affords Ecosim the beneficial trade-off of not having to assume a steady-state observed within the data. Since, heuristically, a behaviorally dynamic model admits a degree of freedom in diet selection, one must then impose the identifying assumption that the behavior observed within the data is an optimum, implying the system has reached a steady-state, in order to complete the calibration. (Section 3.4 will make explicit how the BGE model is calibrated to empirical data.)

In general, input-output system modeling proceeds from a balanced snapshot of the system to a dynamic picture of system behavior by asserting certain behavioral rules or forms for the ecosystem’s participants. The behavior posed must be consistent with the observed snapshot and should be able to “carry” the system forward to

future states. Ecosim describes species' consumption behavior by a Lotka-Volterra framework modified for spatial heterogeneity

$$C_{ij} = a_{ij}B_iB_j \quad (\text{L-V}), \quad (3.8a)$$

$$C_{ij} = a_{ij}B_iB_j \frac{v_{ij}}{v_{ij}+v'_{ij}+a_{ij}B_j} \quad (\text{Ecosim}). \quad (3.8b)$$

Equation (3.8a) gives the traditional Lotka-Volterra model specified in an effective search parameter of predator j for prey i , a_{ij} , and B_i and B_j give biomasses. The Ecosim version (3.8b) modifies the Lotka-Volterra model with parameters giving the rate at which prey i is making itself vulnerable to predator j , v_{ij} , and the rate at which it is making itself invulnerable, v'_{ij} . These rates are equal by default and the entire fraction used to modify the Lotka-Volterra expression effectively reduces the prey population, B_i , in proportion to prey invulnerability. Maximum consumption rates, C_{ij}^{max} are hypothesized by the Ecosim user to estimate the v_{ij} parameter.

Ecosim then poses biomass dynamics with a time derivative of species biomass that parallels the mass-balance equation (3.7) (Kavanagh et al., 2004, eqn. 2)

$$\frac{\partial B_i}{\partial t} = g_i \sum_j C_{ji} - \sum_j C_{ij} + I_i - (M_i + F_i + e_i)B_i, \quad (3.9)$$

where g_i gives species i 's net growth efficiency, $I_i - e_i$ gives net migration, M_i gives other mortality, and F_i harvesting. Ecosim then posits a delay difference model for each species to describe the relation between juveniles and adults. The model is specified in predation risk, biomass, population, body weight, and juvenile-specific growth rates. The specification is based on the Ford-Brody growth model and the "Deriso-Schnute equations for biomass and numbers dynamics" (Kavanagh et al., 2004, p. 73).

The most prominent frailty in this structure is that the specified rates are not the result of (meta-) individual decisions. The model is driven by fixed rules that

parameterize both zeroth and first order behavior. This phenomenological approach does not allow adaptive substitution and generally obscures relevant micro-dynamics, thereby missing how they drive macro-level outcomes. The bioeconomic approach taken by Tschirhart and co-authors, summarized in the next section, helps address these shortcomings.

Bioeconomic approaches – GEEM

Tschirhart has built and employed a “General Equilibrium Ecosystem Model” (GEEM) whose departure from traditional ecosystem models and similarity with the BGE model constructed here warrants detailed treatment. Noting the consistency of this approach with economic general equilibrium models (or *applied* general equilibrium (AGE) models), Tschirhart argues:

[w]hat is needed is to link AGE models of economies with general equilibrium models of ecosystems so that the critical interactions of the two systems are accounted for when developing policies. The first step in such a linkage is to develop a general equilibrium ecosystem model that is both biologically sound and flexible enough to be combined with its economic counterpart. (J. T. Tschirhart, 2000, p. 15)

Toward that end, Tschirhart proposed an energy-budget approach to modeling species interactions, casting the model in a market framing where each species is a net energy surplus maximizer.

In Tschirhart’s 2000 GEEM (J. T. Tschirhart, 2000), species are rank-ordered by trophic hierarchy and not allowed to forage “up” the food chain. Each species is specified with a net energy function in mass quantities (except in the case of solar gain) and corresponding net energy gains (i.e. energy density of prey less cost to secure prey) for each consumed prey, net energy losses when other species prey on it,

and energy losses from activity and rest. Specifically,

$$R_i = [e_0 - e_{i0}]x_{i0} + \sum_{j=1}^{i-1} [e_j - e_{ij}]x_{ij} - \sum_{k=i+1}^m e_i y_{ik} - f^i \left(\sum_{j=0}^{i-1} x_{ij} \right) - \beta_i. \quad (3.10)$$

Biomass supply and demand functions are derived through energy profit maximization. Populations are then updated such that energy profits are driven to zero via a modified Verhulst-Pearl model. Energy is implied conserved in equilibrium. Tschirhart then applies the model to modified data from an Aleutian ecosystem with four trophic levels and six stylized species yielding numerical results that exhibit stable oscillatory behavior.

Tschirhart later (2004) expanded this model (J. T. Tschirhart, 2004), including additional background on economic general equilibrium theory, and additional text dedicated to examining many of the common outcomes analyzed in the biology literature (e.g. functional and numerical responses, switching). With respect to the model, Tschirhart reduces it to fewer species and changes the treatment of population updates from an explicitly modified Verhulst-Pearl to a similar form based on energy profits and fixed natality and mortality rates. In particular, GEEM's latter population update equation modifies the steady-state population growth rate, equal to the death rate (inverse of lifespan), by the amount of actual energetic surplus relative to that required for steady-state. When actual surpluses fall short of (exceed) steady-state levels, the population declines (grows). GEEM's population update equation then takes the form (cf. (Finnoff & Tschirhart, 2005, eqn. 9))

$$N_i^{t+1} - N_i^t = N_i^t \frac{1}{s_i} \left[\frac{\hat{R}_i + r_i}{r_i^{ss}} - 1 \right], \quad (3.11)$$

where the N_i 's represent the population levels of species i at times t and $t + 1$, s_i is the lifespan, \hat{R}_i is the current-period bioenergetic profit, and r_i and r_i^{ss} are the actual and steady-state variable respiration costs, respectively. When bioenergetic profits,

\hat{R}_i , equal zero r_i and r_i^{ss} are equal, implying no population change.

Last, novel to the 2004 GEEM simulation (J. T. Tschirhart, 2004), Tschirhart applies shocks to a model of the Bering Sea ecosystem, showing that 20% shocks to predator and prey species (in opposite directions) takes approximately twenty years to equilibrate with the majority of convergence happening within the first ten years. Tschirhart suggests that future research take on abiotic resources, age structure, and spatial heterogeneity.

Strengths of GEEM

Tschirhart (and colleagues (Eichner & Pethig, 2006; Finnoff & Tschirhart, 2003; J. T. Tschirhart & Pethig, 2001)) excepted, a wide gulf in the biological literature remains between the bioenergetic optimization employed in solving individual problems and the more phenomenological and behaviorally static approaches taken by many ecosystem models. Tschirhart's work is pioneering in this way and it is evident from reading the ecosystem modeling literature that such an approach is desired (if not readily recognized). For example,

[T]here are precious few advances towards truly synthesizing the connections between individuals, populations and large interconnected food webs (A. Beckerman et al., 2010, p. 1).

[T]here is still no comprehensive theory ... showing that activity [costs] could be a limiting factor for predator populations (Giacomini et al., 2013, p. 250).

GEEM exploits the rich bioenergetic optimization principles underpinning optimal foraging (cf. Stephens and Krebs (1986)) and dynamic energy budget (cf. Kooijman (2000)) theories to drive macro-outcomes. Beckerman et al. recently emphasized the importance of this linkage noting that, as “the central theory linking resource and

consumer traits to patterns of resource selection,” optimal foraging “form[s] the interface between selection pressures and population dynamics,” thereby holding a critical position in advancing “food web biology . . . as a new focal point for understanding the interplay between adaptive behaviour [sic], population dynamics and the complexity and structure of ecosystems” (A. Beckerman et al., 2010, p. 1). This is precisely the campaign of the GEEM and BGE approaches.

GEEM then offers a critical departure from traditional ecosystem models in tracing individual behavior to general system outcomes. Grounding a model like GEEM’s dynamics in physically-constrained individual behavior enables a deeper articulation of its theoretical basis. For example, at the individual level one can posit (and verify experimentally) the extent to which species members alter their inputs in the face of changing environments, or the metabolic relationships among inputs and outputs. In contrast, many contemporary ecosystem models miss this opportunity by specifying overly static diet or inter-specific competition rules, or even largely abandoning a theoretical approach in Markov chain diet selection models (Murdoch & Oaten, 1975; van Leeuwen et al., 2013).

Species adaptation is an essential component of ecosystem dynamics. Too often ecosystem modeling has been unable to capture adaptation in a rich and useful way, whether as a result of the phenomenological approach taken or coarse behavioral rules employed. Recognizing the combination of the inherent energy budget constraint and selection pressures exerted on species naturally leads one, as in optimal foraging, to identify the optimum toward which species are being competed. The method of GEEM is to identify, given a set of marginal energy costs that obtain in an environment, toward what optimal allocation of resources selection pressures will drive the ecosystem. Common properties of interest such as population levels then emerge from the optimization framework instead of being a near consequence of the model

parameterization (e.g. in carrying capacities).

Though GEEM is posed with a rather limited number of species, it is done such that additional species richness can be incorporated. The power of GEEM, and the ideal power of any ecosystem model, is that it be sufficiently general that it can be adapted to a wide cast of settings. Basing the model structure on physical principles of energy and mass conservation furthers this generalizability. GEEM is also general in the sense of the equilibrium solutions it identifies. They are quite simply all optimal outcomes that obey basic conservation principles given the prevailing conditions in the ecosystem. One challenge to such a parsimonious definition is that it can admit multiple equilibria. Yet, amongst a variety of limitations, the generality of equilibria is the most potent advantage of general equilibrium models in that it allows for rich, and often counterintuitive, interactions. As quoted by Tschirhart (J. T. Tschirhart, 2000, p. 17), Ken Arrow provided a rather pithy explanation of this potency.

Whatever the source of the (economic equilibrium) concept, the notion that through the workings of an entire system effects may be very different from, and even opposed to, intentions is surely the most important intellectual contribution that economic thought has made to the general understanding of social process (Arrow, 1968, p. 376)

Indeed, in GEEM, and in the BGE model constructed here, the campaign for a general equilibrium representation is premised on the notion that there is nothing uniquely “social” about the law of unintended consequences.

Critiques of GEEM

Tschirhart’s optimization is done for a linear profit function in fixed marginal benefits and varied marginal costs (the equilibrium price). This means that substitution is unconstrained for predators (Beckerman et al.’s diet breadth model is similarly limited

(A. P. Beckerman, Petchey, & Warren, 2006)), which has not likely posed problems for Tschirhart’s empirical investigation due to the extremely narrow diet breadths and small systems evaluated. Moreover, the range of prey is artificially constrained by food chain order where it could be determined empirically from input-output data. Though foraging “up” the food chain was not likely prevalent in the Aleutian ecosystem examined, it often occurs where lower-trophic adults feed on higher-trophic juveniles. This may require distinguishing adults and juveniles and possibly specifying a sub-model of stock recruitment (similar to Ecosim).

Tschirhart notes that “[i]n an economy, consumers or firms typically pay the same price to other firms for the latter’s goods, but in an ecosystem organisms from different predator species pay different energy prices to capture biomass from a prey species” (J. T. Tschirhart, 2000, p. 16). This apparent foil led Tschirhart to pose his equilibrium in a multiplicity of prices, which were not constrained by the fact that they were driven in part by common scarcity costs for prey. This under-determined price structure also obscures how prices, through GEEM’s profit function, likely imply the functional responses observed numerically in later work (J. T. Tschirhart, 2004).

Second, the economic ‘law of one price’ for “consumers or firms” ought not be taken strictly. While there is often, though certainly not always, a common core explicit cost to market transactions, market participants also incur a variety of heterogeneous non-market costs. For example, economic search costs can vary by consumers’ location or familiarity with the market and product. Economic models typically either average away or incorporate this heterogeneity into preferences by altering the marginal benefit of the good. Differences in expenditure can be accounted by introducing fixed predator-specific “taxes” or modifying marginal benefits in calibrating a bioenergetic production function. This enables one to maintain a common, systemic (or market), scarcity-based cost to foraging while still incorporating heterogeneous responses to

that scarcity.

In some instances GEEM poses lower-order parameterization where other techniques are available. For example, marginal energy benefits to consumption are fixed. One of the major strengths of general equilibrium methods is that their parameterization is generally restricted to second-order behavior; i.e., substitution elasticities. First-order behavior is implied by the optimization and calibrated from empirical observation (assuming one observes a steady-state). Zeroth-order behavior, or level outcomes, are emergent but generally constrained by the zeroth-order initial conditions; i.e., the fixed quantities of initial resources (also empirical).⁵ One of the great shortcomings of many biological models is their zeroth-order *parameterization*; e.g. through carrying capacities. In a move toward general equilibrium then, Tschirhart's first-order parameterization does not capture the full benefit of a general equilibrium structure.

Though numerical simulations based on empirical ecosystem data are given for GEEM, the model could better capitalize on the information within the ecosystem empirics. Specifically, general equilibrium models exploit the assumption of an observed steady state in the input-output data to calibrate the model. Particularly for fisheries, both stomach content (input) and population level (output) data are available, in some cases with time-series. For example, a variety of data used for empirically-based fisheries modeling conducted with the Ecopath with Ecosim software are maintained on the Ecopath website.⁶ Mass-balanced data such as these are the target to which the Biological General Equilibrium (BGE) model developed here tunes its specification. This approach is also available with the data on the Aleutian

⁵In an economic setting these quantities classically include labor and capital stocks. In an ecosystem, these correspond to biomasses, light, and nutrient quantities available to the system at the start of the period. In the abstract, these are simply the system's initial conditions that will be updated to next period's stocks by the specified first-order differential equations.

⁶See www.ecopath.org.

ecosystem Tschirhart compiled for GEEM (Finnoff & Tschirhart, 2003) as will be shown in the calibration and application of the BGE model.

Tschirhart finds a conflicting analogue in the patterns of value flows within economies and ecosystem. In particular, he contrasts that “in a marketplace trade, material and money flow in opposite directions, but in an ecosystem trade, biomass and energy flow in the same direction” (J. T. Tschirhart, 2000, p. 16). It is crucial that, in adapting the tools of one discipline to the context of another, these conceptual differences are highlighted and examined.

First, biomass and energy are metrics for evaluating both the benefits and the costs of consuming prey. Species face costs of expended energy and ultimately mass (wastes) to secure the benefits of mass and energy their prey offer. So, while mass and energy benefits flow from predator to prey, mass and energy exertion costs also flow from predator to the environment. A key difference here, and perhaps the true crux of the issue Tschirhart raises, is that the expenditures accrue to the environment instead of the prey who supply them (as in an economic setting). This does raise certain challenges, but careful accounting can resolve this issue.

Second, a bidirectional flow of value is a prevalent feature of the marginal cost-benefit tradeoffs that drive economic reasoning, but it is not the only type of flow. Depreciation and technological inefficiencies are both examples of unidirectional flows in economics. Just as with an ecosystem’s prey, these kinds of unidirectional costs mean that system participants must give up some of their product without receiving anything in return. There may not exist any “free lunches,” but ‘free costs’ abound.

In sum, the essential concern here is not the direction of the flows, but the completeness of the accounting system. Provided all flows, whether neatly bi-directional among two parties, multi-directional among several, or truly unidirectional (costs), are accounted, the zeroth-order requirements of the input-output modeling structure

will function as intended. Also, provided mass or energetic benefits come at some cost to system participants, the first-order conditions of the input-output modeling structure will also function as intended.

To ensure the latter, marginal costs must eventually match or outstrip marginal benefits. This can happen by diminishing benefits, rising costs, or some combination of the two. It does not matter to whom the costs are paid, only that there are no “free lunches” and all flows are accounted. The aforementioned differences between economies and ecosystems do not preclude a model with economic reasoning, but they do require modified structure and interpretations.

Other bioeconomic approaches

Hannon offered an early adaptation of input-output accounting and modeling techniques to an ecosystem application (Hannon, 1985, 1986). Input-output modeling is a predecessor to general equilibrium modeling in economics. While both share a common accounting structure, general equilibrium modeling goes further to specify the adaptive optimizing behavior of the system participants with the critical addition of endogenous “prices” driven by competition and resource scarcity. The lack of adaptive behavior and endogenously-imposed resource constraints is a critical limitation of input-output approaches. Indeed, the inherently static behavior of the input-output approach requires that Hannon make “a myriad of assumptions to successfully constrain the results to the reasonable and stable equilibria” (Hannon, 1985, p. 99), which he develops further in later work (Hannon, 1986).

The adaptive behavior of the general equilibrium approach dampens the propagation of shocks, reducing the tendency toward instability and chaos, and offers a parsimonious set of parameters by which one can fine-tune the system’s dynamical behavior to biologically “reasonable” outcomes. Although Hannon discusses certain resource scarcity considerations, the input-output approach cannot endogenously al-

locate system resources in response to the adaptive, competitive behavior of system participants. Last, Hannon’s work offers much text relating economic analogies to ecosystem dynamics. While Hannon is one of the few to have extended these analogies to the development of analytical tools, there is no shortage of literature offering qualitative explorations of ecologic-economic analogies (cf. Ruth (1993)) that I do not cover.

Mullon, Shin, and Curry (Mullon, Shin, & Cury, 2009) outline a Network Economics Approach to Trophic Systems (NEATS) that operates on a marginal cost-benefit assessment for trophic exchanges. Their model expresses linear predation costs complementary to trophic exchange quantities. The overall system is a linear program that solves for a feasible equilibrium given first-order parameters such as fixed assimilation efficiency (γ_i), other losses (μ_i), predation costs (κ_i), and inter-specific competition costs (λ_i). The linear program solves for steady-state population levels; i.e., it does not allow for steady-state growth as an equilibrium outcome.

The NEATS model draws in part on Network Economics work by Nagurney (Nagurney, 1998) who has also recently applied Network Economics to modeling ecosystem dynamics (Nagurney & Nagurney, 2011) as a “spatial price equilibrium.” This work provides a formalization to the basic approach taken by Mullon et al. (Mullon et al., 2009); i.e., it develops a linear program with first-order parameterization of efficiencies and marginal costs.

Summary

Beckerman and Petchey recently lamented that “there are precious few advances towards truly synthesizing the connections between individuals, populations and large interconnected food webs” (A. Beckerman et al., 2010, p. 1). Much attention has been paid to the role of adaptive behavior in driving food web complexity, stability, and topology (Abrams, 2010; Křivan & Schmitz, 2003; Kondoh, 2003; Piltzko, Drossel, &

Guill, 2012; Van Leeuwen et al., 2007; van Baalen, Křivan, van Rijn, & Sabelis, 2001), and some have offered valuable first steps toward integrating micro-founded bioenergetic dynamics in population dynamic models (Brose, 2010; Diekmann & Metz, 2010; Eichner & Pethig, 2006; Garcia-Domingo & Saldaña, 2007; J. T. Tschirhart, 2000), but a general, bioenergetic approach to the role of adaptive behavior in population dynamics does not appear to have been established.

The bioenergetic, “bottom-up” approach to macro dynamics seems to enjoy nearly exclusive attention from economists (e.g. Tschirhart (J. Tschirhart, 2009; J. T. Tschirhart, 2004), Pethig (Eichner & Pethig, 2006; J. T. Tschirhart & Pethig, 2001), Finnoff (Finnoff & Tschirhart, 2003, 2008), Nagurney (Nagurney & Nagurney, 2011)). Micro-macro integration is, after all, an eminent and long-studied issue in economics. Yet these approaches still take a linear, low-order parametric approach that begs extension given the general equilibrium tools available from economics. The research attention in economics to general equilibrium modeling has yielded a robust tool set for modeling macro-outcomes from micro-founded behavioral forms in economics. It offers an obvious template for constructing such a model in a biological setting. Doing so will require abstracting just the basic structure of the economic general equilibrium framework so as to accommodate the biological dynamics I want to represent.

3.3 Biological General Equilibrium Model

3.3.1 Overview

A micro-founded approach to ecosystem modeling posits behavioral forms to generate activity within the system. For example, for each type of predator in the system, a micro-founded model will provide a *behavioral function* that identifies how much of each prey it will consume if competed to an optimum. In the BGE model, and in optimal foraging, these decisions are determined by an adaptive trade-off of costs and

benefits associated with various prey. Behavioral functions alone do not constitute a model. First, behavior describes activity within the period relative to the state of the system at the beginning of the period. For this reason, the system must be initialized with certain data such as population levels. That is, the model requires *initial conditions*. The behavioral forms update the initial conditions to new system conditions, but modifications that produce physically impossible states must be excluded. In particular, the behavior of the system participants will modify the initial conditions in a manner consistent with mass and energy conservation. Imposing these *system conditions* requires that I enforce a complete accounting of the mass and energy flows within and across the boundaries of the system. In addition to the behavioral forms, which describe the flows within the system and within the period, I must also specify functional forms to describe mass and energy flows across the system boundaries, spatial and temporal, to give *boundary conditions*.

To summarize, a micro-founded model posits individual *behavioral functions* for species behavior that carry the ecosystem forward from particular *initial conditions* to new states where, given certain *boundary conditions* describing flows in and out of the system, energy and mass are conserved to satisfy *system conditions*. Optimal behavior consistent with all three conditions constitutes a steady-state equilibrium of the system. The modeling section will describe each of these model components in detail. An input-output data structure will aid the accounting and intuition with respect to conserving mass and energy. First, I offer additional qualitative description of each component, relating it to the existing modeling literature.

Behavioral Function

The behavioral forms of the model are perhaps the most complex because they must be derived from an optimization process. The most basic aspect of behavior I would like to represent is how species select their prey. To do so, I describe what benefit con-

suming these prey inputs generates. In the BGE model, the assimilation of consumed prey generates a certain quantity of available energy for the predator. The benefit of this available energy is that the predator can use it to support the propagation of its genetic material. I first specify a function that will map prey inputs to bioenergetic output for a given predator.

Benefits

To represent consumption benefits I pose a constant elasticity of substitution (CES) bioenergetic “production function” calibrated on empirical observation and parameterized by empirical estimates of substitution possibilities (percent-for-percent changes in inputs yielding equivalent output). This function, common in economics, is a generalization of the log-linear, “power-law switching” functions common to the biology literature. A “nesting” feature of this function permits differentiating substitution across multiple prey, something absent from the power-law switching literature in theoretical biology.⁷ The functional response and switching literatures have made substantive progress in understanding species adaptive capacities and limitations in prey selection. This work can inform the CES function’s specification in the BGE model applications. An essential feature of the CES function is its many-to-one mapping of bundles of prey inputs to bioenergetic output. The ability of the predator to generate the same level of bioenergetic benefit from a variety of combinations of inputs is what affords it the luxury of substitution. This substitution is motivated by the relative costs and benefits of the prey inputs.

⁷Van Leeuwen et al. note recently that power-law models introduce “an inconsistency” with multiple species in that, “if one chooses three prey species A, B and C such that the exponents for switching between A/B and between B/C are identical, then it follows that the predator will always switch between A/C with exactly the same exponent” (van Leeuwen et al., 2013, p. 90). This has a straightforward remedy in a CES function, which was originally posed by Arrow et al. (Arrow, Chenery, Minhas, & Solow, 1961). In particular, given the later generalization by Sato (Sato, 1967) of the initial CES function to a “nested form,” one simply nests A and C together to admit differential switching behavior. This will be covered in detail further below.

Costs

The search, handling, and digestive costs associated with a given prey will depend on predator traits and behavior. So while all predators search costs are driven by the same observed scarcity for a given prey within the system, the effective cost of acquiring that prey will differ by predator. These differences can be modeled in two ways: either in the (CES) benefit or (linear) cost function. Marginal benefits of prey differ across predators depending on the specification of the benefit function. One can also assign predator-specific “taxes” that modify predators’ perceived prey abundance. Foraging costs then play a clear and prominent role in driving predator-prey dynamics in an energy budget framing. Remarkably, Giacomini et al. note in recent work that “there is still no comprehensive theory . . . showing that activity [costs] could be a limiting factor for predator populations” (Giacomini et al., 2013, p. 250). In the BGE model, competitive selection pressures drive predators to maximize the energetic benefits gained, modeled by the CES function, for a given level of prey acquisition costs.⁸ Solving this optimization gives the functional forms needed to generate species behavior as a function of model variables, in particular, marginal costs and output levels.

Specification

A nested CES function gives both analytical tractability and mutual consistency of multi-prey functional responses, properties highlighted recently by van Leeuwen et al. (van Leeuwen et al., 2013). Where prices are taken as scaling with inverse population densities, the switching parameter of the foraging literature is simply the economist’s elasticity of substitution, which parameterizes the CES function. Further,

⁸By the duality of the optimization problem, one can equivalently minimize the acquisition costs for a given level of bioenergetic benefit. In fact, this is the preferred approach in CGE modeling.

van Leeuwen et al. (van Leeuwen et al., 2013) summarize surveys of such estimates (Elliott, 2004, 2006; Greenwood & Elton, 1979) citing values in the range 0.4 – 2.0, which are well within the norm of economic elasticity values and in accord with an upper bound of 2 derived from van Leeuwen et al.’s model (van Leeuwen et al., 2013, p. 97).

For the BGE model, I will argue that marginal handling and digestive costs for a given prey can be taken as fixed and predator-specific, but search costs will vary depending on prey scarcity and not depend on the predator. (Marginal benefits will be declining in total consumption, which could be interpreted as rising digestive costs.) Total foraging costs are then a function of fixed, predator-specific attributes and variable, system-wide scarcities.

Initial Conditions

The ecosystem starts each period with species population and resource quantities on which the intra-period activity depends. While the intra-period activity can generate a variety of production and consumption outcomes, nothing can be done within the period to change the value of these initial quantities. The initial conditions are the result of past “decisions” and processes exogenous to the ecosystem. Modeled species must compete for resources such as light and basic nutrients as they do for other prey. Again, the distinction here is that no intra-period dynamics will change the supply of these resources to the species. This does not mean that the quantity of initial resources actually consumed must be fixed. For example, in the case of light and nutrients, primary producers will not utilize the entire quantity available to them (in fact the vast majority will go unassimilated), rather they will use quantities up to the point where the marginal benefit falls to meet the marginal cost of securing the benefits.

By contrast, modeled species may be more or less abundant depending on the

system's prevailing scarcities and level of competition within the period. Species' starting biomasses are assumed, as an analytical abstraction, to be entirely assimilated via their species' bioenergetic production function. As a result, there is no competition for a species' own starting biomass, though maintenance costs do obtain and its scarcity does imply an opportunity cost. Including starting biomasses in the bioenergetic production function limits the amount of growth the species can undergo within the period. Since the starting biomass is fixed, marginal additions of other inputs represent substitution away from the standard consumption-to-biomass ratio. Additions beyond common ratios will face diminishing returns, which must exceed the marginal costs of securing the additional inputs (prey).

Boundary Conditions

There are two types of boundary conditions, spatial and temporal. Spatial boundary conditions describe the quantities of mass and/or energy leaving the system within the period. These include wastes, migration, and energy expenditures not mass-embodied (e.g. costs associated with thermal regulation or exertion). Temporal boundary conditions describe mass and energy quantities being carried forward to the next period within the system, or leaving this period's system for next period's. A full expression of the inter-temporal dynamics would allocate total ending biomasses to structure and storage as well as progeny. These quantities comprise the sum of genetic material the species will propagate to the future to further its survival objective.

System Conditions

Finally, I must require that the outcomes generated by the behavior are physically realistic. The model is constructed with an input-output structure, which enables the natural requirement that mass and energy inputs equal outputs. I then require a complete accounting system that will identify all mass and energy inputs and how

their transformed outputs are allocated within and across the boundaries of the system. Behavioral functions track flows within the system, the initial conditions track flows across the temporal boundary (past-to-present), and boundary conditions track flows across the spatial and temporal (present-to-future) boundaries.

Next, I explore how these components come together to form a biological general equilibrium model. Prior to giving the general mathematical expression of the model, the following section outlines a stylized BGE model to demonstrate how these pieces are assembled into an internally consistent model and to motivate the accounting with additional examples.

3.3.2 Stylized Model Example

Figure 3·3 gives a sample set of accounting matrices for a stylized marine ecosystem. Six species are modeled in this system: primary producers (PP), zooplankton (ZP), benthic organisms (BO), small fish (SF), big fish (BF), and marine mammals (MM). Primary resources of light (L) and nutrients (N) are given as part of the initial conditions for the system along with starting biomasses (SB). Boundary conditions are summarized by respiration (R), metabolism (M), harvesting (H), and ending biomass (EB).

	PP	ZP	BO	SF	BF	MM	R	M	H	EB
PP		x	x	x			x	x		x
ZP		x	x	x			x	x		x
BO			x	x	x	x	x	x	x	x
SF				x	x	x	x	x	x	x
BF					x	x	x	x	x	x
MM						x	x	x		x
L	x									
N	x									
SB	x	x	x	x	x	x				

Figure 3·3: Stylized input-output ecosystem accounting matrices

Notice the symmetry of the upper left matrix. This matrix accounts for mass flows from one species (the row) to another (the column). These interspecies exchanges occur during the period and values for these cells (non-zero where x's are present) are generated by the behavioral functions described in the previous section.

The array of columns and rows across the matrices is structured consistently with species inputs and outputs, respectively. For example, primary producers (PP) take only own-biomass (SB), light (L), and nutrients (N) as inputs. These inputs are converted into available energy according to the bioenergetic production function described in section 3.3.1. It is the primary producer's objective to allocate as much of the available energy produced from its inputs to ending biomass (EB) as possible to propagate its genetic material. It must also satisfy the other non-zero demands for its available energy across its row. In this example, that includes demands by zooplankton (ZP), benthic organisms (BO), and small fish (SF) as well as its own respiratory (R) and metabolic (M) demands. Predation and metabolic costs are exogenous to the species while the respiratory costs depend on activity. For the primary producer, whose "foraging" is passive, activity-driven costs will be negligible, while the activity-driven costs incurred by marine mammals, for example, to secure a diet of prey comprised of benthic organisms through other marine mammals will be significant.

The conservation conditions require that the energetic and mass values of inputs must equal the outputs. Taking zooplankton as an example this time gives

$$\underbrace{SB_{ZP} + ZP_{ZP} + PP_{ZP}}_{input} = \underbrace{ZP^{ZP} + BO^{ZP} + SF^{ZP} + R^{ZP} + M^{ZP} + EB^{ZP}}_{output} \quad (3.12)$$

where all quantities are given in mass, this gives the mass conservation condition for zooplankton. If I knew the energy density of each of these masses, I could multiply these by their corresponding masses and generate an energy balance condition

provided I also had expressions for massless energy losses.

Since the species objective is to maximize ending biomass (EB^{ZP}), the conservation condition suggests that its energy expression, as opposed to the mass expression above, will be given as the difference between the energetic benefits of the zooplankton's inputs and the energetic costs (fixed and variable) it must pay as part of its output. For the benefits, I know that a specific amount of available energy will be produced from the two chosen and one exogenous input of the zooplankton as determined by the bioenergetic production function. This production function, which I denote by $F(PP_{ZP}, ZP_{ZP}, SB_{ZP})$, takes a constant elasticity of substitution (CES) form (given explicitly in section 3.4). I also posit a linear cost function, $\Xi(PP_{ZP}, ZP_{ZP}, SB_{ZP})$. Variable costs depend on prey and starting-biomass inputs, which are accounted in output under respiration (R) and metabolism (M), respectively. Losses to harvesting (H) are given exogenously.

I now have a means for expressing the zooplankton's objective as maximizing the difference between bioenergetic benefits and costs

$$\Pi = F(PP_{ZP}, ZP_{ZP}, SB_{ZP}) - \Xi(PP_{ZP}, ZP_{ZP}, SB_{ZP}). \quad (3.13)$$

The zooplankton, and all other modeled species, is assumed to be competed toward the optimal selection of inputs given an output level (Y) and the marginal costs of inputs, both of which are model variables. The modeled species then choose within the period only what to consume based on the costs of predating and the benefits of assimilating the various prey. Less-abundant prey are more costly to forage – they are ‘harder to find.’ Prey abundances are calculated net of all predation. In this way, competition among predators for a given prey species are reflected in higher foraging costs for both.

For each species, there is an optimal selection of prey for any set (or vector) of

population scarcities. The optimal behavior implied by a given vector of population scarcities, which incorporates the initial and boundary conditions, may not satisfy the conservation conditions. The task of the modeling exercise is to find a set of scarcities and output quantities for which the implied optimal behavior for all species satisfies the system conditions. That is, the biomasses produced and consumed by all the modeled species, which are optimally selected based on the species' relative scarcities, must be physically realistic – they must conserve mass and energy.

3.4 Model Structure – Intra-Temporal Dynamics

3.4.1 General Structure

I represent the ecosystem in an input-output framework with five matrices (M, R, X, D, and E). Matrix entries in matrices M, R, X, and D represent *mass* quantities that flow among the I species in the ecosystem and the surrounding environment. Matrix entries in matrix E give *energy* quantities that flow from the ecosystem species to the surrounding environment.

$$\begin{array}{c} \uparrow \\ \text{Input} \\ \downarrow \end{array} \left\{ \begin{array}{l} \overbrace{\left[\begin{array}{ccc} x_{11} & \cdots & x_{1I} \\ \vdots & \ddots & \vdots \\ \vdots & & \vdots \\ x_{I1} & \cdots & x_{II} \end{array} \right]}^{\leftarrow \text{Output} \rightarrow} \left[\begin{array}{ccc} d_{11} & \cdots & d_{1L} \\ \vdots & & \vdots \\ \vdots & & \vdots \\ d_{I1} & \cdots & d_{IL} \end{array} \right] \left[\begin{array}{ccc} e_{11} & \cdots & e_{1N} \\ \vdots & & \vdots \\ \vdots & & \vdots \\ e_{I1} & \cdots & e_{IN} \end{array} \right] \\ \left[\begin{array}{ccc} r_{11} & \cdots & r_{1I} \\ \vdots & & \vdots \\ r_{K1} & \cdots & r_{KI} \end{array} \right] \begin{array}{l} \text{M: prior-period Masses} \\ \text{R: exogenous-produced Resources} \\ \text{X: inter-species eXchange} \\ \text{D: final Disposition} \\ \text{E: massless Energy flows} \end{array} \\ \left[\begin{array}{ccc} m_{11} & \cdots & m_{1I} \\ m_{21} & \cdots & m_{2I} \end{array} \right] \end{array} \right.
 \end{array}$$

Figure 3-4: Biological Accounting Matrix of input-output data

A column spanning the X, R, and M matrices represents inputs to the j^{th} species corresponding to that column. A row spanning the X, D, and E matrices represents allocations of mass (X and D) and energy (E) by the i^{th} species (corresponding to

the row) to its predators (X), final uses such as ending biomass and wastes (D), and massless energy losses to the environment (E). For each species and resource there is a corresponding fixed energy density ρ_i, ρ_f . These densities are used for energy accounting below.

Matrix M contains each species structural ($m = 1$) and storage ($m = 2$) biomasses, which are determined in the prior period. These include, for example, skeleton and muscle (structure) and fat (energy storage). In the initial applications of the BGE, I will take the simplifying assumption of only one aggregate starting biomass, but it is reasonable to posit that optimal consumption behavior would differ relative to different levels of structure and storage.

Matrix R contains K exogenously-produced ecosystem resources. For example, these might include light, nutrients, or even primary producers. The M and R matrices are similar in that they both represent exogenously-produced (or supplied) resources for the ecosystem. In the case of matrix M, the exogeneity comes from the fact that starting biomasses were determined by past periods' activity. In the case of matrix R, the exogeneity represents the assumption that the total availability of resources for the period cannot be changed within the period. For example, no realistic action by the species will change the amount of available sunlight to the ecosystem – the supply of sunlight is effectively fixed with respect to ecosystem dynamics. Individuals will compete for access to the fixed supply of these resources driving the exertion costs required for a species to consume the resource.

So the defining assumption for an input to be included in matrix R (as opposed to matrix X) is that the quantity supplied (or produced) within the period is unaltered by the intra-period activity of the ecosystem species. If the total supply of a resource (energy, nutrient, or species) is thought to depend on species' behavior, its production should be modeled and included in matrix X.

Matrix X elements, x_{ji} , represents the flow of mass from species j to species i so that a column of X is species i 's input vector in other species' masses. Likewise, a row of X is species i 's output vector of masses to its predators. Diagonal entries would represent cannibalism. The defining feature of matrix X is that both the input and output quantities for the species defining its columns and rows are endogenously determined within the period. For example, say in a marine setting I wish to model Atlantic cod. Both the input and output (column and row) of the cod depends on the behavior and abundance of its prey and predators, as will be explained further in the behavior section below.

Matrix D summarizes each species' final disposition of accumulated mass to different mass categories. There are $L = 5$ final disposition categories for each species. The sum of $d_1 - d_3$ represents the the amount of energy a species can carry forward to the next period embodied in its own biomass – its behavioral maximand. The allocation among $d_1 - d_3$ is determined by inter-temporal dynamic optimization (discussed in section 3.2.2). For simplicity, this allocation can be done in fixed shares or collapsed into an ending biomass aggregate. Wastes (d_4) are jointly determined by prior-period structural mass and current period activity levels. Net migration and natural deaths (d_5) could be exogenously specified or be modeled in some way.

d_1 : structural biomass	d_2 : storage biomass	d_3 : progeny
d_4 : wastes	d_5 : net migration & natural deaths	

Matrix E gives energy losses not embodied within system mass flows. There are $N = 3$ massless energy loss categories for each species. Ambient losses (e_1) are determined by the difference between ambient and (optimal) body temperatures. Metabolic transformation losses (e_2) are driven by the inefficiency of the bioenergetic production function in converting energy embodied within prey to energy available

for its own uses (further explanation below). Activity losses (e_3) are driven by the scarcity of the species' prey and the mass quantities consumed. This is the energy expended to locate and compete for prey.

e_1 : metabolic transformation losses e_2 : ambient losses
 e_3 : activity losses

All matrix quantities are constrained positive except net migration (d_5). Quantities are described in greater detail below.

The defining feature of the D and F matrices is that they are contingent on the activity within the period, but cannot be directly “chosen” by the species in the way the values of the X matrix can. This exogeneity is similar to how M and E matrices represent quantities whose total values are determined at the start of the period; i.e., the initial conditions. The D and F matrices represent quantities leaving the system; i.e., the boundary conditions. This can happen spatially, via mass or energy leaving the species and accumulating outside the modeled ecosystem (i.e. wastes d_4 , migration d_5 , and energy losses $e_1 - e_3$), or temporally, via biomasses that carry mass and energy over from the current period to the next (i.e. $d_1 - d_3$).

Given these initial and boundary conditions, I also impose conservation identities on the system's mass and energy quantities so that the modeled outcomes are physically realistic. With these three sets of conditions in place, I can then propagate the system dynamics with species behavior, which I will derive through optimization. Specifically, I assume that the species are competed toward optimal foraging strategies, which are defined by the maximization of the amount of mass and energy carried forward within its genetic material to the next period (i.e. $\rho_i[d_{i1} + d_{i2} + d_{i3}]$).

3.4.2 Behavior

Costs

Each species' input value for the X, R, and M matrices is derived from behavioral assumptions. Behavior in the model is propagated by the bioenergetic function F_i (introduced above) and restored to an interior value by the attendant maintenance and activity costs. These costs are paid to the environment in the form of dissipative losses and mass wastes. Assuming only a single starting biomass, m_i , and marginal (energy per unit mass) scarcity costs of inputs, ϕ , I can express these costs as a function

$$\Xi(\phi, m, r, x) = \phi_{m_i} m_i + \sum_k \phi_{k_i} r_{k_i} + \sum_j \phi_{j_i} x_{j_i}. \quad (3.14)$$

That is, species i pays to the environment costs linear in its inputs of own-biomass (m_i), resources (r_{k_i}), and prey (x_{j_i}). Part of the energetic value of these costs will account for the mass wastes captured by the environment from species i .

Stock recruitment is a critical driver of these costs that is abstracted away in this presentation. As presented, species end the period with a certain generic quantity of biomass. In reality, the total quantity of ending species biomass is allocated across progeny and different types of own biomass (structure and storage). The juvenile population could be modeled as a distinct "pseudo-species," with its own intra and inter-temporal dynamics, but this approach is left to future work.

Setting aside the structure and storage categories, there is an implicit stock recruitment relationship embedded in the current abstraction. Specifically, biomass devoted to reproduction that does not lead to a surviving juvenile population is assumed to be part of the waste category (in addition to excreta and natural death). Given a total quantity of a species' energetic input, losses to predators, and net migration, a baseline growth rate calibrates the allocation of remaining energy between ending

biomass and wastes. (Chapter 5 deals explicitly with calibration to species-specific growth rates.) To increase (decrease) recruitment rates, we can decrease (increase) the relative amount of waste produced by modifying the calibrated relationship between *total* biomass and waste production.

Scarcity costs

The ϕ_{-i} 's give energetic scarcity costs per unit mass as a function of system scarcity (inverse prey abundance) and predator-specific costs (φ_{ji}). Species abundances (or densities) are given by $n_i = N_i/A$, where A is the relevant area (or volume depending upon the application) of the ecosystem and N_i is the raw number of individuals of the species. For simplicity, I will ignore the allocation of ending biomass to structure (d_1), storage (d_2), and progeny (d_3). Using ending biomass to calculate scarcity implies that it is determined at the margin of the last-predated mass of the species. (A similar calculation is used for resources.)

Given species and resource abundances, scarcity costs are given by the product of their scarcity and species-specific energy costs, φ ,

$$\phi_{ji}(n_j; \varphi_{ji}) = \frac{\varphi_{ji}}{n_j}, \quad (3.15)$$

and similarly for resources. The φ terms give energy expenditure per scarce-unit of prey. That is, φ_{ji} times prey scarcity ($1/n_j$) times units of prey consumed (x_{ji}) gives total energy expended by species i to consume prey j . This characterization of scarcity is based on optimal foraging theory. In the model, species scarcities are endogenous variables. For consistency between the ecological scarcity measure and the model variable actually employed the two should be linearly related. I confirm this behavior for each species in model testing.

Objective

Having specified the costs for the model species, I am ready to express the propagating benefits driving species consumption. To do so, I maximize the net energetic “profit” of the species (eqn. 3.17). First I must specify F , which I do in constant elasticity of substitution (CES) form common to economics (cf. Arrow et al. (1961); Sato (1967)).

$$F(X_i, R_i, m_i) = \tau_i \left(\alpha_X \left(\sum_j \alpha_{ji} x_{ji}^{\varrho_{X_i}} \right)^{\varrho_{0i}/\varrho_{X_i}} + \alpha_R \left(\sum_k \alpha_{ki} r_{ki}^{\varrho_{R_i}} \right)^{\varrho_{0i}/\varrho_{R_i}} + \alpha_M m_i^{\varrho_{0i}} \right)^{\eta_g/\varrho_{0i}}. \quad (3.16)$$

The arguments X_i and R_i give species i 's vector of prey and resource inputs, respectively. This form will imply that species i will make aggregate substitutions across its prey, resources, and own-biomass inputs in a parametrically distinct manner from substitutions among prey or resources (i.e. ϱ_{0i} versus ϱ_{X_i} or ϱ_{R_i} , respectively). In a biological setting, the ϱ 's parameterize the “degree of switching” among prey or, more generally, inputs. Given the bioenergetic production and cost functions, the corresponding profit function is given by

$$\Pi(F, \Xi) = F(X_i, R_i, m_i) - \Xi(X_i, R_i, m_i) \quad (3.17)$$

The intra-temporal objective is then to maximize this bioenergetic profit – the amount of energy carried forward within the species to the next period – by choosing X_i , R_i , and m_i given metabolic costs of own-biomass, ϕ_{mi} , and scarcity costs of resources and prey, ϕ_{ki} and ϕ_{ji} . Note however that own-biomass inputs will be fixed to starting biomass (i.e. $m_i = M_{0i}$).

Maximizing the species energetic profit generates optimal input quantities for X_i , R_i , and m_i . Given these optimal quantities and exogenously specified values for the elasticity parameters (ϱ), the remaining parameters (τ and the α 's) can be tuned to match observed steady-state values within empirical or simulated input-output

matrices. The next subsection details how to derive the optimal quantities and how this derivation implies critical “dual” relationships between model variables. The model solution algorithm will exploit this duality relationship to identify solutions.

Finally, the bioenergetic production function produces energy for both waste and new biomass. The allocation among the two is determined by a functional form similar to that used for inputs,

$$(\alpha_W w_i^{\varrho_{O_i}} + \alpha_B b_i^{\varrho_{O_i}})^{1/\varrho_{O_i}} = F(X_i, R_i, m_i). \quad (3.18)$$

For the baseline specification of the BGE model, I will require that waste and biomass be produced in fixed proportion, implying a fixed bioenergetic efficiency for each species. Parametrically, this behavior holds for $\varrho_{O_i} = 0$, a counterintuitive result that works out in the limit of $\varrho_{O_i} \rightarrow 0$. The remaining parameters can be calibrated to observed data based on the relative values of waste and new biomass produced (determined by the ecotrophic efficiency in Ecosim data).

3.4.3 Optimization & Duality

This subsection shows the derivation of optimal bioenergetic profit through the primal and dual presentations of the optimization problem. The values of a Biological Accounting Matrix (BAM) from ecosystem input-output data can then be used to calibrate these demands *assuming* that they represent a steady-state outcome for the ecosystem; i.e., that the intra-period behavior represented in the BAM is optimal given the conditions faced by the species.⁹ One could identify ways to parameterize an ecosystem that is not in steady-state if this assumption is untenable. For example, species choices could be randomly shocked to sub-optimal levels by transferring energetic profit from species to the environment or other species.

⁹The benchmark BAM need not be a single-year snapshot. One could, for example, take a multi-year average or more sophisticated approximation to an equilibrium for the ecosystem.

Objective

To avoid unnecessary complexity in these examples I will assume that species have two or three inputs, own-biomass plus one or two prey. For a species with one prey, the bioenergetic production function takes the form

$$F(x_{ji}, m_i) = \tau_i \left(\alpha_{i0} x_{ji}^{\varrho_{i0}} + \alpha_{i1} m_i^{\varrho_{i0}} \right)^{1/\varrho_{i0}}, \quad (3.19)$$

where x_{ji} gives species i 's singular prey input, j denoting the prey species, and m_i species i 's starting biomass. The associated costs that depend on inputs are given as

$$\Xi(x_i, m_i) = \sum_j \phi_{ji} x_{ji} + \phi_{mi} m_i. \quad (3.20)$$

For species with multiple prey, an aggregate of both prey will take the place of x_{ji} in equation (3.19),

$$\mathcal{X} = \left(\sum_j \alpha_{ji} x_{ji}^{\varrho_{xi}} \right)^{1/\varrho_{xi}}. \quad (3.21)$$

The construction of the bioenergetic production function allows it to be sequentially optimized when there is a multi-prey aggregate as in (3.21). That is, to derive optimal levels of inputs X_i , I can find optimal levels of the j inputs x_{ji} given a level of the aggregate \mathcal{X} while holding the other input, m_i , fixed; i.e., as if \mathcal{X} were an independent CES function. This aggregate is also called a “nest” of the CES function. The ability to sequentially optimize is due to the *weak separability* of the CES function, particularly that

$$\frac{\partial}{\partial r_{ji}} \frac{\partial x_{ji}}{\partial x_{j'i}} = 0. \quad (3.22)$$

That is, the optimal demands for inputs x_{ji} , which are determined by their relative marginal bioenergetic products, $\partial F/\partial x_{ji}$, are independent of the level of inputs outside the \mathcal{X} nest.

Duality

There are two equivalent formulations of the species optimization problem, primal and dual. In the primal formulation, bioenergetic costs are minimized through the choice of input quantities subject to the production of a unit of output. In the dual formulation, bioenergetic costs are minimized for a given level of output over the choice of marginal products. In economics, duality is often treated through the use of certain lemmas particular to the discipline (e.g. Shephard's lemma). Mathematically, the primal and dual problems are related through the Euler-Legendre transform, which is also used in physics to relate Lagrangian and Hamiltonian mechanics.

The primal formulation solves in terms of extensive variables (i.e. 0th-order quantities), while the dual posing solves in terms of intensive variables (i.e. 1st-order marginals or unit costs). Letting Z_i give a stacked vector of prey inputs (x_{ji}) and own biomass (\bar{m}_i), I can specify the primal and dual posings of the bioenergetic optimization problem as

$$\text{Primal: } \mathcal{L}(Z_i, \lambda^F) = \Xi(Z_i) - \lambda^F(F(Z_i) - 1) \quad (3.23a)$$

$$\text{Dual: } \mathcal{L}^*(Z_i^*, \lambda^F) = \inf_{Z_i \in \mathbb{R}_+^I} \{\mathcal{L}(Z_i) - Z_i^* \cdot Z_i\}. \quad (3.23b)$$

Using this definition for the Euler-Legendre transform, the primal and dual posings are both minimization problems.¹⁰ Solving for the infimum in Z_i of the dual expression via the first-order conditions gives

$$Z_i^* = \nabla \mathcal{L}(Z_i). \quad (3.24)$$

Inserting the value for the convex conjugate or dual variable Z_i^* into the expression of the dual problem demonstrates that it is equivalent to minimizing the marginal cost

¹⁰It is common in other applications to flip the sign within the infimum of the transform, making it a supremum and the dual posing a maximization problem (opposite the primal).

of a unit of production, λ^F .

$$\begin{aligned}
\mathcal{L}^*(Z_i^*, \lambda^F) &= \Xi(Z_i) - \lambda^F(\nabla F(Z_i) - 1) - [\nabla \Xi(Z_i) - \lambda^F \nabla F(Z_i)] \cdot Z_i \\
&= \Xi(Z_i) - \lambda^F \nabla F(Z_i) + \lambda^F - \Xi(Z_i) + \lambda^F F(Z_i) \\
&= \lambda^F,
\end{aligned} \tag{3.25}$$

where the second line exploits Euler's homogeneous function theorem; i.e., $kF(Z) = \nabla F(Z) \cdot Z$, where k gives the degree of homogeneity and $F(Z)$ and $\Xi(Z)$ homogeneous of degree 1. The Lagrange multiplier represents the marginal value to the objective for an additional unit of constraint. Here, this means the marginal cost (objective) of an additional unit of bioenergetic production (constraint), which the species seek to minimize.

While the objective of the primal posing is to minimize cost through choice of inputs Z_i , the dual posing minimizes cost through choice of Z_i^* . Z_i must be restricted to $Z_i \geq 0$ for physical relevance (i.e. they are quantities of mass inputs). The domain restriction on the conjugate Z^* is that it ensure a finite solution to the infimum of the dual problem. Since Z_i is unbounded above and I seek an infimum, I require that the dual is increasing in Z_i . That is,

$$\begin{aligned}
\nabla_{Z_i}[\mathcal{L}(Z_i) - Z_i^* \cdot Z_i] &\geq 0 \\
\nabla \mathcal{L}(Z_i) &\geq Z_i^*.
\end{aligned} \tag{3.26}$$

From the solution to the infimum problem (3.24) I know that this weak inequality will hold with equality provided the Lagrangean obeys certain convexity properties. From the solution to the primal problem I know that $\nabla \mathcal{L}(Z_i) = 0$ at an optimum in Z_i .

Last, and somewhat loosely, the convexity properties of $\mathcal{L}(Z_i)$ ensure it has a turning point in the domain \mathbb{R}^I . If I am unable to find the turning point it must be

due to the restriction that $Z_i \in \mathbb{R}_+^I$. In this case I will find a minimum of $\mathcal{L}(Z_i)$ at $Z_i = 0$ with $\nabla \mathcal{L}(Z_i) > 0$. This has important implications for the relationship between the conjugate choice variables Z_i and Z_i^* . The above argument gives that if $\nabla \mathcal{L}(Z_i) = Z_i^* > 0$, I must have the optimal $Z_i = 0$. Conversely, if the optimal Z_i is positive, I must have that $\nabla \mathcal{L}(Z_i) = Z_i^* = 0$. From this I have

$$\begin{aligned} Z_i^* &= \nabla_{Z_i} \mathcal{L}(Z_i) \quad \text{AND} \quad Z_i = \nabla_{Z_i^*} \mathcal{L}^*(Z_i^*) \\ Z_i^* \cdot Z_i &= \nabla_{Z_i} \mathcal{L}(Z_i) \cdot \nabla_{Z_i^*} \mathcal{L}^*(Z_i^*) = 0. \end{aligned} \quad (3.27)$$

This relationship, where at least one of the complementary or conjugate variables must be zero, is known as complementary slackness. The intuition of this result is more clear when the duality is considered with respect to the Lagrange multiplier of a constraint. In this scenario, either the Lagrange multiplier is zero, the constraint (derivative of the Lagrangian w.r.t. its multiplier) equals zero, or, more trivially, both. That is, excluding the trivial case, when the constraint binds (i.e. equals zero), its Lagrange multiplier is positive, else the constraint is left slack (non-zero) and the multiplier equals zero – a familiar result in constrained optimization. This is a helpful property for the success of the numerical solution algorithms employed to identify model solutions.

I can now solve the primal problem given above by taking first order conditions, giving

$$\begin{aligned} \text{w.r.t. } Z_i: \quad \nabla_{Z_i} \Xi(Z_i) - \lambda^F \nabla_{Z_i} F(z_i) &= \vec{0} \\ \frac{\partial \Xi(Z_i)}{\partial x_{ji}} &= \phi_{ji} = \lambda^F \frac{\partial F(Z_i)}{\partial x_{ji}} \quad \forall j \\ \frac{\partial \Xi(Z_i)}{\partial m_i} &= \hat{\phi}_{mi} = \lambda^F \frac{\partial F(Z_i)}{\partial m_i} \end{aligned} \quad (3.28a)$$

$$\text{w.r.t. } \lambda^F: \quad F(Z_i) = 1. \quad (3.28b)$$

Taking first derivatives of the production function $F(Z_i)$ (3.19), gives the first-order conditions above as

$$\phi_{ji} = \lambda^F \left[\frac{1}{\varrho_{i0}} (\tau_i^{\varrho_{i0}} Y_i^{1-\varrho_{i0}}) (\varrho_{i0} \alpha_{i0} x_{ji}^{\varrho_{i0}-1}) \right] \quad (3.29a)$$

$$\hat{\phi}_{mi} = \lambda^F \left[\frac{1}{\varrho_{i0}} (\tau_i^{\varrho_{i0}} Y_i^{1-\varrho_{i0}}) (\varrho_{i0} \alpha_{i1} m_i^{\varrho_{i0}-1}) \right] \quad (3.29b)$$

Note that the Lagrange multiplier, λ^F , is the marginal cost of a unit output, a model variable, which I denote $\hat{\phi}_i$. The mass output, \hat{Y}_i , of the species bioenergetic production function, F , is also a model variable. This enables us to solve for the optimal input level as a function of model variables and parameters only.

$$x_{ji}^* = \left(\alpha_{i0} \frac{\hat{\phi}_i \tau_i^{\varrho_{i0}}}{\phi_{ji}} \right)^{\frac{1}{1-\varrho_{i0}}} \hat{Y}_i \quad (3.30a)$$

$$m_i^* = \left(\alpha_{i1} \frac{\hat{\phi}_i \tau_i^{\varrho_{i0}}}{\hat{\phi}_{mi}} \right)^{\frac{1}{1-\varrho_{i0}}} \hat{Y}_i \quad (3.30b)$$

Benchmark levels of the x , m , and Y terms are observed in the data, allowing the calibration of the remaining parameters assuming a steady-state is observed. The α terms from the first-order conditions can be expressed as

$$\alpha_{i0} \tau_i^{\varrho_{i0}} = \phi_{ji}^{\varrho_{i0}} \left(\frac{\phi_{ji} x_{ji}}{\hat{\phi}_i \hat{Y}_i} \right)^{1-\varrho_{i0}}, \quad (3.31a)$$

$$\alpha_{i1} \tau_i^{\varrho_{i0}} = \hat{\phi}_{mi}^{\varrho_{i0}} \left(\frac{\hat{\phi}_{mi} m_i}{\hat{\phi}_i \hat{Y}_i} \right)^{1-\varrho_{i0}}. \quad (3.31b)$$

The common τ_i term gives a degree of freedom to normalize the α 's such that $\alpha_{i0} + \alpha_{i1} = 1$. Imposing this constraint and taking either of the expressions immediately above over their sum gives

$$\alpha_{i0} = \frac{\alpha_{i0}}{\alpha_{i0} + \alpha_{i1}} = \frac{\alpha_{i0} \tau_i^{\varrho_{i0}}}{\alpha_{i0} \tau_i^{\varrho_{i0}} + \alpha_{i1} \tau_i^{\varrho_{i0}}}, \quad (3.32)$$

and analogously for $\alpha_{i1} = (1 - \alpha_{i0})$. Expressed in this way, the α terms represent the

relative productivities of the inputs in generating bioenergetic output. The φ terms, component to the $\hat{\phi}$'s, can be calibrated based on ecosystem data. This will specify the entire CES function with the exception of τ_i , which I can identify algebraically using the definition of the CES.

Summary

I can express the optimal demand for all inputs as a function of the substitution parameters (ϱ), the coefficients (α and τ_i), along with marginal costs ($\hat{\phi}$) and the level of output \hat{Y}_i yielded by the CES bioenergetic production function F . That is, as functions of parameters and model variables only. The calibration of these demands to empirical data will be conducted in the next chapter. First, I outline how the system conditions can be used to identify physically relevant quantities for the model variables, completing the model.

3.4.4 System Conditions & Equilibria

Conservation identities

System conditions require that inputs equal outputs for conserved quantities, ensuring that there is no unaccounted introduction (loss) of mass or energy to (from) the system. The conditions also provide a means to solve for the model variables. I first express the conservation conditions then show how these conditions are used to identify equilibria.

In an economic model, economic value is the only conserved quantity, but a biological system will conserve both mass and energy. The conservation requirement is set by equating inputs and outputs for the conserved quantity. With respect to the system accounting matrices, this gives that the column sum equals the row sum for each species.

The left-hand side of each line in Table 3.1 gives the output quantity in conserved

Conserved qty.	Conservation identity
<i>Economy</i>	
Economic value:	$\hat{\rho}_i \hat{Y}_i = \sum_j \hat{\rho}_j x_{ji}^* + \sum_f \hat{\rho}_f r_{fi}^*$ $= \sum_j \hat{\rho}_i x_{ij}^* + \sum_l \hat{\rho}_l d_i^*$
<i>Ecosystem</i>	
Mass:	$\hat{Y}_i = \sum_j x_{ji}^* + \sum_f r_{fi}^* + m_i$ $= \sum_j x_{ij}^* + M_{1i}^* + d_i^*$
Energy:	$\hat{\phi}_i \rho_i \hat{Y}_i = \sum_j \hat{\phi}_j \rho_j x_{ji}^* + \sum_f \hat{\phi}_f \rho_f r_{fi}^* + \hat{\phi}_i^m \rho_i m_i^*$ $= \sum_j \hat{\phi}_i \rho_i x_{ij}^* + \hat{\phi}_i \rho_i M_{1i}^* + \hat{\phi}_i \rho_i \omega_i d_i^*$

Table 3.1: Conservation conditions for an economy and an ecosystem

units. The Y_i variable is the mass equivalent of the bioenergetic output produced by F_i . The ρ terms give either marginal economic value (price) or marginal energetic value (i.e. energy density). Here, d_i represents wastes taken up by the environment and M_1^* is ending biomass (final consumption demands and investment in an economic setting). The ω_i scalar gives the waste energy density per unit biomass energy density. In the ecosystem, the r terms represent resources whose supply is exogenous to the system (e.g. light, nutrients). (These are fixed factors of production such as labor and capital in an economic setting.)

“Hatted” characters are model variables. Notice that, while the ρ terms are model variables in the economic setting, they are not model variables in the biological setting. Instead, I let the ρ terms set the fixed energy densities of the species. The $\hat{\phi}$ terms, variables in the BGE model, are set to one in baseline and measure the relative scarcity of the species ($\hat{\phi}_i$), resources ($\hat{\phi}_f$), and starting biomass ($\hat{\phi}_i^m$). Note that, for parsimony, the ϕ terms were subsumed by the ρ terms in the previous section.

In the ecosystem, the relative scarcity variables do the work of economic prices by scaling the energy required to secure various prey and resources in relation to their scarcity. The initial conditions are the ultimate source of scarcity in the ecosystem – they are the only supplies that cannot be influenced by the intra-temporal dynamics

of the system. The $\hat{\phi}$ terms then signal the extent to which the species draws on the variety of scarce resources it takes as its inputs. The more scarce the sources of a species' inputs, the more scarce it will be in turn. The following section will make clear how these scarcity terms “ration” uses of scarce resources to identify physically relevant states for the system.

At an optimum, the scarcity terms will match the marginal product of the bioenergetic production function; i.e., marginal cost will equal marginal benefit. If marginal benefits exceed marginal costs, competitive pressures will ultimately reward those who avail themselves of these net benefits. This framing aids the interpretation of the own-biomass scarcity, $\hat{\phi}_i^m$. The scarcity of own-biomass will rise to the point where the optimal input level equals the fixed quantity of starting biomass available to the species (given that it is the outlet for the biomass). Yet the cost paid by the species to the environment for carrying its starting biomass is only its fixed resting metabolic rate. The difference between the marginal scarcity value and the metabolic rate represents energetic “profit” to the species, or the net marginal benefit to an additional unit of biomass. So while the marginal predation costs accrue wholly to the environment, the species captures some of the “cost” paid for own-biomass. The next section will demonstrate how matching marginals in this way is a necessary implication of our conservation conditions.

Posing the equilibrium problem

The final step in specifying the equilibrium problem is to use the input-output conservation identities to isolate the model variables, particularly \hat{Y} and $\hat{\phi}$, to solve for them. The essential method here is to take derivatives of the input and output equations with respect to the model variables that are common terms. This will generate conjugate relationships between the resulting equations and the variable on which the derivative was taken. These conjugate relationships, as described in section 3.4.3,

can be exploited by numerical algorithms to help solve the BGE model.

In the case of input, the common term is the level of output \hat{Y}_i . Recall that optimal input demands are expressed as a fraction of output, where that fraction is determined by parameters and the model scarcity variables $\hat{\phi}$. In the case of output, the derivative is taken with respect to the species' scarcity variable, $\hat{\phi}$. By summing the conservation identities over species, we can equate the total starting mass and energy of biomass and resource inputs with those of the ending biomass and waste quantities. The species will carry the energy captured in ending biomasses forward to start the next period, while the wastes will be 'absorbed' by the environment (dynamic waste cycles could be modeled if desired). Table 3.2a demonstrates how the conservation identities are transformed to specify the equilibrium problem for an ecosystem.

The scarcity values equal one in the baseline specification, but as system conditions change, these values will shift to capture changes in the relative scarcity of the various species and their resources. Additional prey scarcity implies greater expenditure and thereby additional waste products by the species. Since the bioenergetic inputs taken up by each predator are transformed into both waste and biomass, production should be toward wastes as prey scarcities rise; i.e., as additional energy expenditure generates greater waste. This raises the interpretation of the expenditure to starting biomass. The optimization process will match marginal costs of inputs to the associated marginal benefits of output. To ensure the starting biomass from the initial conditions is the same quantity "foraged" by the species, the scarcity cost of starting biomass will rise to the meet marginal benefit, but in a sense the species captures the benefit of its own scarcity or "pays itself." Explicitly, the scarcity value of own biomass (costs) represents forgone bioenergetic profit (benefit) for the species.

Finally, to ensure energy conservation, I can confirm that energy expenditure on

ECOSYSTEM EQUILIBRIUM PROBLEM

Conserved quantities

Mass

Energy

Conservation identities

$$\begin{aligned}\hat{Y}_i &= \sum_j x_{ji} + \sum_f r_{fi} + m_i \\ &= \sum_j x_{ij} + M_{1i} + d_i \\ \sum_i (m_i + \sum_f r_{fi}) \\ &= \sum_i (M_{1i} + d_i)\end{aligned}$$

$$\begin{aligned}\hat{\phi}_i \rho_i \hat{Y}_i &= \sum_j \hat{\phi}_j \rho_j x_{ji} + \sum_f \hat{\phi}_f \rho_f r_{fi} + \hat{\phi}_i^m \rho_i m_i \\ &= \sum_j \hat{\phi}_i \rho_i x_{ij} + \hat{\phi}_i \rho_i M_{1i} + \hat{\phi}_i \omega_i \rho_i d_i \\ \sum_i \hat{\phi}_i^m \rho_i m_i + \sum_f \hat{\phi}_f \rho_f r_{fi} \\ &= \hat{\phi}_i \rho_i \sum_i (M_{1i} + \omega_i d_i)\end{aligned}$$

Intensive conditions*Marginal mass product* $\perp \hat{Y}_i$ *Marginal energetic product* $\perp \hat{Y}_i$

$$0 \geq 1 - \sum_j \tilde{x}_{ji} - \sum_f \tilde{r}_{fi} - \tilde{m}_i$$

$$0 \geq \hat{\phi}_i \rho_i - \sum_j \hat{\phi}_j \rho_j \tilde{x}_{ji} - \sum_f \hat{\phi}_f \rho_f \tilde{r}_{fi} - \hat{\phi}_i^m \rho_i \tilde{m}_i$$

Extensive conditions*Mass allocations**Energy allocations*

$$0 \geq \hat{Y}_i - \sum_j x_{ij} - M_{1i} - d_i$$

$$0 \leq \rho_i (\hat{Y}_i - \sum_j x_{ij} - M_{1i} - \omega_i d_i) \perp \hat{\phi}_i$$

$$0 \leq M_{0i} - m_i$$

$$0 \leq \rho_i (M_{0i} - m_i) \perp \hat{\phi}_i^m$$

$$0 \geq R_{0f} - \sum_i r_{fi}$$

$$0 \geq \rho_f (R_{0f} - \sum_i r_{fi}) \perp \hat{\phi}_f$$

Table 3.2a: BGE Model Equations**Model variables** \hat{Y}_i : mass of bioenergetic output $\hat{\phi}_i$: relative scarcity**Functions of variables**

$x_{ji} = \tilde{x}_{ji} \hat{Y}_i$, input of species j $r_{fi} = \tilde{r}_{fi} \hat{Y}_i$, input of resource f
 M_{1i} : ending biomass d_i : mass waste quantity
 $m_i = \tilde{m}_i \hat{Y}_i$, own-biomass input

Empirically calibrated parameters

M_{0i} : starting biomass supply ρ : species or resource energy density
 R_{0f} : starting resource supply ω_i : share of energy losses in mass

Table 3.2b: BGE Model Equations – Definitions

initial resources not exceed the energetic value of those resources. This condition is satisfied when the weighted average scarcity of initial resources does not exceed one. Mass conservation can be verified *ex post*, with differences in starting and ending mass quantities attributable to wastes. The convexity of the bioenergetic production functions will no doubt generate differences here.

3.4.5 Model closure

Consumption of prey and the production of waste and biomass cover only a portion of the modeled behavior in the ecosystem. The model requires several more features to be properly closed. There are two sides to each activity in the general equilibrium structure, meaning it remains to specify how the total energy given in the initial conditions is allocated across the different waste and biomass products after predators have taken their share of the latter. For both total waste and ending biomass, ending quantities move percent-for-percent counter to the system scarcity. This behavior can be modeled using a CES function with an elasticity of one. For example, if increased abundance of a species' predators induced a 10% rise in its scarcity, ending biomass for the species would decline by 10%. It can also be shown that this maximizes the entropy of changes to the distribution of ending quantities – implying an agnosticism or least-biased allocation affected by the ecosystem.

As mentioned above, increased expenditures on prey will generate proportionately more wastes relative to biomass. To generate this behavior in the model, the waste aggregation is dynamically calibrated so that more waste is required of species with high predation costs. As wastes requirements rise, the implied scarcity of the species waste will rise, inducing the bioenergetic production function to allocate more output to waste mass over biomass. In the next chapter, I diagram the production structure and model closure in detail prior to testing the model.

3.5 Conclusion

It is evident from the theoretical biology literature, particularly within optimal foraging and bioenergetic allocation, that an economic approach to adaptive species behavior is well-supported. Yet “precious few” examples, if any, exist of macro-scale models constructed from micro-consistent behavior. Economic general equilibrium theory offers an obvious and proven template from which such a model can be adapted. In taking up this task, this work contributes a flexible and robust tool for assessing the impacts of environmental change, anthropogenic or otherwise, on ecosystems.

This work also provides a coherent lens through which the incompletely-connected fields of optimal foraging, bioenergetic optimization, and ecosystem modeling can be viewed. The optimal foraging literature has made a strong case that species exhibit switching or substitution behavior – whether through passive means (e.g. encounter rates) or an active cognitive selection process. It is clear from the literature on switching that parametric switching behavior is needed to capture heterogeneity. This work has shown how this can be implemented through an energetic optimization scheme that admits differential switching behavior across multiple prey in a manner consistent with optimal foraging theory.

The energetic presentation creates a direct link with literature on bioenergetic optimization and its implications on evolutionary dynamics. Future work on the BGE model will incorporate inter-temporal trade-offs along the lines of, e.g., (Giacomini et al., 2013). This posing enables incorporating hypothetical or empirical observed behavior at an individual level into a dynamic ecosystem. This “micro-macro” linkage is a key contribution of the BGE model. Much of the ecosystem modeling literature has had to rely on phenomenological or atheoretic characterizations of complex ecosystems. Modeling system dynamics as the emergent consequence of adaptive individual behavior establishes an important linkage with the actual “agents” of the ecosystem

dynamics and offers the ability to analyze the impacts a wide cast of shocks to the system species in a physically relevant way.

CHAPTER 4: TESTING THE BIOLOGICAL GENERAL EQUILIBRIUM MODEL

4.1 Introduction

This chapter calibrates the Biological General Equilibrium (BGE) model specified in Chapter 3 to two empirical data sets of the marine ecosystem surrounding the Aleutian Islands. The two datasets are from the GEEM model (Finnoff & Tschirhart, 2003) and an Ecosim dataset with much higher species resolution (Gu enette & Christensen, 2005). In each case, the data must be pre-processed in different ways to satisfy the Biological Accounting Matrix (BAM) input-output balance requirements. Differences in the type and completeness of data provided warrant different treatment of each dataset. Given the large number of the Ecosim datasets, a generalizable approach is presented for preparing those data.

With a balanced BAM, I calibrate the biological general equilibrium (BGE) model and simulate stylized “shocks” to the system comparing the results across the two datasets and a variety of parameterizations. This confirms the stability and plausibility of the model behavior and sheds some light on how differences in underlying data may drive model results.

4.2 Calibration – GEEM

I first calibrate the data employed in the GEEM model presented by Finnoff and Tschirhart (Finnoff & Tschirhart, 2003, Table 1), which I transform into mass and energy Biological Accounting Matrices (BAMs) compatible with the BGE model. The next section details the calibration of Ecosim data for the same ecosystem. These data have a much more detailed representation of the ecosystem with more than 30 species.

Table 4.1 presents GEEM mass data in a BAM. The key feature of the accounting

matrix, to satisfy the system conditions, is that the row and column sums are equal; i.e., input equals output. For example, the sum of phytoplankton mass inputs of own biomass (0.993 MMT) and nutrients (10.5 MMT) equals the sum of allocations to ingestion losses (0.114 MMT, column [B]), predators (7.52 MMT, column [C]), mass wastes (2.9, column [D]), and ending biomass (0.993, column [E]). Similarly for the energy BAM given in Table 4.2, the sum of energy from sunlight, nutrients, and starting biomass equals the sum of columns [B]-[F].

4.2.1 Costs

For the initial calibration, ecosystem populations are assumed to be in a no-growth state so that ending biomass equals starting biomass. The model can also be calibrated to observed or specified growth rates, but these rates are not given in the GEEM data.¹ I can deduce mass wastes [D] as total mass input [A] less ingestion losses [B], predator losses [C], and ending biomass [E]. In order to do so, I must calibrate ingestion losses.

In the energy presentation (Table 4.2), I use estimated energy densities from GEEM (ρ_i) to calculate total energy input [A] as mass inputs times their corresponding densities. Ending energy [F] and predator losses [C] are transformed from their corresponding masses in Table 4.1 at the species energy density. Mass wastes [D] are transformed at a separate waste energy density estimated as half the density of the species' prey. Transformation losses [B] are estimated by parameterizing an initial value for γ (equal to 0.05 here). Transformation losses here equal total energy input times $\gamma/(1 + \gamma)$. Last, massless (or radiative) energy losses [E] are taken as the remainder of total energy input less [B], [C], [D], and [F].

For the cost function Ξ I isolate the energetic value of rest metabolism and activity.

¹As a sensitivity, I have calibrated the model to a variety of baseline growth rates. In each case, populations converged to a steady-state level within several years.

This value is equal to total energy input [A] less transformation losses [B], predator losses [C], and ending biomass [F] – or mass wastes [D] plus massless wastes [E]. From the energy BAM in Table 4.2,

$$[\text{D}] + [\text{E}] = \chi_i = \sum_j \phi_{ji} x_{ji} + \beta m_i. \quad (4.1)$$

That is, activity costs for species i , χ_i , are driven by the prey it forages x_{ji} and the mass it carries m_i . The mass quantities, x_{ji} and m_i , are observed in the data and the resting metabolic rate, β_i , is given parametrically or from empirical estimates. All are given in the GEEM data. I estimate the marginal cost of a unit of prey in the GEEM data as

$$\phi_{ji}(N_j) = \varphi_i N_j^{-1}. \quad (4.2)$$

	Inter-Species Mass Exchange (MMT) ¹								Mass Allocations				
	PP	ZP	PO	SL	OW	SO	UR	KE	Mass Input [A]	Ingestion Losses [B]	Predator Losses [C]	Mass Wastes* [D]	Ending Biomass* [E]
	<i>Phytoplankton</i> PP	-	7.52	-	-	-	-	-	-	11.5	0.549	7.52	2.46
<i>Zooplankton</i> ZP	-	-	1.19	-	-	-	-	-	7.54	2.40	1.19	3.93	0.016
<i>Pollock</i> PO	-	-	-	0.333	-	-	-	-	1.35	0.637	0.333	0.222	0.160
<i>Steller sea lion</i> SL	-	-	-	-	0.005	-	-	-	0.364	0.156	0.005	0.172	0.031
<i>Orca whale</i> OW	-	-	-	-	-	-	-	-	0.009	0.001	-	0.004	0.004
<i>Sea otter</i> SO	-	-	-	-	0.000	-	-	-	0.340	0.210	0.000	0.126	0.004
<i>Urchin</i> UR	-	-	-	-	-	0.336	-	-	117	5.57	0.336	86.5	24.5
<i>Kelp</i> KE	-	-	-	-	-	-	92.40	-	718	34.2	92.4	2.77	589
Starting Biomass	0.993	0.016	0.160	0.031	0.004	0.004	24.5	589					
Nutrients* ²	10.5	-	-	-	-	-	-	129					
Pop. (units / km ²)	87.7	162	6.16	0.096	0.008	0.051	10.8	1,077					

Notes:

* Asterisked items are derived from GEEM data, all others come directly from GEEM data (Finnoff & Tschirhart, 2003, Table 1).

1. Biomasses given in million metric tonnes. Biomasses are calculated from GEEM data as predator population (N / Km²) times biomass flow (Kg / N) corresponding area (Km²).

2. Nutrients inputs are assumed to be 40% greater than predator losses.

[A]: Sum of all mass inputs.

[B]: Mass inputs times mu divided by one plus mu to correct for mass losses during ingestion process.

[C]: Row sum of inter-species exchange matrix.

[D]: Total mass input less predator losses and ending biomass.

[E]: Set assuming no growth for initial calibration.

Table 4.1: Balanced mass Biological Accounting Matrix (BAM) based on GEEM mass data (Finnoff & Tschirhart, 2003)

	Inter-Species Energy Exchange (Bn. Kcal) ¹								Energy Allocations*						
	PP	ZP	PO	SL	OW	SO	UR	KE	Energy Input [A]	Trans. Losses [B]	Predator Losses [C]	Mass Wastes [D]	Massless Losses [E]	Ending Energy [F]	
<i>Phytoplankton</i> PP	-	3,009	-	-	-	-	-	-	15,454	11,063	3,009	73.8	910	397	
<i>Zooplankton</i> ZP	-	-	666	-	-	-	-	-	3,018	144	666	15.7	2,183	8.86	
<i>Pollock</i> PO	-	-	-	375	-	-	-	-	847	40.3	375	62.1	188	181	
<i>Steller sea lion</i> SL	-	-	-	-	9.97	-	-	-	438	20.9	9.97	97.2	247	62.5	
<i>Orca whale</i> OW	-	-	-	-	-	-	-	-	20.7	0.987	-	3.78	5.72	10.2	
<i>Sea otter</i> SO	-	-	-	-	0.525	-	-	-	248	11.8	0.525	45.3	184	6.67	
<i>Urchin</i> UR	-	-	-	-	-	241	-	-	93,447	13,602	241	35,506	26,511	17,587	
<i>Kelp</i> KE	-	-	-	-	-	-	75,860	-	866,084	304,653	75,860	170	2,102	483,298	
Starting Biomass	397	8.86	181	62.5	10.2	6.67	17,587	483,298							
Nutrients*	10.0	-	-	-	-	-	-	150							
Sunlight	15,046	-	-	-	-	-	-	382,636							
Energy Densities ² (Kcal / Kg)															
Own-Biomass ³	400	559	1,128	2,000	2,500	1,810	717	821							
Prey ⁴	300	400	559	1,128	1,990	717	821	616							
Waste ⁵	30.0	4.00	280	564	995	359	411	61.6							

Notes:

* Asterisked items are derived from GEEM data, all others come directly from GEEM data (Finnoff & Tschirhart, 2003, Table 1).

1. Energy quantities given in billion kilocalories and are given by the corresponding mass quantities times the relevant density with the exception of sunlight, transformation losses [B], and massless losses [E].

2. Own-biomass energy densities are given by GEEM.

3. Energy density for Orca whales a rounded estimate based on Williams et al. (2004, Table 1).

4. Nutrient energy densities are taken as 75% of plant density. Orca whale prey density is an input-mass weighted average of prey densities.

5. Equal to one half of prey density.

[A]: Sum of all mass inputs times their corresponding energy densities plus energy from sunlight.

[B]: Transformation losses determined by gamma parameter.

[C]: Row sum of inter-species energy exchange matrix.

[D]: Mass wastes times corresponding waste density.

[E]: = [A] - ([B] + [C] + [D] + [F])

[F]: Ending biomass times own energy density.

Table 4.2: Balanced energy Biological Accounting Matrix (BAM) based on GEEM energy data (Finnoff & Tschirhart, 2003)

The number of kilo-calories expended by species i per scarce-tonne of prey foraged is given by φ_i . The inverse of species j 's population density, N_j^{-1} , gives a measure of its scarcity. This gives the marginal cost, ϕ_{ji} , of predating species j to species i in Kcal per tonne. Population densities are also observed (in the GEEM data) leaving only φ_i for calibration based on equation (4.1) as

$$\varphi_i = \frac{\chi - \beta m_i}{\sum_j N_j^{-1} x_{ji}}, \quad (4.3)$$

so that φ_i is calibrated uniformly for all prey. One could differentiate if relative efforts for different prey were known or hypothesized. The calibration differs slightly for autotrophs who predate scarce-calories of sunlight. For autotrophs φ_i represents Kcal expenditure per unit Kcal gained from its “prey.” I implicitly assume a scarcity of 1 for both sunlight and nutrients, though model species could be required to compete for these resources, which could increase foraging costs through higher scarcity of sunlit surface area or nutrient quantities. Table 4.3 shows the φ_i calibration for each species.

The final task in calibrating species' costs is to determine what fraction of the environment's energy “budget” is borne by massive and massless losses. This fraction, ω_i , completes the specification of the environment's boundary condition. Here I make use of a certain fiction in the model and value mass losses at the full energy density of the species. In the energy BAM, I introduced a waste energy density. By using the full energy density I am effectively shifting energy from the environment's massless losses category [E] to its massive wastes category [D]. This enables consistent accounting of all masses on a given species row – a helpful feature for the equilibrium problem. If the actual energy flows of mass wastes are of biological interest, one can always perform a simple conversion.²

²Note that this method may generate negative implied massless losses, but the accounting can always be trued to the actual energy values.

	Activity Costs (Bn Kcal)				Marginal Cost Calibration		
	Mass Wastes	Massless Losses	Metabolic Costs $\beta_i m_i$	Activity Losses $\Sigma_j \phi_{ji} x_{ji}$	Scarce-Tonnes $N_i^{-1} x_{ji}$	Kcal per Scarce-Kg φ_{ji}	Kcal per Kg $\phi_{ii} = \varphi_{ii} N_i^{-1}$
	[A]	[B]	[C]	[A + B - C]	[D]	[A + B - C] / [D]	[E]
Heterotrophs							
<i>Zooplankton</i> ZP	15.7	2,327	752	1,591	0.086	18,541	211
<i>Pollock</i> PO	62.1	229	200	90.9	0.007	12,384	76.3
<i>Steller sea lion</i> SL	97.2	268	91.4	274	0.054	5,074	823
<i>Orca whale</i> OW	3.78	6.71	1.33	9.16	0.058	159	1,736
<i>Sea otter</i> SO	45.3	195	42.4	198	0.031	6,348	589
<i>Urchin</i> UR	35,506	40,113	18,965	56,654	0.086	660,303	613
Autotrophs							
<i>Phytoplankton</i> PP	73.8	11,973	903	11,145	11.5	967	967
<i>Kelp</i> KE	170	306,755	22,958	283,967	718	395	395

Notes:

[A]: Energy value of mass wastes from energy-denominated BAM.

[B]: Energy value of massless losses from energy-denominated BAM.

[D]: Prey mass consumed times scarcity of prey, summed over both prey for Orca whales. For autotrophs, total sunlight consumption.

[E]: Kcal per scarce tonne times scarcity = Kcal expenditure per tonne of consumed prey.

Table 4.3: Calibration of marginal cost of foraging prey

4.2.2 Benefits

With costs calibrated I can focus on the bioenergetic production function, F . The mass and energy BAMs above provide the necessary data to complete the calibration. In total, I know the function will yield the calibrated mass quantity Y_i , the sum of existing and new biomass and waste masses, with energy $\rho_i Y_i$. Recalling the derivations in section 3.4.3, I can set the observed input quantities equal to their expressions from equation 3.30

$$x_{ji}^* = \left(\alpha_{i0} \frac{\hat{\phi}_i \tau_i^{\varrho_{i0}}}{\hat{\phi}_{ji}} \right)^{\frac{1}{1-\varrho_{i0}}} \hat{Y}_i \quad (3.30a)$$

$$m_i^* = \left(\alpha_{i1} \frac{\hat{\phi}_i \tau_i^{\varrho_{i0}}}{\hat{\phi}_{mi}} \right)^{\frac{1}{1-\varrho_{i0}}} \hat{Y}_i. \quad (3.30b)$$

All values in these expressions are either parameterized (φ_{i0}) or calibrated from observed data ($x_{ji}^*, m_i^*, \hat{Y}_i, \hat{\phi}_i, \hat{\phi}_{ji}$) with the exception of the α_i 's and τ_i , which I calibrate

		Energy Allocations (Bn Kcal)				
		Total	Species	Environment		
		Energy Input	Ending Energy	Energy Budget	Massive Wastes ¹	Mass Share
		$(1 + \hat{\gamma})\rho_i\hat{Y}_i$	$\hat{\phi}_i\hat{M}_{1i}$		$\hat{\phi}_i\hat{d}_i$	ω_i
		[A]	[B]	[A] - [B]	[C]	[C] / ([A] - [B])
Heterotrophs						
<i>Zooplankton</i>	ZP	3,018	8.86	3,009	666	0.221
<i>Pollock</i>	PO	847	181	666	375	0.564
<i>Steller sea lion</i>	SL	438	62.5	375	9.97	0.027
<i>Orca whale</i>	OW	20.7	10.2	10.5	-	-
<i>Sea otter</i>	SO	248	6.67	241	0.525	0.002
<i>Urchin</i>	UR	93,447	17,587	75,860	241	0.003
Autotrophs						
<i>Phytoplankton</i>	PP	15,454	397	15,056	3,009	0.200
<i>Kelp</i>	KE	866,084	483,298	382,786	75,860	0.198

Notes:

1. Massive wastes are valued at the species energy density, not their actual waste density.

Table 4.4: Environment energy budget allocation

following equations (3.31), (3.32), and the definition of F_i for τ_i . A similar calibration is performed for sharing total output, Y_i , to new biomass and mass wastes.

I have now fully articulated the bioenergetic production function with calibration help from the observed ecosystem data. To perform the same process for the multi-prey sub-problem for Orca whales and autotrophs, I simply take the x_{ji} term in the production above as yet another production function of the same form, this time aggregating the two prey instead of prey and own biomass. The resulting production function is given as

$$F(x_{1i}, x_{2i}, m_i) = \tau_i \left(\alpha_{i0} (\theta_{i1} x_{1i}^{\varrho_{i1}} + \theta_{i2} x_{2i}^{\varrho_{i1}})^{\varrho_{i0}/\varrho_{i1}} + \alpha_{i1} m_i^{\varrho_{i0}} \right)^{1/\varrho_{i0}}. \quad (4.5)$$

I have thereby set the initial and boundary conditions and calibrated the intra-period dynamics. The final task is to impose the system conditions and confirm that the model solves, reproducing the BAM data as an equilibrium.

4.3 Calibration - Ecosim

The Ecosim data used for this calibration are also for the marine ecosystem surrounding the Aleutian Islands. Data for a variety of ecosystems are provided on the Ecopath with Ecosim website.³ The dataset assembled by (Gu enette & Christensen, 2005) provide the basis for the calibration here. The data provide information on the diet shares of 37 species and data on masses for two primary producers and a detritus category. Some of the 37 are actually sub-species types, e.g. stellar sea lion pups and adults. For simplicity within the BGE model, sub-species types are collapsed into a single species representative. Table 4.5 gives the mapping from the set of species as-provided to that used in the model.

To collapse the diet share data to the new species scheme I sum the diet shares and re-normalize.⁴ The diet share matrix for the Ecosim data is 81.2% sparse relative to the 90.1%-sparse GEEM data.⁵ For each predator, the matrix gives the fraction of total consumption supported by each of its prey. By definition, with predators arrayed along the columns, each column must sum to one down the rows. The “group by group” data given in the Ecosim model (Gu enette & Christensen, 2005) preserve this relation up to a *de minimus* error. Additional “group information” given within the database provides estimates of biomasses, ratios of production and consumption to biomass and of production to consumption, net “exports” out of the system, and ecotrophic efficiency.⁶

³See “Ecopath Models” www.ecopath.org/models

⁴This would ideally be a biomass-weighted average of the diet shares, but biomasses are incomplete.

⁵Sparseness is measured as the fraction of the diet share matrix, excluding primary producers and detritus, that equal zero. By way of comparison, a sample “intermediate demand” matrix for a highly disaggregated representation of the US economy (360 sectors) is 38.8% sparse. There may be some endogeneity with how economic sectors are defined that could down-bias this sparseness measure.

⁶The exports reported in the Ecosim data are identical to the species catch, implying that migration was likely not considered. Ideally, migration would be part of the net export rate.

BGE Model Species with Count of Represented Ecosim Species											
No.	Code	Description	Ct.	No.	Code	Description	Ct.	No.	Code	Description	Ct.
<i>Higher-trophic species</i>			<i>Mid-trophic species</i>			<i>Lower-trophic species</i>			<i>Primary producers & Det.</i>		
1.	ORC	Transient orca	1	11.	PEL	Lg. pelagics	2	22.	FFS	Flatfish	1
2.	TWL	Toothed whales	1	12.	MCK	Atka mackerel	1	23.	DSM	Sm. demersals	1
3.	HWL	Baleen whales	1	13.	SDL	Sandlance	1	24.	LPD	Lg. demersals	1
4.	SSL	Stellar sea lion	4	14.	HER	Herring	1	25.	DEL	Lg. deep water	1
5.	SMM	Sm. mammals	1	15.	PLK	Adult pollock	2	26.	MYC	Myctophids	1
6.	SOT	Sea otters	1	16.	POP	Pacific perch	1	27.	SHR	Shrimps	1
7.	BRD	Birds	1	17.	RKF	Rockfish	1	28.	BEI	Benthic inverts	1
8.	SME	Shark mml. pred.	1	18.	SBF	Sablefish	1	29.	EPC	Epiben pred.	1
9.	SKT	Shark & skates	1	19.	COD	Pacific cod	1	30.	CPH	Cephalopods	1
10.	SAL	Salmon	1	20.	HLB	Halibut	1	31.	ZPK	Lg. zooplankton	2
				21.	RWT	Arrowtooth	1				

Table 4.5: BGE model species with Ecosim species count

As outlined in the previous chapter, column-row or input-output balance is an essential property of the accounting tableau for the BGE model. Where the diet matrix represents the intra-period or intermediate exchange of biomass and energy, I must also account the initial conditions of the system for the exogenously modeled supplies of inputs from primary production, detritus, and starting biomass. Last, I must specify the boundary conditions of the system including ending biomass, wastes, and net exports. Consumption of primary producers is included within the diet shares matrix and estimates of starting biomasses are provided for approximately half of the species. Although consumption-to-biomass ratios are also sparse, I can combine the production-to-biomass and production-to-consumption ratios to generate a complete set of consumption-to-biomass ratios. Growth rates and net exports are given for all species, and ecotrophic efficiencies are given for approximately half of the species.⁷

In sum, given the information provided by the Ecosim dataset (Guénette & Christensen, 2005), I can populate all predator-prey interactions via the diet matrix, all boundary conditions except waste quantities for those species with missing ecotrophic efficiencies, and the initial conditions for consumption of exogenously supplied re-

⁷Zero values for growth rates and exports may be missing data.

sources but not for starting biomass. The main caveat is that the quantities of resources, all quantities in the diet share matrix, and the growth and waste quantities depend on starting biomasses, which are incomplete. To complete the biomass accounting matrices, I must first determine whether there exists a vector of biomasses that can satisfy the matrix structure I have assembled from the Ecosim data.

4.3.1 Accounting identities

To demonstrate the generality of the method, and given the large number of species, I present the data procedures abstractly. Figure 4-1 defines the set of matrices that can be partially or wholly populated using the Ecosim data. All matrix elements are expressed as fractions of the corresponding species' starting biomass. For example, the elements in the inter-species exchange matrix, X , are diet shares times the corresponding consumption-to-biomass ratio so that multiplying by biomass gives the total mass consumed of the row prey by the column predator.

$$\begin{bmatrix} x_{11} & \cdots & x_{1S} \\ \vdots & \ddots & \vdots \\ x_{P1} & \cdots & x_{PS} \end{bmatrix} \quad \begin{bmatrix} f_{11} & \cdots & f_{13} \\ \vdots & \ddots & \vdots \\ f_{P1} & \cdots & f_{P3} \end{bmatrix}$$

$$\begin{bmatrix} r_{11} & \cdots & r_{1S} \\ \vdots & \cdots & \vdots \\ r_{E1} & \cdots & r_{ES} \\ 1 & \cdots & 1 \end{bmatrix} \quad \begin{array}{l} x_{ps} = d_{ps}c_s \\ r_{es} = d_{es}c_s \\ f_{p1} = (1 + g_s) \\ f_{p2} = c_s(1 - \eta_s) \\ f_{p3} = m_s/b_s \end{array}$$

- d_{ps} : Prey p share of predator s 's total consumption
- c_s : Predator s consumption-to-biomass ratio
- g_s : Growth rate of species s
- η_s : Ecotrophic efficiency of species s
- m_s : Net exports of species s
- b_s : (Starting) biomass of species s
- $P = S$: Number of modeled species (= 31)
- E : Number of exogenously supplied species +1 for detritus (= 3)

Figure 4-1: Biomass accounting matrices for Ecosim data

The question remains whether, using the column-row identity, a set of feasible

biomasses can satisfy the accounting matrices as populated from the Ecosim data.⁸

Imposing the column-row identity gives the relation

$$\underbrace{\hat{B}}_{s \times s} \cdot \underbrace{\left[\left(\begin{array}{cc} \vec{1} \cdot X & \vec{1} \cdot R \\ 1 \times s & s \times s \end{array} \right)^T \right]}_{\text{column} = \text{input}} = \underbrace{X \cdot B + \hat{B} \cdot F \cdot \vec{1}}_{\text{row} = \text{output}}, \quad (4.6a)$$

$$\hat{B} \cdot \underbrace{\left[\left(\vec{1} \cdot X + \vec{1} \cdot R \right)^T - F \cdot \vec{1} \right]}_{\substack{N \\ s \times 1}} - \underbrace{X \cdot B}_{s \times s \cdot s \times 1} = 0, \quad (4.6b)$$

where the “hat” operator $\hat{\cdot}$ sets the vector elements along the diagonal of a symmetric matrix with zero off-diagonal elements and the $\vec{1}$ are summing vectors. The bracketed term on the left-hand side of equation 4.6b gives the net output available for inter-species exchange. That is, total input, equal to total output, less final uses (F) gives total mass available for use by predators. This is an $s \times 1$ vector I denote as N . Equivalently, the second term gives the explicit row-sum of predators’ uses of each species. If I diagonalize the net inter-species exchange output vector N I can re-arrange the equation to isolate the biomass vector B as

$$\left(\hat{N} - X \right) \cdot B = 0, \quad (4.7)$$

where I have used the relation $\hat{B} \cdot N = \hat{N} \cdot B$. Excluding the degenerate solution $B = 0$, equation 4.7 requires that

$$\text{Det} \left(\hat{N} - X \right) = 0. \quad (4.8)$$

I can interpret this statement as a requirement that there be no spontaneous production or loss of mass from inter-species exchange. Since not all ecotrophic efficiencies and starting biomasses (needed for the net export rate, m_s) are given, these matrices

⁸Note that I have assumed net exports as a fraction of species biomass.

cannot be fully populated from the Ecosim data; however, I can examine the size of the determinant using average values for those species with missing data. Table 4.6 presents the known biomasses and growth rates along with the known and estimated values for consumption-to-biomass ratio, ecotrophic efficiency, export rate, and energy densities.

Energy densities are not provided in the Ecosim data but are essential for the energy presentation of the BGE model's accounting matrices. A limited set of energy densities are available from Tschirhart's General Equilibrium Ecosystem Model (GEEM) as given in (Finnoff & Tschirhart, 2003). The GEEM data contain eight species leaving twenty-five species energy densities to be estimated. I exploit the inverse relationship between trophic sequence and energy density and estimate a 2nd-order polynomial as

$$\tilde{\rho} = 2,571.8 - 99.26\tau + 1.25\tau^2, \quad (4.9)$$

where ρ is the energy density and $\tau \in [1, 40]$ the trophic sequence, taken as the average trophic sequence in cases where multiple Ecosim species are contained within a BGE species definition.

Using the values presented in Table 4.6, the determinant from equation 4.8 does not evaluate to zero. The determinant is several orders of magnitude large, suggesting that minor *ad hoc* revisions will likely be insufficient. To proceed I will resort to numerical methods to identify a minimally-revised set of accounting matrices satisfying column-row balance for a given vector of biomasses.

4.3.2 Data revision

The numerical program will accept the complete diet share matrix, consumption-to-biomass ratios, and growth rates as correct and revise only the incomplete data; i.e., energy densities (ρ), starting biomasses (B), ecotrophic efficiencies (η), and export

Ecosim data for BGE model initial and boundary conditions							
Trophic Seq.	BGE Code	Biomass (t km ⁻²)	Cons. / Biomass	Eco-trophic Efficiency	Growth Rate	Export Rate	Energy Density
<i>Higher-trophic species</i>							
1.	ORC	0.001	10.830	0.860	0.000	0.000	2,473.8
2.	TWL	0.013	11.073	0.860	-0.025	0.042	2,378.3
3.	HWL	0.145	6.990	0.860	-0.020	0.046	2,285.3
4.	SSL	0.045	92.328	0.860	0.000	0.006	2,063.8
5.	SMM	0.022	22.741	0.860	-0.010	0.017	1,858.0
6.	SOT	0.004	86.400	0.860	0.000	0.002	1,780.1
7.	BRD		65.350	0.950	0.000	0.000	1,704.6
8.	SME	0.050	0.625	0.860	0.000	0.006	1,631.7
9.	SKT	2.600	0.795	0.860	0.000	0.006	1,561.3
10.	SAL		4.330	0.500	0.000	0.014	1,493.4
<i>Mid-trophic species</i>							
11.	PEL		2.560	0.950	0.000	0.000	1,396.3
12.	MCK	13.500	1.700	0.860	0.000	0.000	1,304.8
13.	SDL		3.650	0.950	0.000	0.000	1,246.9
14.	HER		0.970	0.950	0.000	0.000	1,191.6
15.	PLK	3.376	3.340	0.860	0.000	0.004	1,113.3
16.	POP	1.109	0.680	0.860	0.000	0.028	1,040.6
17.	RKF		1.000	0.950	0.000	0.014	995.3
18.	SBF	1.799	1.030	0.860	-0.020	0.006	952.5
19.	COD	2.400	2.280	0.860	0.030	0.004	912.2
20.	HLB		1.267	0.900	0.030	0.014	874.5
21.	RWT	0.500	2.000	0.860	0.000	0.004	839.2
<i>Lower-trophic species</i>							
22.	FFS		1.720	0.500	0.000	0.014	806.4
23.	DSM		3.000	0.950	0.000	0.000	776.2
24.	LPD		2.000	0.950	0.000	0.014	748.4
25.	DEL		2.000	0.950	0.000	0.000	723.2
26.	MYC		3.650	0.950	0.000	0.000	700.5
27.	SHR		10.200	0.950	0.000	0.000	680.3
28.	BEI		8.430	0.950	0.000	0.000	662.6
29.	EPC		5.000	0.950	0.000	0.014	647.4
30.	CPH		7.160	0.950	0.000	0.000	634.7
31.	ZPK		64.210	0.950	0.000	0.000	620.4
Pct. estimated:			22.6%	45.2%	0.0%	19.4%	80.6%
Notes:							
1. Growth rates are from the Ecosim bio-accumulation variable.							
2. Export rate equals net exports over biomass.							
3. Italicized figures are estimated.							
4. Energy densities are estimated using GEEM data by a 2 nd -order polynomial in the average trophic sequence of the Ecosim species represented by the BGE species.							

Table 4.6: Ecosim original & est. values for BGE calibration

rates ($\chi_s = m_s/b_s$). I will introduce one additional variable, a massless energy losses multiplier (μ), to facilitate the energy balance. A sum-of-squares objective function will penalize deviations from the known values of the revised parameters. The mathematical program is stated as

$$\begin{aligned}
 \mathbf{Given:} \quad & X \in \mathbb{R}^{S \times S}, R \in \mathbb{R}^{E \times S}, G \in \mathbb{R}^S \\
 & B, \eta, \chi \in \mathbb{R}^S, \rho \in \mathbb{R}^{I=S+E} \\
 \\
 \mathbf{Find:} \quad & B', \eta', \chi', \mu \in \mathbb{R}^S, \rho' \in \mathbb{R}^I \text{ to minimize} \\
 & \textit{Sum of squared deviations} \\
 f(\rho', B', \eta', \mu) = & \sum_s [(100[(1 - \eta_s) - \mu_i(1 - \eta'_s)])^2 + \\
 & (b_s - b'_s)^2] + \sum_i (0.01(\rho_i - \rho'_i))^2 \\
 \\
 \mathbf{Subject to:} \quad & \textit{Mass balance} \quad \eta'_s(b'_s(1 + \sum_e r_{es} + \sum_p x_{ps})) \\
 & = \sum_p x_{sp}b'_p + b'_s((1 + g_s) + \chi'_s) \quad \forall s \\
 & \textit{Energy balance} \quad b'_s(\rho'_s + \sum_e \rho'_e r_{es} + \sum_p \rho'_p x_{ps}) \\
 & = \rho'_s \left(\sum_p x_{sp}b'_p + b'_s((1 + g_s) + \chi'_s) \right) \\
 & + \mu_s(1 - \eta'_s)E_{\text{in}} \quad \forall s \\
 & \textit{Realistic bounds} \quad e^{-5} \leq B' \leq e^4, \\
 & 0.05 \leq \eta' \leq 0.95, \\
 & -0.05 \leq \chi' \leq 0.05, \\
 & 0.10 \leq \mu \leq 10, \\
 & 0.75\rho \leq \rho' \leq 1.25\rho,
 \end{aligned}$$

where E_{in} equals the left-hand side of the energy balance equation or total energy input and I have scaled the variables' squared errors to comparable orders of magnitude.⁹ The massless losses multiplier adjusts for the fact that I incorrectly value mass wastes at the higher biomass energy density (ρ'_s) and for the fact that certain energetic losses are not mass embodied. While growth rates are held fixed at the given values, the program can solve for alternative growth rates, including a no-growth steady state or population declines.

⁹Note that this is somewhat analogous to the economic matrix balancing conducted in Chapter 2. There I relied on an entropy metric instead of the simpler least-squares metric used here.

	ORC	TWL	HWL	SSL	SMM	SOT	BRD	SME	SKT	SAL	PEL	MCK	SDL	HER	PLK	POP	RKF	SBF	COD	HLB	RWT	FFS	DSM	LPD	DEL	MYC	SHR	BEI	EPC	CPH	ZPK	EX	EB	EW	
ORC																																1.98	39.6	349	
TWL								0.519																								-0.017	30.1	129	
HWL	3.96							1.57																								11.4	325	893	
SSL	286							2.38																								3.99	79.8	3,564	
SMM	48.3							0.232																								2.04	40.5	426	
SOT	9.26																															0.139	2.79	89.7	
BRD	2.96							0.213																								-0.004	0.087	0.171	
SME								4.08																								2.55	81.7	28.0	
SKT	0.225		39.0					7.54	9.68																							203	4,059	1,433	
SAL	34.2	2.88	600	14.9		0.155	1.02	136		25.6																						-92.0	1,839	2,562	
PEL	10.0	202		59.0		1.00	1.43	25.8		111									112	0.094	52.4			52.2				716			-54.7	1,094	125		
MCK	2.82	177	1,757	65.9	7.07	0.096		111							259				1,077	14.1	255	15.1		83.7						410	17,615	10,715			
SDL		46.6	11.1	21.8	6.74	0.522		23.2					56.5				1.15		40.3	1.93		26.0					161				-11.8	235	32.6		
HER	1.37	2.17		25.0		0.132	0.260	49.3		112											2.31		73.7								-28.4	569	42.4		
PLK	1.76	101	93.5	62.9		0.142	0.868	152		22.4	1,559				31.6		1.03		252	7.07	122	7.74	15.0	7.59						-188	3,758	4,999			
POP						0.003	0.065												11.2			14.5									-57.7	1,154	491		
RKF	0.143	1.31	58.7	6.96		0.003	0.559	14.4																							-6.58	132	10.9		
SBF	0.137			2.86			0.208	80.7											10.3	1.09	10.2										85.7	1,679	985		
COD	0.394	2.03	241	18.7		0.107	0.228	20.7											9.85	0.431	1.77									109	2,255	4,007			
HLB							0.409	43.4																							2.38	48.9	10.6		
RWT			36.0				4.13	24.3																							21.0	420	801		
FFS			95.1	10.5			0.277	65.0											13.1	0.218										54.3	1,085	1,324			
DSM	3.36	29.0	566	47.3	31.5		1.19	41.7				35.3			153		0.616		687	2.57	30.8	16.2	75.1	0.882					-34.8	697	125				
LPD			148				0.560	52.6		6.04									60.6	0.961	23.9		46.3	23.0						10.6	213	30.8			
DEL							0.586	10.5								1.64			66.3	0.928	23.1	11.7								0.121	65.6	9.50			
MYC	2.01		32.3	10.4		0.191	0.326	33.1		13.3	142				988	13.1	0.092		150	1.27	179	339	3.74	0.395	0.759	5.08		180		-34.7	695	145			
SHR				3.39			0.042	247		21.2	77.0				536	0.512	33.6		1,036	0.870	122	206	104	12.7	80.6			2.01	87.4	-14.5	290	150			
BEI	1.85			3.20	52.1	0.024	0.120	183		86.6	786				692	11.6	20.0	23.8	270	0.780	23.6	611	1,057	32.0	9.67	65.4	1,119	64.8	1,294	827	13.6	961	432		
EPC				3.15	1.71		0.079	53.5		330					21.4	4.75			215	7.67		58.5	217	89.6				84.0	651	18.7	373	112			
CPH	68.4	8.60	179	120		0.875	4.95	208	383	71.8	1,715				110	2.71	1.14	129	279	16.0	3.48	137	25.1	2.45	33.4					-2.26	518	215			
ZPK	1.74	331		0.302		0.085		80.0	1,773	827	10,293		375	280	4,426	429	23.8	989	16.3		32.2	120	143	143		2,024	527		256	935	8,733	6.80	538	1,756	
PHY																																			21,453
MPH										1,129	61.0		41.7														110		145	51.9	156				
DET							0.776	28.9			13.8				31.0		0.161		170	2.13	3.53			8.28		1,060	7,469	180		4,336					
SB	39.6	30.9	331	79.8	40.9	2.79	0.087	81.7	4,059	1,839	1,094	17,615	235	569	3,758	1,154	132	1,714	2,189	47.5	420	1,085	697	213	65.6	695	290	961	373	518	538				

Table 4.7: Energy Biological Accounting Matrix (eBAM) for Ecosim data

The final results of the revision process are summarized in the form of an energetic BAM in figure 4.7. The revised initial and boundary conditions for the BGE model stay close to the given values with the exception of export rates, whose deviations are not penalized but whose levels are tightly bound in the interval $\pm 5\%$. Table 4.8 presents the given and revised values for the BGE model for comparison.

The final outcome of the revision process is a balanced set of mass and energy accounting matrices for the 31 modeled species, two exogenous primary producers, and one detritus stock. Given balanced accounting matrices, the next section will specify the structure for the BGE model.

4.4 Model structure

The model is programmed and solved numerically using the Mathematical Programming System for General Equilibrium analysis (MPSGE) within the General Algebraic Modeling System (GAMS) software.¹⁰ The constant elasticity of substitution (CES) function is a key feature of this modeling system, enabling a simplified and thereby less error-prone specification of the model equations. This software handles the calibration tasks described in Chapter 3.

A structure of linkages among the system species and environment underlies the data calibration procedures from the previous sections. This structure is commonly depicted in a stylized ‘stick figure’ diagram that details both input and output linkages along with substitution parameters. For example, in addition to depicting the linkage between Orca whales and their prey, the diagram will provide the degree of switching (or elasticity of substitution) between these prey. Figure 4-2 diagrams the structure of Orca whale biomass and waste production for the model as calibrated to the GEEM data, with only two prey, and to the Ecosim data, with five prey. The structure is generalized for the Ecosim data to demonstrate how the same general bioenergetic

¹⁰See www.mpsge.org/mainpage/mpsge.htm and www.gams.com.

Ecosim data as given and as revised for BGE model											
Trophic	BGE	Biomass (t km ⁻²)		Eco-trophic Efficiency			Export Rate		Energy Density		
		Seq.	Code	Given	Revised	Given	Revised	Energy	Given	Revised	Given
<i>Higher-trophic species</i>											
	1.	ORC	0.001	0.016	<i>0.860</i>	0.089	0.107	0.000	0.050	2,474	2,474
	2.	TWL	0.013	0.013	<i>0.860</i>	0.082	0.192	0.042	-0.001	<i>2,378</i>	2,378
	3.	HWL	0.145	0.145	<i>0.860</i>	0.129	0.277	0.046	0.034	<i>2,285</i>	2,285
	4.	SSL	0.045	0.039	<i>0.860</i>	0.050	0.095	0.006	0.050	2,064	2,064
	5.	SMM	0.022	0.022	<i>0.860</i>	0.094	0.176	0.017	0.050	<i>1,858</i>	1,858
	6.	SOT	0.004	0.002	<i>0.860</i>	0.050	0.120	0.002	0.050	1,780	1,780
	7.	BRD		0.000	0.950	0.561	0.950	0.000	-0.050	<i>1,705</i>	1,705
	8.	SME	0.050	0.050	<i>0.860</i>	0.665	0.759	0.006	0.031	<i>1,632</i>	1,632
	9.	SKT	2.600	2.600	<i>0.860</i>	0.593	0.751	0.006	0.050	<i>1,561</i>	1,561
	10.	SAL		1.231	0.500	0.261	0.500	<i>0.014</i>	-0.050	<i>1,493</i>	1,493
<i>Mid-trophic species</i>											
	11.	PEL		0.788	0.950	0.612	0.950	0.000	-0.050	<i>1,396</i>	1,388
	12.	MCK	13.500	13.500	<i>0.860</i>	0.459	0.671	0.000	0.023	<i>1,305</i>	1,305
	13.	SDL		0.189	0.950	0.566	0.950	0.000	-0.050	<i>1,247</i>	1,245
	14.	HER		0.477	0.950	0.719	0.950	0.000	-0.050	<i>1,192</i>	1,192
	15.	PLK	3.376	3.376	<i>0.860</i>	0.368	0.546	0.004	-0.050	1,113	1,113
	16.	POP	1.109	1.109	<i>0.860</i>	0.579	0.696	0.028	-0.050	<i>1,041</i>	1,041
	17.	RKF		0.132	0.950	0.787	0.950	<i>0.014</i>	-0.050	995	995
	18.	SBF	1.799	1.799	<i>0.860</i>	0.538	0.655	0.006	0.050	953	953
	19.	COD	2.400	2.400	<i>0.860</i>	0.370	0.399	0.004	0.050	912	912
	20.	HLB		0.054	0.900	0.883	0.900	<i>0.014</i>	0.050	874	874
	21.	RWT	0.500	0.500	<i>0.860</i>	0.401	0.387	0.004	0.050	839	839
<i>Lower-trophic species</i>											
	22.	FFS		1.346	0.500	0.448	0.500	<i>0.014</i>	0.050	806	806
	23.	DSM		0.898	0.950	0.855	0.950	0.000	-0.050	776	776
	24.	LPD		0.284	0.950	0.918	0.950	<i>0.014</i>	0.050	748	748
	25.	DEL		0.091	0.950	0.917	0.950	0.000	0.002	723	723
	26.	MYC		0.998	0.950	0.853	0.950	0.000	-0.050	700	696
	27.	SHR		0.428	0.950	0.876	0.950	0.000	-0.050	680	678
	28.	BEI		1.499	0.950	0.905	0.950	0.000	0.014	663	641
	29.	EPC		0.592	0.950	0.950	0.950	<i>0.014</i>	0.050	<i>647</i>	631
	30.	CPH		0.720	0.950	0.950	0.949	0.000	-0.004	635	719
	31.	ZPK		0.889	0.950	0.950	0.950	0.000	0.013	620	604
		Min:	0.001	0.000	0.500	0.050	0.095	0.000	-0.050	620	604
		Mean:	1.826	1.167	0.894	0.564	0.678	0.014	0.005	1,229	1,229
		Max:	13.500	13.500	0.950	0.950	0.950	0.046	0.050	2,474	2,474

Notes:

1. Italicized figures are estimated.
2. Energy densities are estimated using GEEM data by a 2nd-order polynomial in the average trophic sequence of the Ecosim species represented by the BGE species.
3. Energy eco-trophic efficiency includes the effect of the massless losses multiplier.

Table 4.8: Given & revised values for initial & boundary conditions

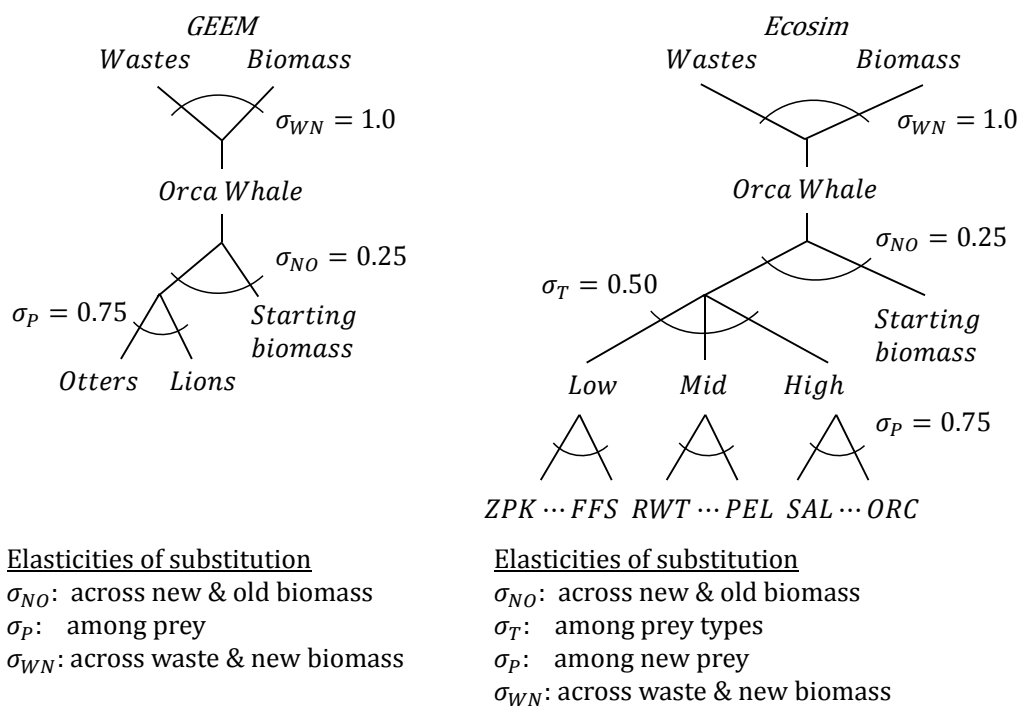


Figure 4.2: Production structures for Orca whales

production structure applies to all species.

In the baseline specification, all species have the same elasticities of substitution among prey, across prey and existing biomass, and between waste and new biomass. Only primary producers and Orca whales have multiple prey (sunlight and nutrients for primary producers) in the GEEM data, which simplifies the structure for all other species. Species' ability to substitute between prey and starting biomass is limited relative to their ability to substitute among prey. This feature of the production structure imposes diminishing returns to consuming additional prey, thereby limiting the extent to which species grow each period. Last, substitution among waste and new biomass is permitted to allow for proportionally more waste to be produced when

a species prey are more scarce; i.e., they are expending more energy, and thereby generating more waste, per unit of prey.

The supply of exogenous resources is also elastic. These are nutrients and sunlight in the GEEM data or primary producers and detritus in the Ecosim data. Species preying on exogenous resources can draw more into the system but only with increasing effort. The energy expended to draw in additional resources is assumed to rise 1.11% for each additional 1% in resource quantities taken in by primary producers (i.e. an elasticity of 0.9). Species are assumed to compete for the same pool of exogenous resources, which drives the energetic expenditure required to secure them.

To close the model, I require that the quantity of system energy embodied in wastes and ending biomasses at the end of the period equal the starting quantity from biomass plus additional energy from exogenous resources. The model equations require the conservation of expended energy, or starting energy times its scarcity value as determined in the model. The discrepancy between this measure and the quantity of supplied energy has proven slight in model runs and in practice the difference in starting and ending energies can be apportioned to additional wastes. For the purposes of model specification, wastes and biomasses are aggregated into a final quantity whose energetic value must equal the starting value of energy supplied to the model. Section 3.4.5 provides an alternate description of the closure assumptions. Figure 4-3 diagrams the overall model structure illustrating how exogenous resources and starting biomasses are converted to wastes and biomass, which are aggregated to total ending energy.

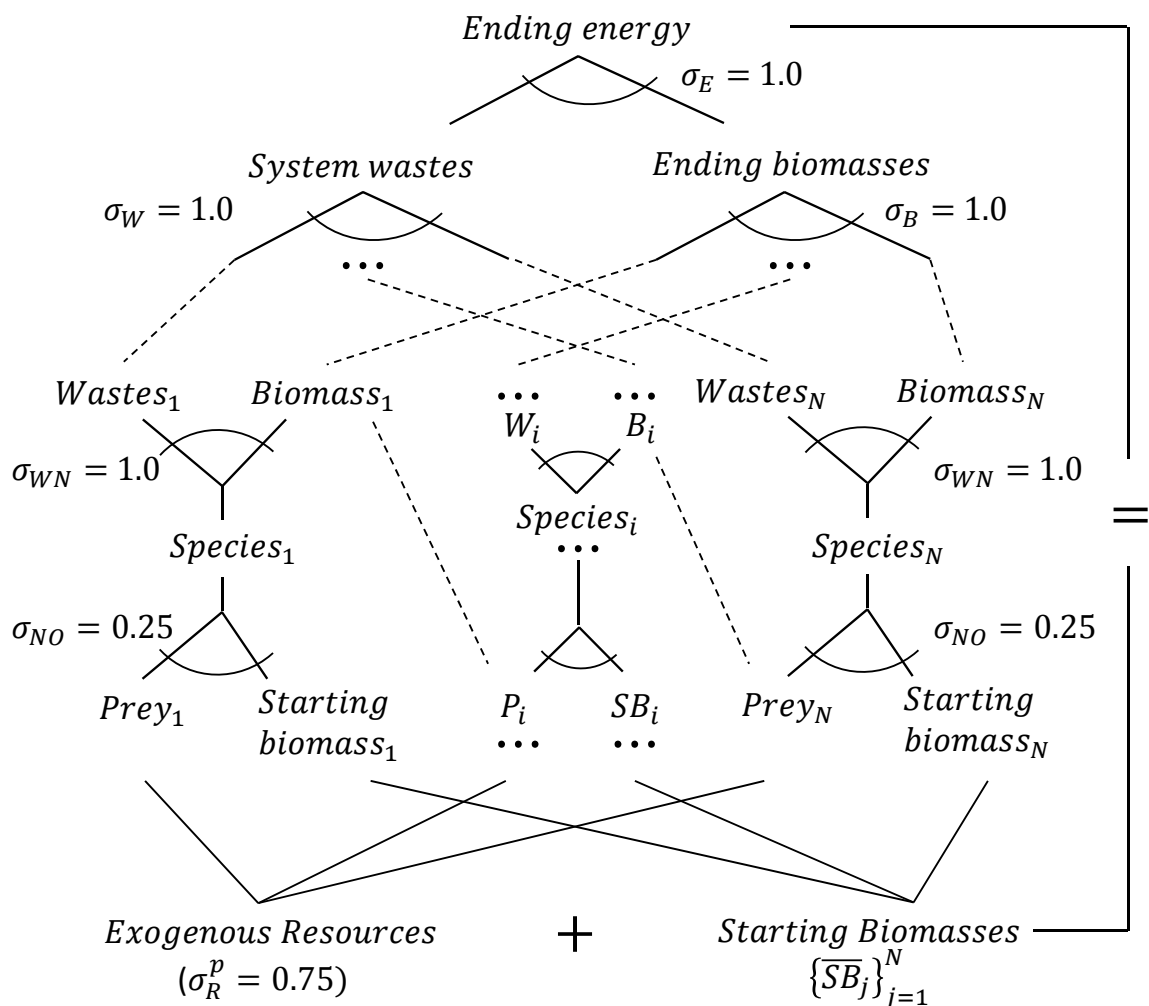


Figure 4-3: Ensemble of modeled ecosystem's production structures

4.5 Results

4.5.1 Overview

I evaluate one baseline and four counter-factual scenarios to demonstrate the BGE model's behavior. The model is solved for twenty-five consecutive periods (each a representative year) for each scenario run. After the model solves for ending biomass levels in each period, those biomasses are used to set the following period's starting biomasses. In all model runs with the benchmark parameterization, the twenty-five year period proved sufficient for perturbed populations to reach a new steady-

state equilibrium. For each scenario, I compare results from the GEEM and Ecosim datasets along with an aggregated version of the Ecosim data intended to mimic the species resolution of the GEEM data. All results are presented relative to the unperturbed baseline scenario outcomes of the model. This is important for the Ecosim dataset where baseline growth rates are non-zero.

I conduct monte carlo analyses to examine the sensitivity of the model outcomes to changes in the benchmark parameterization. I report the distribution about the benchmark biomass outcomes generated from 250 draws from a distribution of parameter values. The monte carlo analyses first vary five parameter values one at a time for 25 iterations each. Results from these iterations indicate the relative sensitivity of model outcomes to each of the key model parameters. I use a mean squared error metric to assess the amount of variation induced by each parameter's variation. Next, I take a "buckshot" approach to model sensitivity by taking random draws for all parameters over 125 monte carlo iterations. Table 4.13 reports the benchmark values and range of the parameters varied in the monte carlo analysis.

4.5.2 Baseline diagnostics

To provide an initial assessment of the ecosystems represented in the model runs, Table 4.9 provides summary metrics for all three datasets. The most marked difference is in the aggregates between the GEEM and Ecosim data. Total energy and mass measures are significantly larger in the GEEM data. Aggregate measures will not challenge comparison, which is done in relative terms, but could mute shock responses to species that are represented as "larger" in the GEEM data. The weighted average energy density also appears lower in the Ecosim data. Ascendancy declines for the Ecosim data on aggregating, to an even smaller measure than the GEEM data the aggregation is intended to mimic. In general, intra-period flows and system exports are closer together across datasets than the aggregates.

System metrics by model				
Metric	Units	Baseline		
		GEEM	EwE	EwE-Sm
<i>Aggregate System Metrics</i>				
Total system throughput (energy)	Bn. Kcal	875,847	135,267	135,138
Total system throughput	MMT	971	252	253
Total biomass		614	36	36
Primary production		730	60	60
Ascendancy	None	0.63	1.28	0.45
<i>Intra-Period Flows</i>				
Respiratory flows	Bn. Kcal		20,678	22,196
Consumption	MMT	101.8	91.0	87
Detrital flows		139.9	43.5	45
<i>System Exports</i>				
Net exports	MMT		0.4	-0.8
Total catch		(N/A)	0.8	0.2
Mean trophic sequency of catch	None		14.1	7.5

Table 4.9: Ecosystem metrics for model datasets

The first benchmark model scenario generates a set of population levels over the 25-year period to demonstrate the stability of baseline model behavior. Baseline growth rates are all zero for the GEEM data so these results are not presented. Absent external estimates, zero-growth was assumed in order to calibrate the GEEM data, but growth rates from the Ecosim data for GEEM species were also zero (or perhaps missing). (Population levels for baseline solves with zero growth do not change over the model period.) Three different stylized growth scenarios (given in Tables 4.10 and 4.11) are run to examine the behavior of the model on GEEM data with growth and the Ecosim data under alternate growth assumptions.¹¹

¹¹Given the volume and dimensionality of figures produced, some figures are rather small; however, all are vectorized and will zoom to a readable size.

Growth Scenario	PP	ZP	PO	SL	OW	SO	UR	KE
1. Uniform	0.020	0.020	0.020	0.020	0.020	0.020	0.020	0.020
2. Discrete	0.020	-0.020	0.000	-0.020	0.000	0.020	0.020	-0.020
3. Random	0.029	0.009	0.048	-0.037	0.008	0.027	-0.023	-0.023

Table 4.10: GEEM species growth rates for growth scenarios

BGE Model Species with Growth Rates by Scenario											
Species			Growth			Species			Growth		
No.	Code	Description	Base	Disc.	Rand.	No.	Code	Description	Base	Disc.	Rand.
<i>Higher-trophic species</i>						<i>Mid-trophic species (cont.)</i>					
1.	ORC	Transient orca	0.00%	0.00%	-3.70%	17.	RKF	Rockfish	0.00%	-1.00%	0.31%
2.	TWL	Toothed whales	-2.50%	-1.00%	0.91%	18.	SBF	Sablefish	-2.00%	0.00%	-2.75%
3.	HWL	Baleen whale	-2.00%	1.00%	1.12%	19.	COD	Pacific cod	3.00%	0.00%	4.95%
4.	SSL	Stellar sea lion	0.00%	-2.00%	-1.56%	20.	HLB	Halibut	3.00%	-2.00%	-2.80%
5.	SMM	Sm. mammals	-1.00%	2.00%	1.27%	21.	RWT	Arrowtooth	0.00%	2.00%	-3.88%
6.	SOT	Sea otter	0.00%	-1.00%	-2.59%	<i>Lower-trophic species</i>					
7.	BRD	Birds	0.00%	-1.00%	1.45%	22.	FFS	Flatfish	0.00%	-1.00%	-3.45%
8.	SME	Shark mml. pred.	0.00%	1.00%	0.33%	23.	DSM	Sm. demersals	0.00%	-1.00%	-2.99%
9.	SKT	Shark & skates	0.00%	2.00%	-1.81%	24.	LPD	Lg. demersals	0.00%	-1.00%	0.11%
10.	SAL	Salmon	0.00%	1.00%	4.96%	25.	DEL	Lg. deep water	0.00%	0.00%	-3.81%
<i>Mid-trophic species</i>						26.	MYC	Myctophids	0.00%	2.00%	-2.12%
11.	PEL	Lg. pelagics	0.00%	2.00%	-3.61%	27.	SHR	Shrimps	0.00%	2.00%	-0.34%
12.	MCK	Atka mackerel	0.00%	-2.00%	3.98%	28.	BEI	Benthic inverts	0.00%	0.00%	1.21%
13.	SDL	Sandlance	0.00%	-1.00%	1.17%	29.	EPC	Epiben pred.	0.00%	-2.00%	1.69%
14.	HER	Herring	0.00%	-2.00%	-2.80%	30.	CPH	Cephalopods	0.00%	1.00%	-0.41%
15.	PLK	Adult pollock	0.00%	1.00%	3.57%	31.	ZPK	Lg. zooplankton	0.00%	2.00%	0.99%
16.	POP	Pacific perch	0.00%	0.00%	-1.78%						

Table 4.11: Ecosim species growth rates for growth scenarios

Three BGE models are run on the two datasets. The first model is calibrated to GEEM data, the second and third are calibrated to Ecosim data, but the third model aggregates to nine species to mimic the resolution of the GEEM data. Figure 4.12 shows how the Ecosim species are mapped to the smaller species set for Model 3 (Ecopath with Ecosim Small - EwE-Sm).

The base growth scenario for the Ecosim species are as given in the Ecosim data (zero for many). The uniform scenario simply grows all species at 2% (not presented in

Ecosim Species Mapping								
No.	Code	Description	No.	Code	Description	No.	Code	Description
<i>Whales (WHL)</i>			<i>Large fish (LGF)</i>			<i>Small fish (SMF)</i>		
1.	ORC	Transient orca	11.	PEL	Lg. pelagics	23.	DSM	Sm. demersals
2.	TWL	Toothed whales	12.	MCK	Atka mackerel	24.	LPD	Lg. demersals
3.	HWL	Baleen whales	13.	SDL	Sandlance	25.	DEL	Lg. deep water
						26.	MYC	Myctophids
<i>Other mammals (MML)</i>			<i>Harvested fish (HVF)</i>			<i>Bottom feeders (BTM)</i>		
4.	SSL	Stellar sea lion	10.	SAL	Salmon	27.	SHR	Shrimps
5.	SMM	Sm. mammals	14.	HER	Herring	28.	BEI	Benthic inverts
6.	SOT	Sea otters	15.	PLK	Adult pollock	29.	EPC	Epiben pred.
			16.	POP	Pacific perch	30.	CPH	Cephalopods
<i>Birds (BRD)</i>			19.	COD	Pacific cod	31.	ZPK	Lg. zooplankton
7.	BRD	Birds	20.	HLB	Halibut			
<i>Big fish (BGF)</i>			<i>Medium fish (MDF)</i>					
8.	SME	Shark mml. pred.	17.	RKF	Rockfish			
9.	SKT	Shark & skates	18.	SBF	Sablefish			
			21.	RWT	Arrowtooth			
			22.	FFS	Flatfish			

Table 4.12: Mapping of Ecosim species to small species set

Table 4.11). The discrete random scenario grows species at a rate randomly selected from the set $\{-2\%, -1\%, 0\%, 1\%, 2\%\}$. Last, the random growth scenario selects rates from the interval $[-5\%, 5\%]$. Tables 4.10 and 4.11 report the selected growth rates.

The baseline model runs (with or without growth) ultimately reach steady-state population levels in nearly all cases. The flatness of the steady-state outcomes are largely a result of the baseline model runs' unrealistic assumption of no variability in resource availability. I add these features in the counter-factual scenarios, but the steadiness of the baseline solves gives confidence that the baseline activity is not unduly influencing the counter-factual outcomes.

Figure 4-4 shows stable population levels for all species in all growth scenarios on the GEEM data after 5 – 10 years of the simulation (see e.g. Table 4.1 for a list of

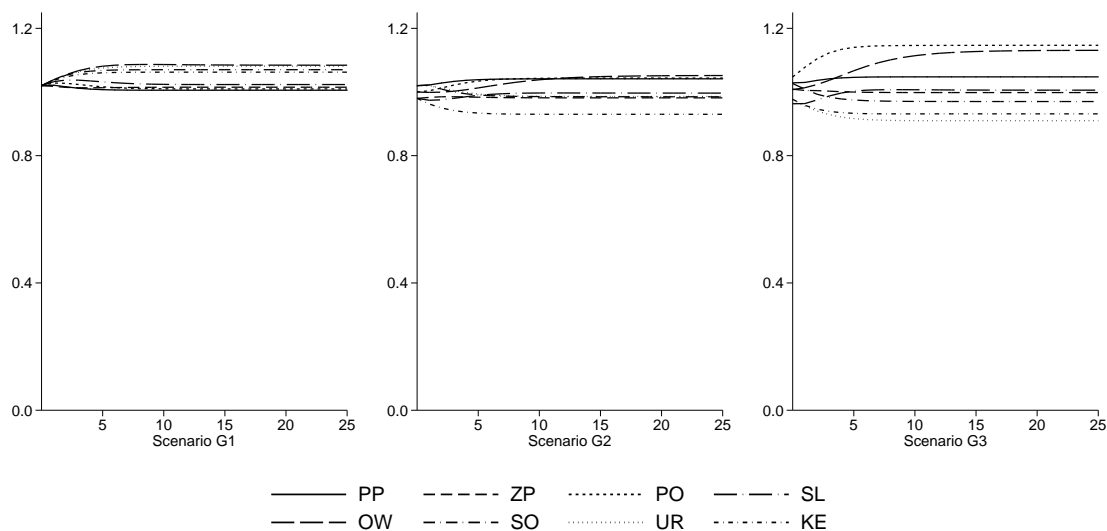


Figure 4-4: Model 1 (GEEM) growth scenarios' population outcomes

species codes). The calibrated zero-growth scenario is not presented – it simply produces straight lines. Results are qualitatively similar for Model 3 (EwE-Sm) although the trajectories are somewhat more smooth. This likely owes to the greater richness in the species diets. Figure 4-5 presents these results including the baseline-growth scenario (G0) based on the growth rates given in the Ecosim data.

The population trajectories are more varied for the full set of Ecosim species in Model 2 (EwE) presented in Figure 4-6.¹² This is particularly evident for certain mid-trophic species in the discrete (G2) and random (G3) growth scenarios. Halibut (HLB) and herring (HER) populations show marked and persistent declines in the discrete scenario, where each species had the lowest possible growth rate (-2%). Three other species (stellar sea lions, SSL; mackerel, MCK; epibenthic predators, EPC) were assigned this growth rate but achieved stable population levels early in the simulation. In the random growth scenario pelagics (PEL) are assigned a -3.61%

¹²To balance the figure, arrowtooth flounder (RWT) are not presented. They were chosen for omission since they have relatively few predators that depend heavily on them and they have little to no commercial value.

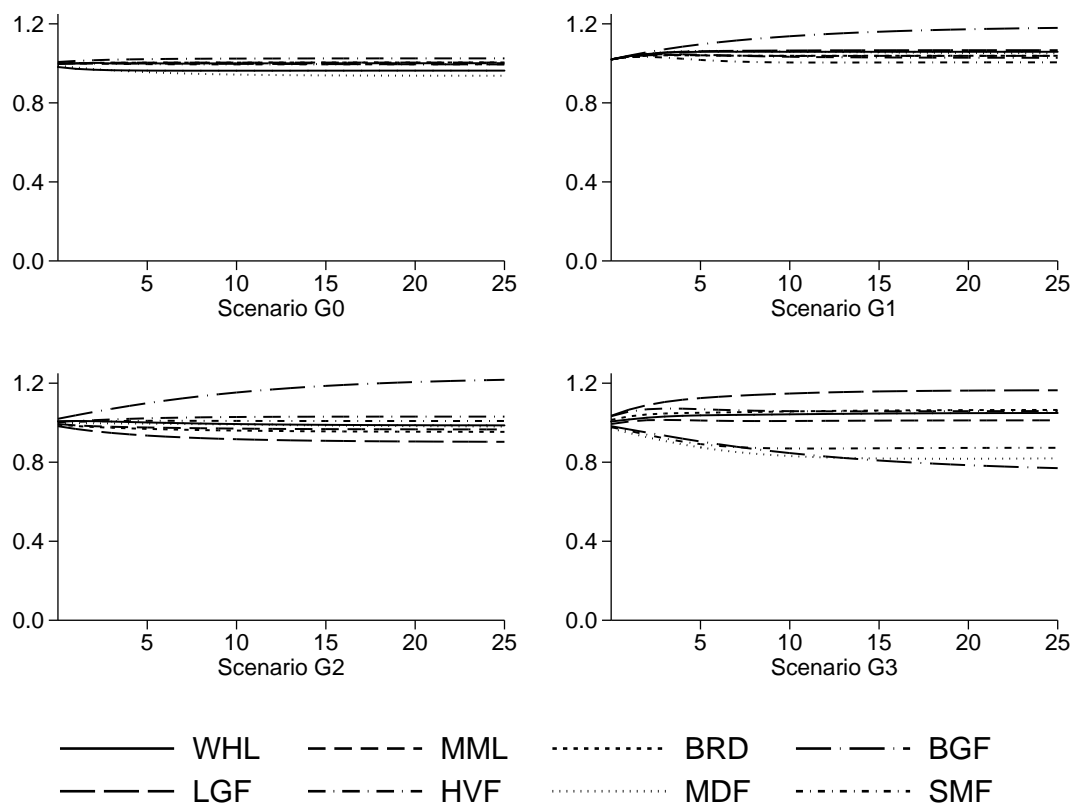


Figure 4-5: Model 3 (EwE-Sm) growth scenarios' population outcomes

growth rate and are not able to recover, exhibiting a persistent decline throughout the period. This is the fourth most negative growth rate assigned. The Orca population is robust to the assigned -3.70% decline with a roughly commensurate decline in population levels whereas large deep-water fish (DEL, -3.81%) and arrowtooth flounder (RWT, -3.88% , not presented) populations declined by approximately 20% before stabilizing.

The results for all three baseline growth scenarios are encouraging. In each case the assumed or observed growth rates generate stable population levels from which I can measure the divergence induced by the stylized shocks imposed on the model. The observed population outcomes are emergent from the dynamics of the specified micro-

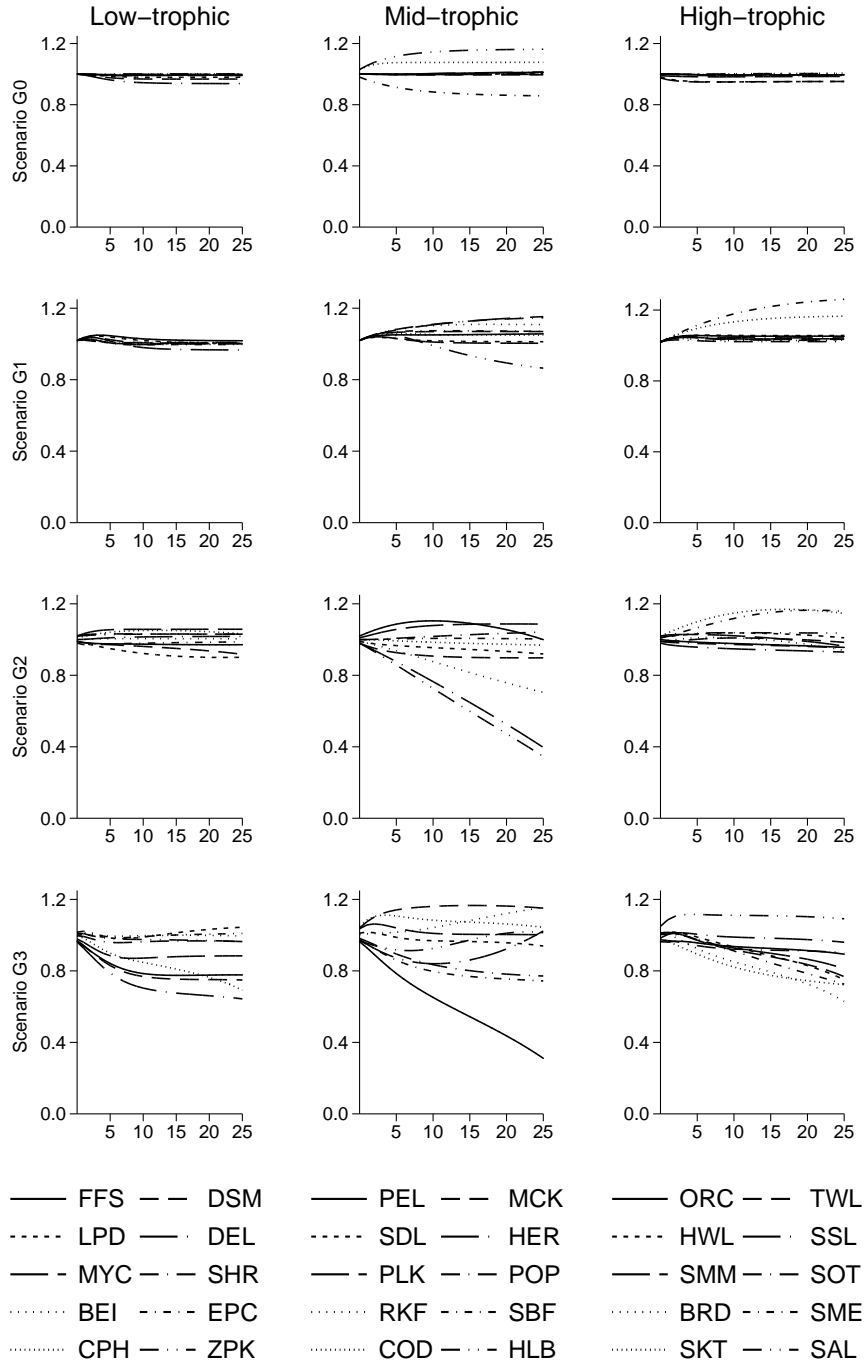


Figure 4-6: Population outcomes for Model 2 (EwE) growth scenarios

level bioenergetics. Emergent outcomes in complex systems are not always intuitive and sometimes intractable. For key outcomes of the counter-factual scenarios, I will offer additional “forensics” on the causal mechanisms at play.

4.5.3 Benchmark counter-factual scenarios

Four stylized scenarios are presented below to examine the BGE model’s behavior. Each scenario targets different aspects of the ecosystem structure with the intent of inducing certain population outcomes. Population levels for all model species across the three models are presented relative to their baseline outcomes. This preserves the baseline growth dynamics of the species (null in Model 1) within the model while depicting only the impact of the shocks imposed by the scenario. That is, as presented, the population levels would be constant at 1 absent any shocks.

Scenario 1: Starve The System (STS)

The first scenario shocks the system’s primary producers and resources. In the GEEM data, the relevant primary producers are phytoplankton and kelp and in the Ecosim data they are phytoplankton and macrophytes, or just primary producers for the small set in Model 3. Detrital resources are also shocked for the Ecosim-based models (2 & 3). Shocks are implemented by reducing their productivity by 10% for Model 1, where primary production is endogenously modeled. The starting quantity of resources is reduced by 10% for Models 2 & 3, where primary production is exogenous.

The population effects are pronounced but generally not very large in magnitude. In both Ecosim models all populations experience a subtle decline with a smooth transition (Figures 4-7 & 4-8b). The population effects are larger and more varied for Model 1 (GEEM, Figure 4-8a). The kelp population is more sensitive to the 10% productivity shock than the zooplankton population. Kelp prey, urchins, and in turn urchin prey, sea otters, experience marked declines of approximately 40%.

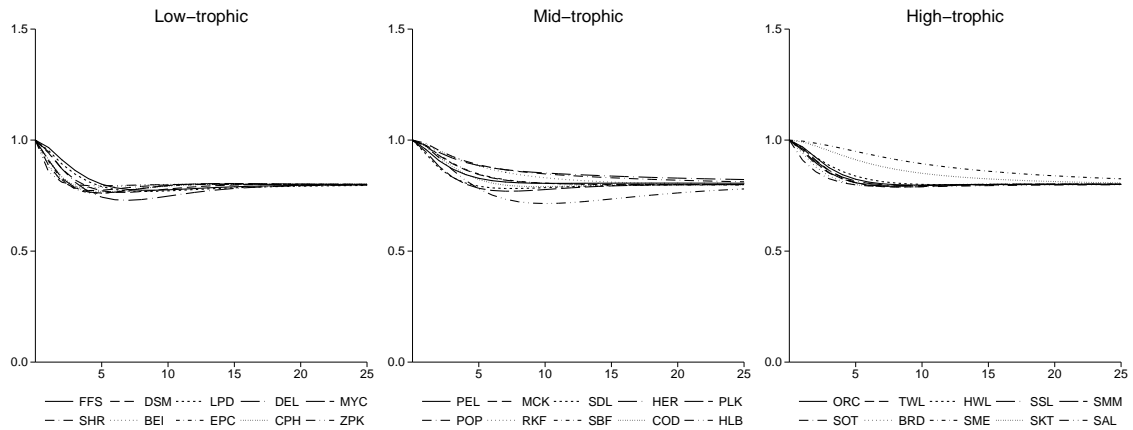


Figure 4.7: Population outcomes for STS scenario - Model 2 (EwE)

The remaining species experience initial shocks of approximately 20% but recover to between 0 and 10% below baseline levels. Sea lion populations suffer in part from Orca whale switching in the face of increased sea-otter scarcity.

Scenario 2: Stochastic Species Harvest (SSH)

The stochastic species harvest (SSH) scenario is intended to model a stylized representation of random fluctuations in harvesting activity. For the GEEM data and Model 1, harvesting shocks are only imposed on the pollock population. No baseline harvesting is specified for the GEEM data, so random harvests are implemented as fractions of baseline starting biomass. Harvests vary between 15 and 35% of the initial period's starting biomass. Shocks vary by year within the 25-year period. For Models 2 and 3 shocks are imposed as a multiple of baseline harvesting so that harvesting varies between one half and three times the baseline levels as a fraction of initial-period biomass. There are 19 species with non-zero harvesting rates ranging from fractions of a percent (of starting biomass) to 14.6%. According to the Ecosim data, the majority of harvest rates are on the order of 1% of starting biomass. In Model 3 the harvest rates are the weighted average of the sub-species of the functional group.

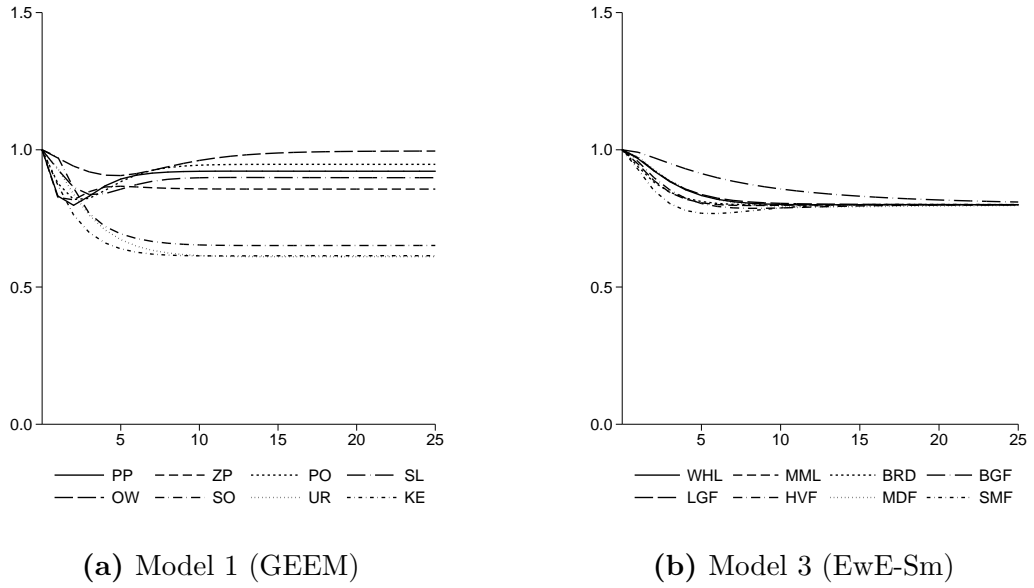


Figure 4.8: Population outcomes for STS scenario

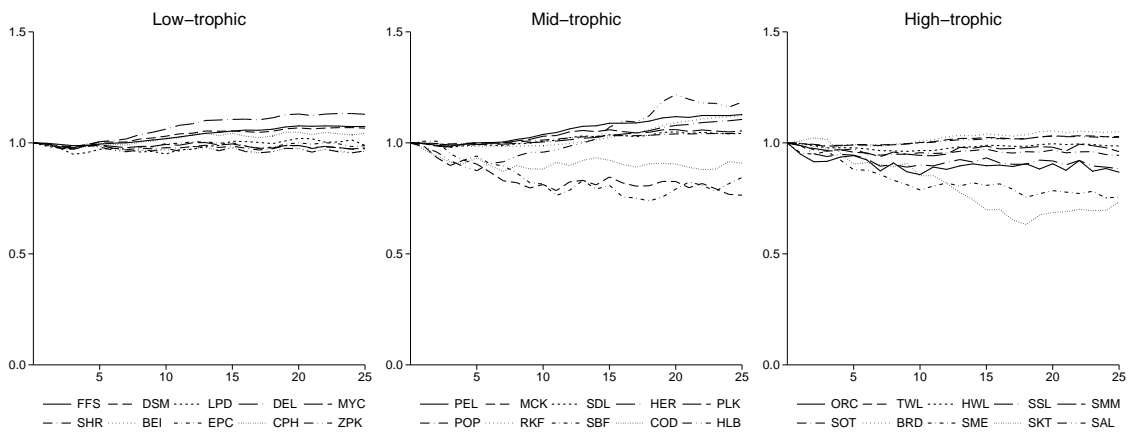


Figure 4.9: Population outcomes for SSH scenario - Model 2 (EwE)

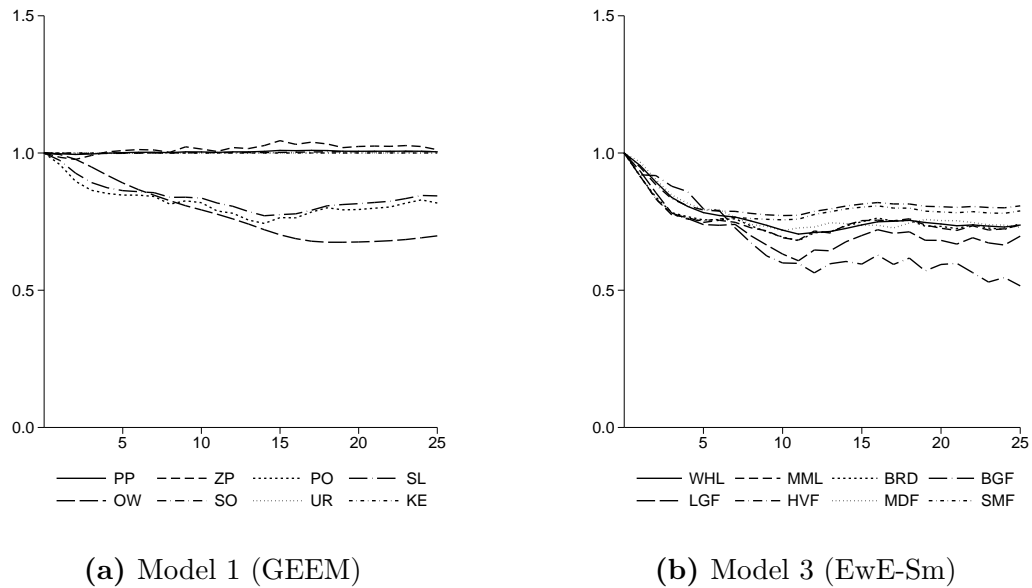


Figure 4.10: Population outcomes for SSH scenario

As revealed by Model 2 in Figure 4.9, the SSH scenario has the most dramatic impact on mid-trophic species where the majority of extant harvesting occurs. These shocks have a larger cascade up the food chain than down. The impacts on low-trophic species are positive as expected from the harvesting of their predators and largely negative for their higher-trophic predators. Pacific ocean perch are substantially impacted by the imposed shocks dropping to approximately 50% of pre-shock levels. This species has the highest baseline export rate of mid-trophic species. Model 1 results, presented in Figure 4.10a show comparable dynamics, where the harvested species, pollock, exhibit population declines along with their predators, sea lions, and their predators, Orca whales. Dynamics are similar although muted in Model 3 as presented in Figure 4.10b.

Scenario 3: Stochastically Perturbed System (SPS)

The stochastically perturbed system (SPS) is intended to induce fluctuations in species populations qualitatively similar to those that might be observed empirically.

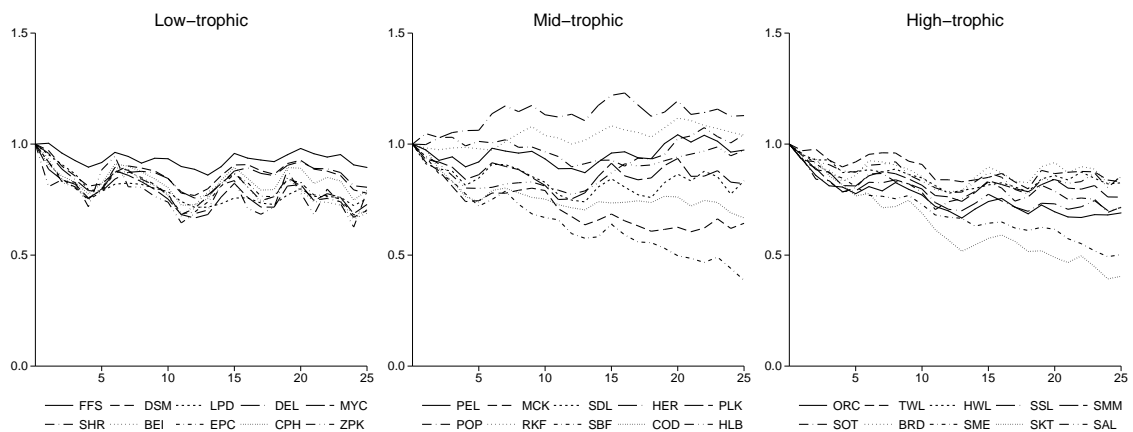


Figure 4-11: Population outcomes for SPS scenario - Model 2 (EwE)

Operating strictly through the boundary conditions of the system, the SPS scenario randomly shocks primary production and harvesting. In Model 1 primary producers' (phytoplankton and kelp) starting biomasses are shocked between -10 and 10% . Similar to the SSH scenario, pollock harvesting is varied between 15 and 35% . In Models 2 and 3 primary producers' starting biomasses are shocked between -40 and 5% and harvests vary between one half and three times baseline levels. Shocks vary across primary producers (for Models 2 and 3) and across years within the 25-year period.

The outcomes from the SPS scenario show the greatest variation in population levels of all scenarios. Here the ecosystem is shocked both at its primary production and mid-trophic production. In a sense, the SPS scenario combines the shocks imposed in the STS and SSH scenarios. Combining the shock sources in this way generates shocks throughout the ecosystem as evident in Figures 4-11, 4-12a, and 4-12b. Here low and high trophic species' populations trend closer together than mid-trophic species. Here again pacific ocean perch are heavily decimated by the shocks. The highest-trophic species, whales and sharks (HWL and SME), experience the smoothest transition to the new system dynamics.

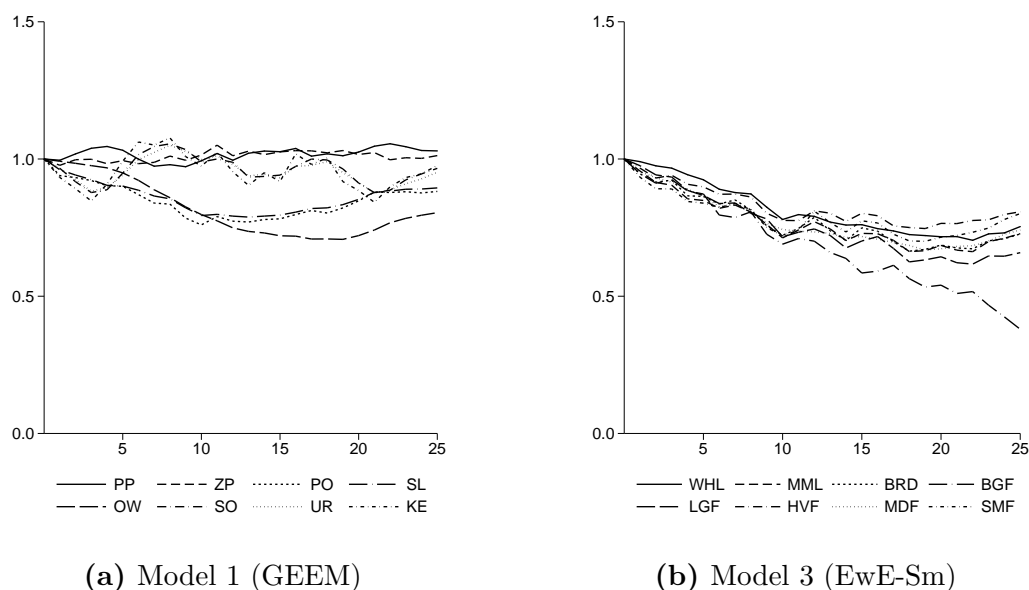


Figure 4-12: Population outcomes for SPS scenario

Figure 4-12a shows similar variability in population outcomes for Model 1. Higher-trophic species such as the Orca whale and sea lions show smoother transitions than mid-trophic species, whose populations are more variable but less impacted on net. Last, Figure 4-12b presents more muted population responses among Model 3 species. Variation is evident and the net effect on populations is negative, but all populations move more tightly together than in either Model 1 or 2.

Scenario 4: Extinction event (EXT)

The extinction scenario (EXT) examines how the loss of the ecosystem's apex predator, the Orca whale, influences other species in the system. In Models 1 and 2 this shock is implemented by simply removing the Orca whale's production function from the BGE model. Additional steps must be taken in Model 3 not to perturb the efficiencies of other species that eat whale species. While the Orca whale has no predators by account of the Ecosim data, other whale species with which it is aggregated for Model 3 do have predators. These predators' biomass production functions

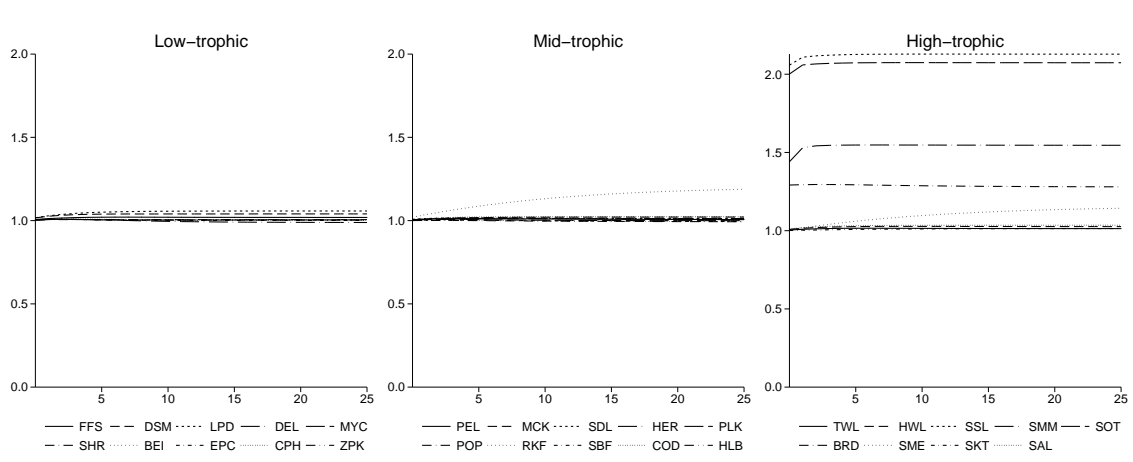


Figure 4.13: Population outcomes for EXT scenario - Model 2 (EwE)

are recalibrated to exclude whales as part of their diet. Better empirical data might inform how these predators' diet shares could change disproportionately in the event of a whale extinction. I expect the scenario will produce large rises in Orca prey (i.e. primarily marine mammals). Less clear is how a rise in these populations will in turn influence their prey and to what extent limited productivity of marine mammals' prey may limit their ability to grow under reduced predation pressure.

Results from the extinction scenario are comparable across Models 2 and 3 in direction and degree. Only the former similarity holds for Model 1 in Figure 4.14a. Figures 4.13 and 4.14b show dramatic effects on the marine mammal prey of the Orca whale species. Sea otter and lion populations more than double in Model 2 and the same holds for marine mammals in Model 3. Sea otter and lion populations also benefit in Model 1 but much less dramatically - only by 5 – 10%.

4.5.4 Monte carlo counter-factual scenarios

This section examines the sensitivity of the model outcomes for each scenario to variations in the benchmark specification of the elasticity parameters. These parameters determine the degree to which different inputs can be substituted to yield the same

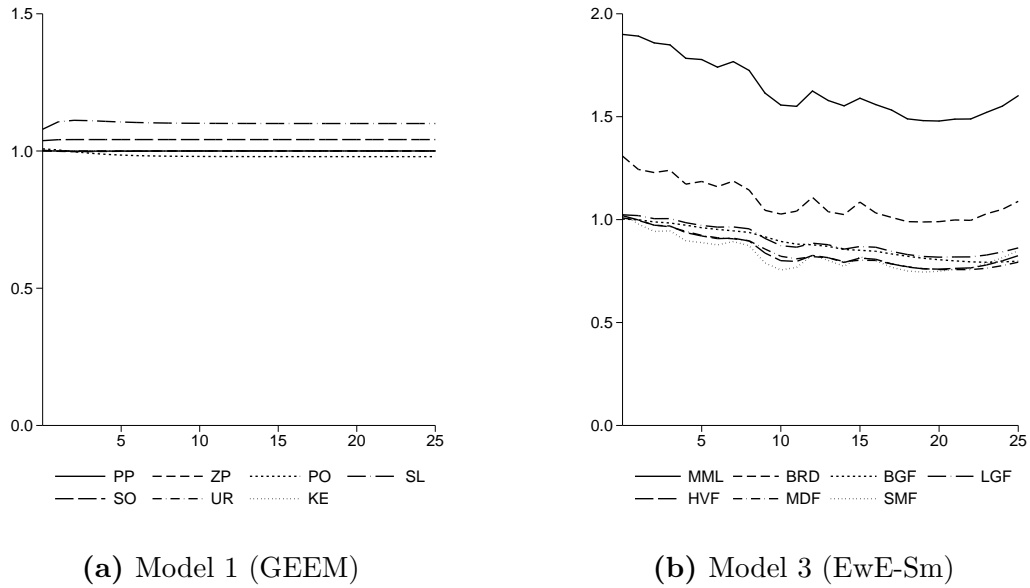


Figure 4-14: Population outcomes for EXT scenario

output. The smaller the elasticity, the more difficult it is to make substitutions. An elasticity of zero means that no substitution is possible - the inputs must be used in fixed proportion. An elasticity of one means that substitution can occur on a percent-for-percent basis relative to the benchmark calibration.

Table 4.13 outlines the five elasticity parameters that are varied for the monte carlo simulations. The parameters are first varied individually with 25 random draws each. The five parameters are then drawn all at once over 125 draws. The results will reveal to which parameters model outcomes are most sensitive and demonstrate the overall sensitivity of the model to its chosen parameters. Aside from the chosen

	Symbol	Description	Benchmark	Monte Carlo Distribution
1.	σ_R^p	Resource supply	0.75	0.5 – 2.0
2.	σ_P	New prey	0.75	0.5 – 2.0
3.	σ_{NO}	New-old biomass	0.25	0.0 – 0.5
4.	σ_{EB}	Ending biomass	1.00	0.0 – 1.0
5.	σ_{EE}	Ending energies	1.00	0.0 – 1.0

Table 4.13: Distribution of elasticities for Monte Carlo simulations

functional forms, essentially all other features of the model are empirically observed.

To assess the relative sensitivity of the model to the different parameters, I present the distribution of population outcomes over all species and all iterations of the given parameter. These outcomes are relative to the baseline growth scenario so that all variation is that induced by the scenario shock. The median is presented within the 20 – 80th percentile range of population outcomes. The wider the inter-quintile range, the greater the dispersion induced by the variations in the given parameter. I also present the mean square error of the monte carlo outcomes to the benchmark specification. That is, for a given scenario I take the average squared error between the monte carlo and benchmark results over all populations, time periods, and iterations for the scenario.

For some parameterizations, the test scenarios may produce local extinction events for certain species. In instances where extinctions occur, the model simulation is stopped at the given time period and the next iteration is started. For programming reasons, a non-zero biomass threshold is set to identify extinction events. I report the number of extinction events and the iterations in which they occur for each model in each of the scenarios summarized below.

Scenario 1: Starve The System (STS)

The variation in population outcomes induced by the monte carlo simulations was largest for the all-elasticities iterations for Model 1 and for the new-old biomass elasticity for Models 2 and 3. Table 4.14 shows the mean squared error for each model and each scenario. Model 2 had the highest sensitivity overall at 0.138 or 37.1 percentage points. The new biomass and ending energies elasticities had the least impact on outcomes across models. This is likely a result of the broad and even nature of the shock, which gave an unbiased effect on populations and induced little switching behavior. Conversely, the resource supply and old-new biomass elasticities,

Mean squared errors: Starve the system (STS)						
Scenario	Resource Supply	New biomass	New-old biomass	Ending biomass	Ending energies	All elasts.
Model 1: GEEM	0.023	0.000	0.026	0.013	0.000	0.050
Model 2: Full Ecosim	0.004	0.004	0.138	0.010	0.000	0.014
Model 3: Small-species Ecosim	0.008	0.000	0.054	0.004	0.000	0.004

Table 4.14: Monte carlo mean squared errors for STS scenario

which moderate the level of output relative to starting biomass, are more influential for model outcomes in the STS scenario.

Species extinctions occurred in 10 of the monte carlo iterations of the STS scenario in Model 1. Of the 10 extinction events, 6 occurred in iterations where all elasticities were varied. The remaining occurred in the iterations where the new-old biomass elasticity was varied. There were 23 extinctions in the iterations for Model 2 with 22 occurring during the new-old biomass elasticity iterations and the remainder in the all-elasticities iterations. There were 3 extinctions all in the new-old biomass iterations for Model 3.

Figure 4-15 presents the median and inter-quintile range of population outcomes in the STS scenario over all monte carlo iterations for each model. The populations in Model 1 exhibit a narrow range of responses to the reduction in primary production with the widest ranges coming from the resource supply and biomass elasticities. Results are widest for variations in the new-old biomass elasticity in Model 2. Here nearly all (23 of 25) iterations resulted in an extinction event as is evident in the downward crash of the new-old biomass pane of the Model 2 panel. The species that most often face extinction in these iterations are large deep water fish (Gu nette & Christensen, 2005, p. 54, DEL) and small demersals (Gu nette & Christensen, 2005, p. 51, DSM). Results are less dramatic for Model 3, where the dispersion in

population outcomes is narrowest for all. The species in Model 3 are much more robust against extinctions as suggested by the narrow population distribution.

Scenario 2: Stochastic Species Harvest (SSH)

The variation of population outcomes in the monte carlo runs of the Stochastic Species Harvest scenario is almost exclusively induced by variations in the new-old biomass elasticity. Table 4.15 shows that, across all models, this parameter generates the highest mean squared errors. Also, the mean squared error (MSE) in Model 1 is the highest MSE across all models *and* scenarios, 0.54 or 73.5 percentage points. Moreover, mean squared errors for other parameters are relatively small. In this harvesting scenario, the ability of harvested species to add additional biomass is a critical factor in the extent to which they recover from the shock. That the new biomass elasticity does not generate much variation in outcomes suggests that the breadth of the harvesting shocks is not inducing strong prey substitution among higher-trophic species.

Mean squared errors: Stochastic species harvest (SSH)						
Scenario	Resource Supply	New biomass	New-old biomass	Ending biomass	Ending energies	All elasts.
Model 1: GEEM	0.000	0.000	0.542	0.007	0.000	0.019
Model 2: Full Ecosim	0.002	0.004	0.130	0.016	0.000	0.023
Model 3: Small-species Ecosim	0.008	0.000	0.032	0.005	0.000	0.006

Table 4.15: Monte carlo mean squared errors for SSH scenario

Twenty-nine of the Model 1 monte carlo iterations generated species extinctions in the SSH scenario. Twenty-two of the extinctions occurred in the iterations where all elasticities were varied and the remainder in the iterations where the new-old biomass elasticity was varied. There were 22 extinctions in the iterations for Model 2 with 17 occurring during the new-old biomass elasticity iterations and the remainder in

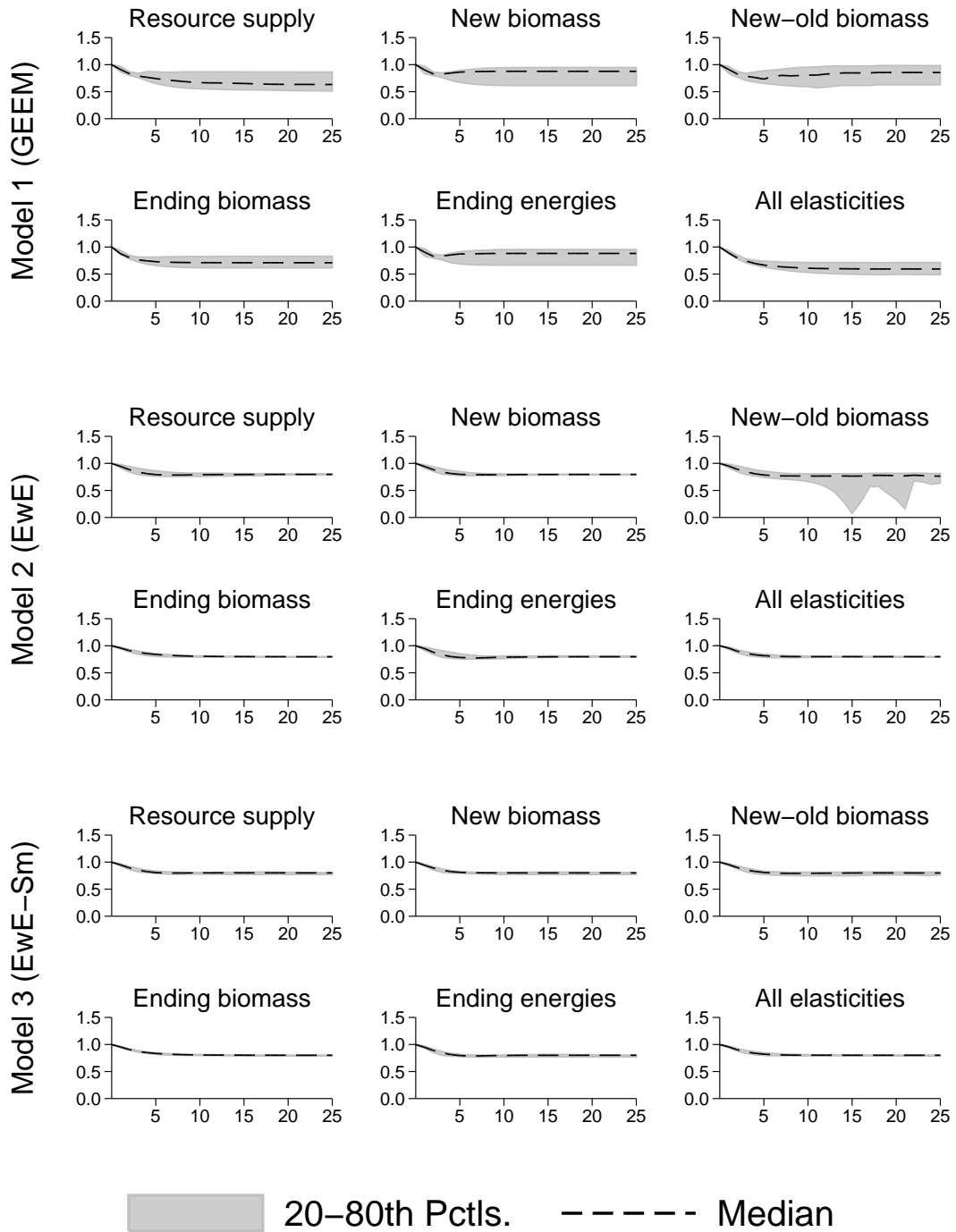


Figure 4-15: Population distributions for STS scenario

the all-elasticities iterations. There was 1 extinction in the new-old biomass elasticity iterations in Model 3.

The variation in population outcomes is more narrow for the SSH scenario and again widest for the new-old biomass elasticity, most dramatically for Model 2. Large deepwater fish (DEL), similar to the STS scenario, experience the largest number of extinctions. Part of the up-tick present in the new-old biomass pane of the Model 2 panel in Figures 4-15 and 4-16 may be the result of survivorship bias. When species go extinct in an iteration the recursive solving is stopped in that time period. If species extinctions tend to happen near year 20 then the median for later years will only include the populations in iterations where extinctions did not occur. The tracking of the median and 80th percentiles in many of the panes suggests that there may be a large gap between those clearly negatively affected by the shocks and other species that are largely unimpacted by the shock. This was evident in some of the benchmark plots where all species were presented (e.g. Figure 4-10a).

Scenario 3: Stochastically Perturbed System (SPS)

The new-old biomass parameter and the all-parameters buckshot iterations generate the largest mean squared errors, as shown in Table 4.16. Largest overall is the MSE for new-old biomass in Model 2 at 0.12 or 33.9 percentage points. The low MSE's generated in the resource supply and new-biomass iterations suggest that the shocks are not driving substitution by predators and that the reductions in mid-trophic species may be accommodating the negative shocks to primary production. Given the stochasticity, the lack of influence of the new biomass parameter is somewhat surprising. I would have also anticipated that variations in the resource supply elasticity would have driven variation in lower-trophic species' population outcomes. It may be the case that the shocks themselves have already driven the population outcomes so strongly that they are not sensitive to the marginal changes in these parameters.

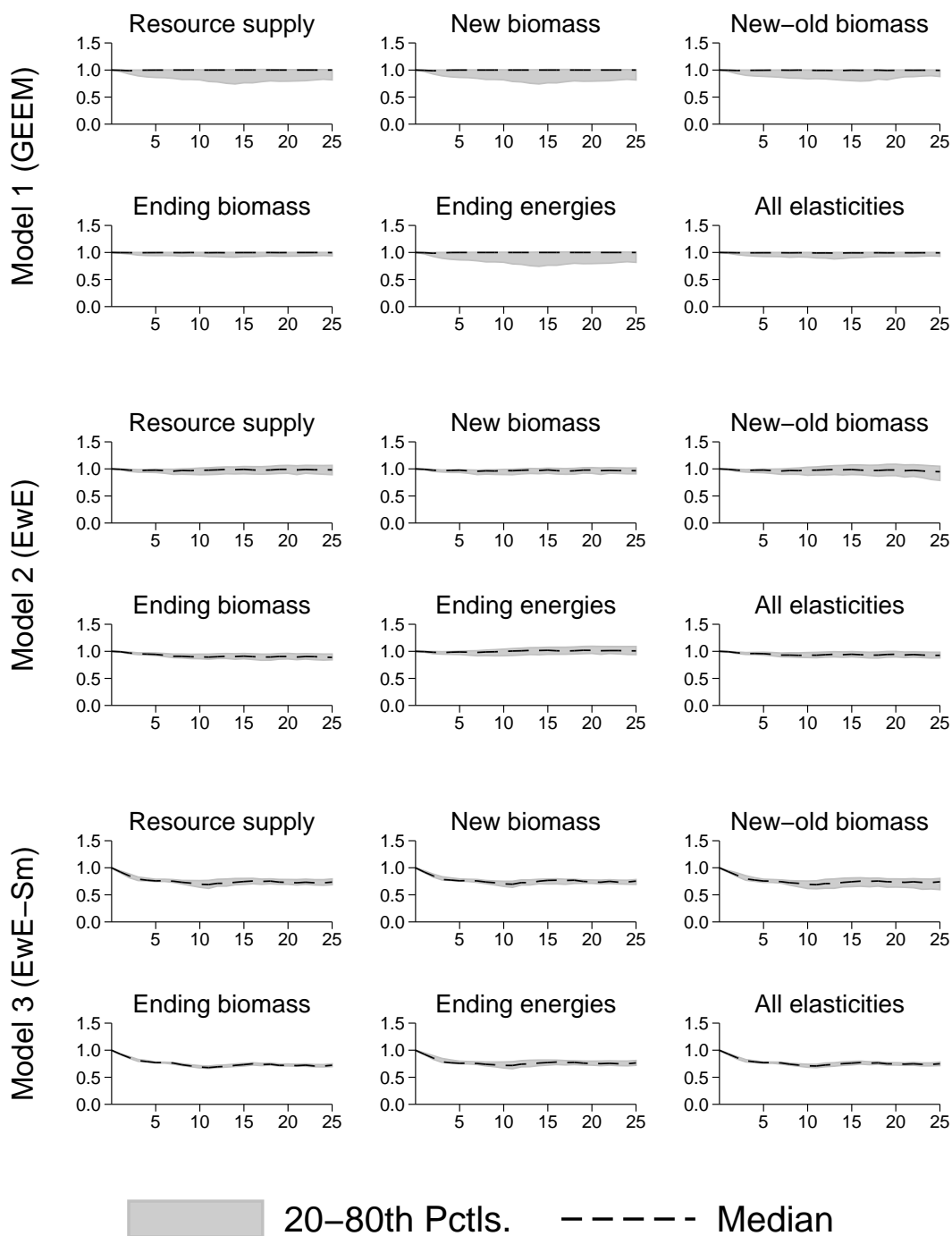


Figure 4-16: Population distributions for SSH scenario

Mean squared errors: Stochastically perturbed system (SPS)						
Scenario	Resource Supply	New biomass	New-old biomass	Ending biomass	Ending energies	All elasts.
Model 1: GEEM	0.001	0.000	0.056	0.005	0.000	0.019
Model 2: Full Ecosim	0.000	0.003	0.115	0.009	0.000	0.013
Model 3: Small-species Ecosim	0.000	0.000	0.079	0.005	0.000	0.004

Table 4.16: Monte carlo mean squared errors for SPS scenario

Thirty of the Model 1 monte carlo iterations generated species extinctions in the SPS scenario. Twenty-two of the extinctions occurred in the iterations where all elasticities were varied and the remainder in the iterations where the new-old biomass elasticity was varied. There were 22 extinctions in the iterations for Model 2 with 18 occurring during the new-old biomass elasticity iterations and the remainder in the all-elasticities iterations. There were 7 extinction events all in the new-old elasticity iterations for Model 3.

Figure 4-17 shows that, again, the extent of the extinction events is most evident in the new-old biomass elasticity iterations of Model 2. Here the rebound of populations is not present in the out years as it was in the SSH scenario and STS to a lesser extent. Despite the stochastic variability evident in the median lines, the distribution of the population outcomes is still relatively narrow.

Scenario 4: Extinction event (EXT)

Significant mean squared errors are present most broadly across parameter iterations for the extinction scenario (Table 4.17). Errors for Models 2 and 3 are comparable, particularly for new-old biomass and all-elasticity iterations. The ending-biomass parameter generates a higher MSE in the extinction scenario than in any other. This is likely owing to the strong growth of marine mammals following the whale extinction. Populations in Model 1 appear least sensitive to iterations in the parameters.

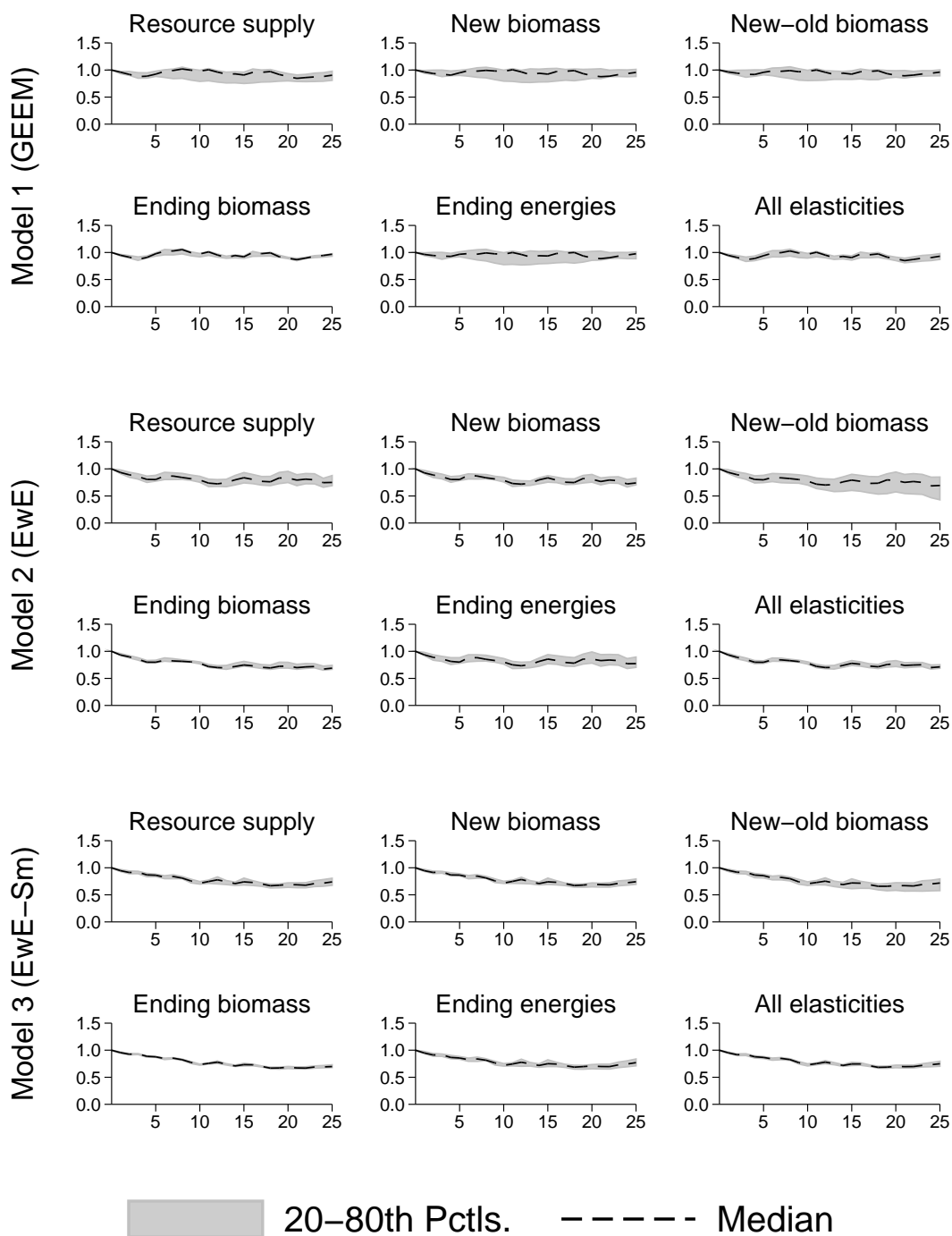


Figure 4-17: Population distributions for SPS scenario

Mean squared errors: Orca whale extinction (EXT)						
Scenario	Resource Supply	New biomass	New-old biomass	Ending biomass	Ending energies	All elasts.
Model 1: GEEM	0.000	0.000	<i>0.013</i>	0.001	0.000	0.003
Model 2: Ecosim	0.019	0.006	<i>0.153</i>	0.033	0.000	0.042
Model 3: Small-species Ecosim	0.001	0.001	<i>0.157</i>	0.062	0.000	0.041

Table 4.17: Monte carlo mean squared errors for EXT scenario

Aside from the modeled extinction, one of the Model 1 monte carlo iterations generated a species extinction in the EXT scenario. The extinction occurred in an iteration where the new-old biomass elasticity was varied. There were 19 extinctions in Model 2 with 17 occurring in the new-old biomass elasticity iterations and the remaining 2 in the all-elasticities iterations. In Model 3 there were 2 extinction events that both occurred in the new-old biomass elasticity iterations. The distribution of population outcomes is remarkably narrow for Model 1 and wider for Models 2 and 3.

4.5.5 Summary

The benchmark growth scenarios demonstrated that the data procedures set up in sections 4.3 and 4.2 allow the BGE model to be calibrated to a variety of growth rates. As evident in Figure 4-6, certain mid-trophic species are more sensitive to negative growth rates than others. Producing a baseline outcome with stable populations is a positive result for the BGE model. This enables clear assessments of the results of counter-factual analyses.

The starve the system (STS) scenario demonstrated how reductions in primary productivity imposes losses on the entire system. This is an essential result given the trophic structure of the ecosystem. The stochastic species harvest (SSH) demonstrated how mid-trophic shocks can ripple up the trophic chain to influence high-

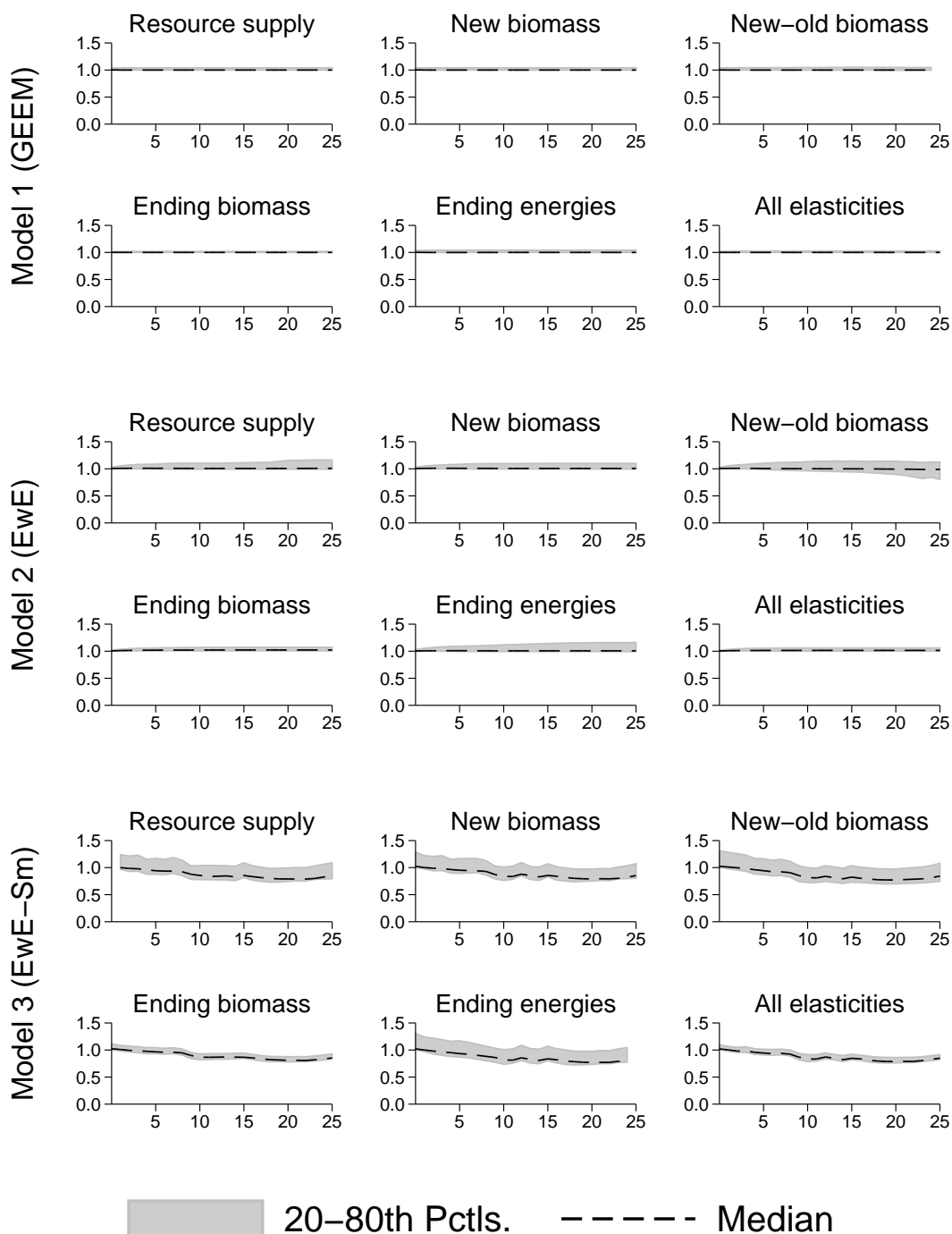


Figure 4-18: Population distributions for EXT scenario

trophic population levels but have limited impact on low-trophic species. The stochastically perturbed system (SPS) combined the STS and SSH scenarios to show how stochastic shocks to the base and middle of the ecosystem can generate ripple effects throughout the system. This variation may more closely resemble empirical observation of population variability. Finally, the extinction scenario demonstrated how the removal of a top predator can have dramatic impacts on the populations of its prey, doubling the sea otter and lion populations in the Ecosim models.

The sensitivity analyses offered a consistent story across scenarios. The new-old biomass parameter was by far the most influential. Moreover, ending biomass and energy parameters had relatively little impact on outcomes. This is a positive result. We learned that the BGE model is sensitive to a physically relevant parameter. We can empirically examine the extent to which additional consumption of prey produces new biomass for various species. For example, lower-trophic species may be able to add much more new biomass relative to their starting biomass than higher-trophic species. Last, the ending biomass and energy aggregations are abstractions imposed by the modeling framework. They are needed to close the model and its mathematical structure. It is encouraging that these parameters, that lack a direct analogue in the physical world, are not driving model outcomes.

4.6 Conclusion

This chapter has demonstrated the power of the Biological General Equilibrium (BGE) model constructed in Chapter 3 to admit multiple data sources and produce robust, biologically relevant results. In particular, section 4.3 demonstrated a general method for organizing Ecosim data, a widely-used standard in ecosystem modeling, into a set of accounting matrices compatible with the BGE framework. This opens a wealth of opportunity for analysis of additional ecosystems and cross-model compar-

ison.

Section 4.4 outlined how the micro-dynamics of species bioenergetic trade-offs “roll up” to macro-ecologic outcomes. Specifying the model in this way permits a unique level of specificity for imposing bioenergetic shocks on model species. These emergent population dynamics proved biologically plausible and largely robust to alternate specifications with the exception of the physically relevant new-old biomass substitution parameter. Incorporating a more nuanced understanding of the extent to which species intra-period growth rates can vary will improve model performance and shed additional light on species’ population dynamics. Ultimately, the BGE model will benefit from specific consideration of inter-temporal trade-offs such as biomass allocation and spatial features such as “patchy” environments.

The BGE model provides a successful integration of optimal foraging, bioenergetic optimization, and ecosystem modeling into a well-founded mathematical structure for representing the complex interactions of species in an ecosystem. Chapter 5 will test the BGE model further by modeling observed phenomena in the Aleutian ecosystem. Verifying the outcomes here against the historical record will support the BGE model’s capacity for generating biologically relevant results.

CHAPTER 5: APPLYING THE BIOENERGETIC GENERAL EQUILIBRIUM MODEL

5.1 Introduction

This chapter applies the Biological General Equilibrium (BGE) model to the Aleutian marine ecosystem to examine the model's ability to represent empirically observed phenomena. The BGE model's external validity will be supported to the extent it is able to mimic key features of these phenomena. I consider two cases of interest for this ecosystem: invasive species and a harvesting-induced trophic cascade. The BGE model is run using only the full Ecosim data set (Gu enette & Christensen, 2005) (Model 2 in Chapter 4). The invasive species scenario incorporates external estimates of bird biomass into the underlying data and shocks the bird population to mimic empirical findings. The trophic cascade scenario highlights how, through prey substitution, exogenous shocks can be transmitted to a seemingly remote part of the ecosystem, though not as strongly as hypothesized.

5.2 Invasive species

The first scenario considers the introduction of an invasive species, the Norway rat, to the Aleutian marine ecosystem. As documented by Kurle and co-authors (Kurle, Croll, & Tershy, 2008), Norway rats impact Aleutian ecosystems by preying on the eggs of Glaucous-winged gulls and Black Oystercatchers. Where rats have been introduced, endemic bird species' populations are significantly lower and the prey species of birds are more abundant. There is one representative bird species encompassing 20 biological bird species in the Ecosim data (Gu enette & Christensen, 2005, p. 28). This means that the model representation is further abstracted from the phenomena observed by Kurle and co-authors, but producing qualitatively similar model dynamics to those observed should still be possible.

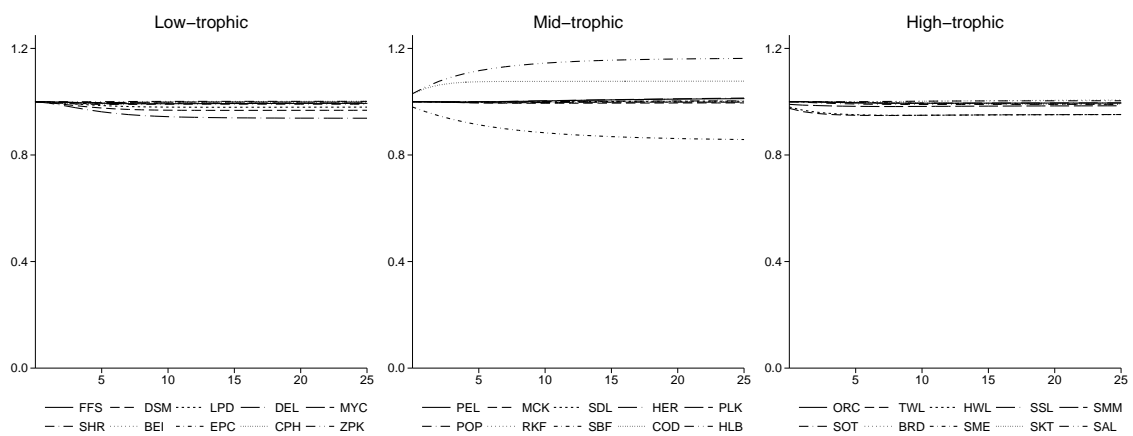
Biomass data are missing for the bird species in the Ecosim data. The benchmark data revision procedure (Section 4.3.2) finds minimal biomass values for the bird species, which limits its potential impact on the ecosystem. Data provided by Kurle et al. (Kurle et al., 2008, Fig. 2) suggest bird biomass densities of approximately 15 tonnes per square kilometer.¹ Adjusting for the relative area between the nearshore and the greater marine environment as in (J. Tschirhart, 2003, Table 1, fn. a) gives a bird biomass density of 0.04 tonnes per square kilometer. I use this “back of the envelope” estimate to set bird biomass levels in the data revision procedure that are likely more realistic and consequential for the ecosystem.

The newly-revised data have different baseline population behavior than in previous iterations of the model. Figure 5.1b presents the baseline outcomes of the model with the increased bird biomass and, for comparison, Figure 5.1a presents the same outcomes without revising the bird biomass levels to those comparable to Kurle et al.’s findings (same as the top panel of Figure 4.6). Results are similar, halibut (HLB) and sablefish (SBF) show the largest population changes, but the revised data show less dispersion in population outcomes among lower-trophic species. Higher-trophic species are effectively unchanged with whales exhibiting slight declines for both data sets. In all, revising the bird biomass levels upward does not have a marked impact on the ecosystem as a whole.

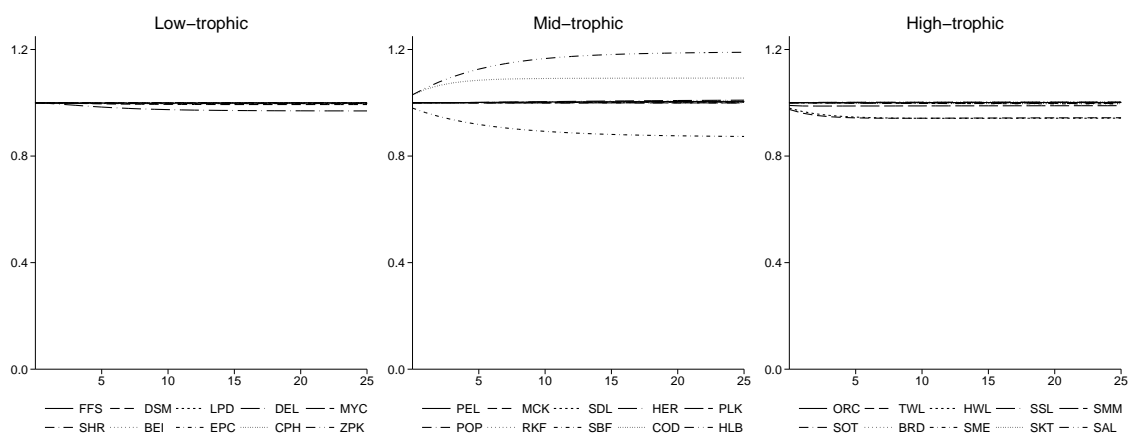
The Norway rat preys on bird species by eating their eggs. To introduce this shock in the model I remove 50% of the birds’ starting biomass each period. This results in an approximate 40% decline in the bird population, which is in the middle of the 19 – 47% range of declines referenced by (Kurle et al., 2008) (citing (Jones et al., 2008)). Figure 5.2 presents the population outcomes relative their baseline levels for all model species (except the Norway rat).

As expected, the bird population is negatively impacted, by about 40% in this

¹Assuming each individual is approximately 1kg on average.



(a) Low bird biomass levels



(b) Revised bird biomass levels

Figure 5.1: Baseline growth population outcomes

case. Birds' major prey are cephalopods (CPH, 36.3%), pelagics (PEL, 21.5%), and sandlance (SDL, 12.5%). Together these species comprise 70% of the birds' diets. The impact on these populations is uniformly positive, with cephalopods experiencing the smallest increase. Although cephalopods are a significant part of the bird diet, birds are responsible for a small fraction of cephalopod predation (4.9%) in the Ecosim data (as revised for the model). Birds account for larger fractions of pelagic (13.4%) and sandlance (18.3%) predation.

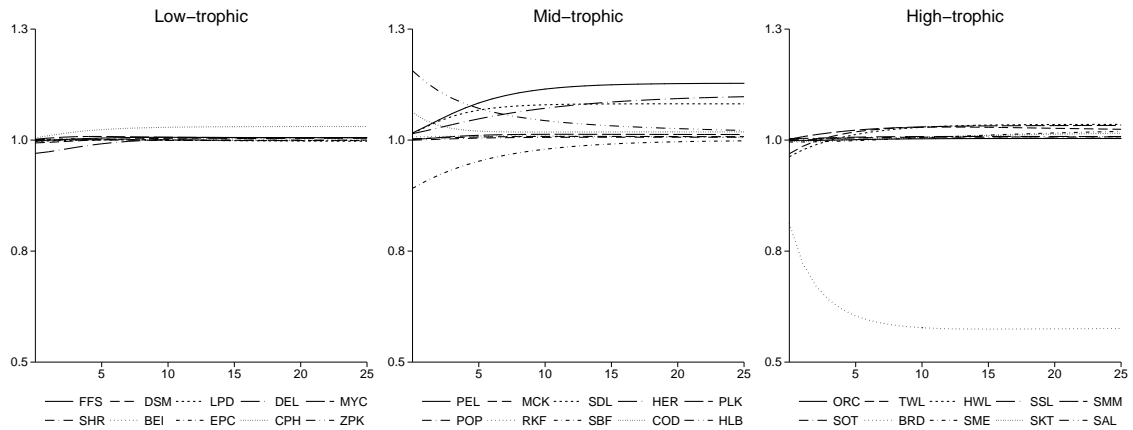


Figure 5.2: Population levels following invasive Norway rat

Halibut (HLB) and sablefish (SBF) show large initial shocks but trend back to baseline levels throughout the period. Figure 5.1b shows how these populations showed the largest population changes in baseline - positive for halibut and negative for sablefish. The relative shocks induced by the bird harvesting appear to have moved these populations to their long-run levels more rapidly than in the baseline. These species are linked - halibut prey on sablefish, but not in significant amounts. Cephalopods comprise the largest share of the halibut diet at approximately a third. The more-rapid population increase experienced by the halibut is attributable to reduced competition with birds for these prey, whose scarcity decreases by 2.5% when the effects of the Norway rat are modeled. Sablefish feed heavily (approximately 90%) on zooplankton (ZPK), who face increased scarcity from the rise in the population levels of two of their primary predators, also birds' primary prey, cephalopods and pelagics. Given the high dependence of sablefish on zooplankton, even slight increases in the latter's scarcity generate noticeable changes in sablefish population outcomes.

5.3 Trophic cascade

The second case considers the impact on higher-trophic species of increased harvesting of mid-trophic species. Estes and co-authors document declines in sea otter populations in the early 1990s following peak abundance in the late 1970s. The authors ultimately propose a trophic cascade among the ecosystem species, one that is ripe for investigation by the BGE model.

... sea otter population declines and the consequent collapse of kelp forest ecosystems almost certainly have been driven by ... a chain of ecological interactions, beginning with reduced or altered forage fish stocks in the oceanic environment, which in turn sent pinniped populations into decline ... killer whales who once fed on [pinnipeds] expanded their diet to include sea otters ... [creating] a linkage between oceanic and coastal ecosystems and in so doing transformed coastal kelp forests from three- to four-trophic-level systems, thereby releasing sea urchins from the limiting influence of sea otter predation. Unregulated urchin populations increased rapidly and overgrazed the kelp forests... (Estes, Tinker, Williams, & Doak, 1998, p. 475)

To summarize, reduced fish stocks from harvesting led to sea lion declines, which induced prey switching by Orca's toward sea otters, whose reduced numbers led to increases in their prey, sea urchins, and in turn decreases in urchin's primary food source, kelp. To characterize the harvesting shocks I use commercial landings data from the National Oceanic and Atmospheric Administration's (NOAA) National Marine Fisheries Service (NMFS)(NOAA, 2015). Figure 5.1 summarizes the primary prey for Orca whales, sea lions, and sea otters.

To identify these prey in the fisheries data, I match the detailed descriptions of the the constituent prey of the Ecosim functional group given in (Gu enette & Christensen,

Affected species and prey diet shares								
Orca Whales			Sea Lions			Sea Otters		
		Diet			Diet			Diet
Prey name	Code	share	Prey name	Code	share	Prey name	Code	share
Stellar sea lion	SSL	80.0%	Atka mackerel	MCK	37.7%	Benthic inverts	BEI	60.0%
Sm. mammals	SMM	15.0%	Salmon	SAL	11.3%	Sm. demersals	DSM	30.0%
Sea otters	SOT	3.0%	Pacific cod	COD	7.4%	Sandlance	SDL	4.0%

Table 5.1: Species of interest and their harvested prey

2005) to search results in the landings data. Stellar sea lion prey also included small demersals (DSM) as 20.4% of their diet and cephalopods (CPH) as 6.9% of their diet; however, the landings data showed small and often zero landings for these species. None of the species comprising the remaining 16.3% of the sea lion diet comprised more than 5.6% on its own. As a result of the limited landings for cephalopods and small demersals, I've modeled shocks to salmon (SAL), cod, and mackerel (MCK) only, which comprise 56.3% of the sea lion diet.

Table 5.2 summarizes the harvest quantities in tonnes and relative to prior-period landings.² As a point of comparison, I've included the relevant Ecosim data. Recall that harvest rates from the Ecosim data have been revised according to the data procedure for Model 2 outlined in Section 4.3.2. The revision procedure assigned all three shocked species corner solutions (i.e. harvest rates were bounded above at 5%), but these rates could be fixed at different levels in the data revision procedure given better external estimates (e.g. using the landings data if they were plausible).

The quantity of tonnes fished from the landings data for mackerel (MCK) are plausible on their face, but salmon (SAL) and cod landings are clearly incommensurate with the Ecosim data. Inaccuracy here can be tolerated since the model will incorporate relative landings data only. That is, the relative movement in harvesting

²Biomass densities given in the Ecosim data are converted to total tonnage using the 56,936 km² study area identified by (Gu nette & Christensen, 2005, p. 8).

Year	Biomass and Landings					
	MCK		SAL		COD	
	Tonnes	Relative	Tonnes	Relative	Tonnes	Relative
<i>Ecosim</i>						
Biomass	768,636		105,724		136,646	
Exports	38,432	5.0%	5,286	5.0%	6,832	5.0%
<i>NOAA-NMFS</i>						
1990	22,263	1.000	298,123	1.000	238,332	1.000
1991	25,668	1.153	314,741	1.056	231,460	0.971
1992	59,714	2.682	298,624	1.002	251,665	1.056
1993	51,314	2.305	373,848	1.254	193,983	0.814
1994	62,547	2.809	362,036	1.214	209,158	0.878
1995	67,497	3.032	428,500	1.437	272,160	1.142
1996	87,871	3.947	355,131	1.191	278,616	1.169
1997	59,165	2.658	240,534	0.807	316,574	1.328
1998	51,198	2.300	283,996	0.953	267,431	1.122
1999	51,436	2.310	363,650	1.220	237,616	0.997
2000	44,592	2.003	275,212	0.923	240,276	1.008
2001	57,096	2.565	311,351	1.044	213,565	0.896
2002	37,759	1.696	237,257	0.796	231,721	0.972
2003	45,152	2.028	286,006	0.959	256,099	1.075
2004	49,180	2.209	316,564	1.062	266,414	1.118
2005	58,733	2.638	395,681	1.327	248,003	1.041
2006	59,337	2.665	287,683	0.965	234,872	0.985
2007	57,589	2.587	390,662	1.310	221,059	0.928
2008	57,620	2.588	290,334	0.974	223,992	0.940
2009	71,164	3.196	304,446	1.021	222,508	0.934
2010	65,865	2.958	343,294	1.152	244,619	1.026
2011	51,073	2.294	334,810	1.123	300,978	1.263
2012	47,168	2.119	277,222	0.930	325,372	1.365
2013	23,326	1.048	459,318	1.541	309,267	1.298
2014*	51,719	2.323	343,818	1.153	280,549	1.177
2015*	47,830	2.148	351,692	1.180	292,157	1.226

Notes: Asterisked rows are moving averages of prior five years.

Table 5.2: Harvesting quantities and rates

is used as a multiplier on Ecosim harvesting rates as produced by the data revision procedure. For the purposes of this scenario, I artificially assume that the Ecosim data depict a snapshot of the ecosystem as of 1990, with the 25-year model horizon carrying the ecosystem to present day. I extend the available landings data using a moving average to cover the final two years of the period.

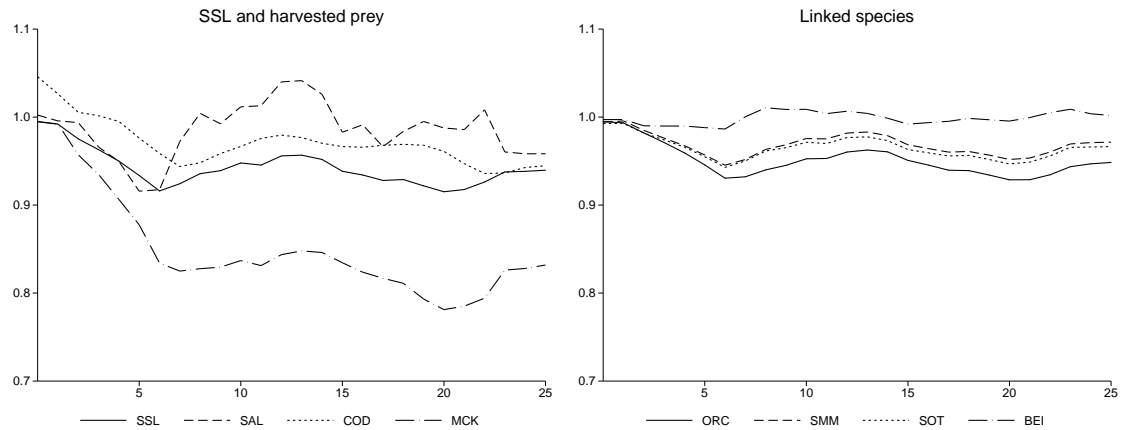


Figure 5.3: Relative population levels for perturbed species

Figure 5.3 plots modeled population outcomes for the harvested species and those linked to the harvested species via the trophic chain described by Estes et al. (Estes et al., 1998). Of the harvested species, mackerel (MCK) are hit hardest by the harvesting shocks generated from the NMFS landings data. Harvesting rates for mackerel more than doubled during the period covered by the landings data. Salmon (SAL) and cod experienced smaller declines consistent with the harvesting shocks imposed.

The trophic cascade outlined by Estes et al. (Estes et al., 1998) is evident in the relative movements of the species, though much more slight than the observed phenomena. Sea lions suffer from the increased harvesting of their prey and Orca whale populations also decline. Sea otters face declines throughout the period but are nearly recovered by the end. The degree of prey switching by Orcas is the limiting parameter on the cascade dynamics. To witness impact of this parameter, I set it to 4 instead of 1. That is, for a 1% rise in the relative scarcity of a particular prey, the Orca will now consume 4% more of the relatively abundant prey (otters in this case).

Figure 5.4 plots the population levels for the top three Orca prey, sea lions (SSL), shark mammal eaters (SMM), and sea otters (SOT), which comprise 98% of the Orca diet. The figure presents outcomes for the benchmark specification (unitary degree

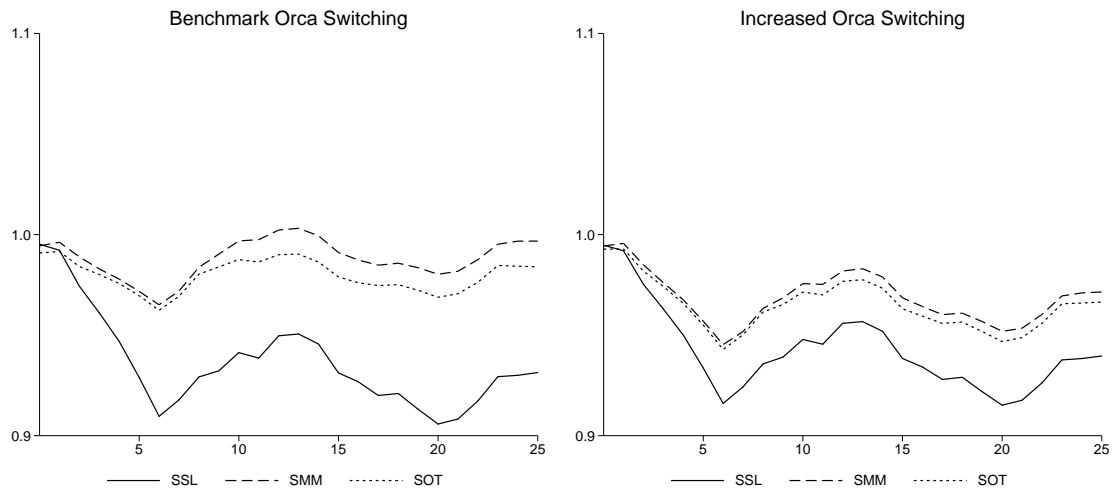


Figure 5-4: Relative population levels for perturbed species

of switching) and the increased switching alternate specification (degree of switching of 4). The otter (SOT) and mammal-eating shark (SMM) populations suffer greater losses while sea lions (SSL) gain some relief from the increased switching. That is, the Orca is able to reduce its expenditures dedicated to securing the now-scarce sea lion by switching to a greater extent to consuming the relatively abundant shark and otter populations. The Orca population (not presented) is slightly better off for this increased adaptability. As hypothesized, otters are worse-off throughout the period for the Orca’s increased switching ability.

The small share of the Orca diet taken up by sea otters (3%) is another mitigating factor here. The alternate switching scenario presented above demonstrated how, even with a relatively high degree of switching, the Orca population’s relative “distaste” for otters prevents them from dramatically increasing predation pressure on this population. This exercise demonstrates one way in which the BGE model can help characterize the impact of switching behavior on trophic interactions in the context of other shocks.

Benthic invertebrates (BEI) comprise the majority of the sea otter diet at approximately 60%; however, sea otters account for less than one percent of benthic invertebrates' predation. While there is a slight increase in benthic invertebrate abundance in the model, the otter population's influence on benthic invertebrates is generally too small to generate the kinds of impacts hypothesized by Estes et al. (Estes et al., 1998). This is likely an artifact of the species aggregation in the Ecosim data (Gu nette & Christensen, 2005), which group sea urchins within a broad aggregate of all benthic invertebrates. If the data identified urchins we may find that otters are responsible for a significant share of their predation, in which case we would expect the BGE model to yield significant impacts on the urchin species.

There are two critical caveats to note here. First, the Ecosim data are incomplete and likely do not depict the true state of the ecosystem at the desired period. Second, the harvesting shocks are taken in isolation and there were no doubt myriad other exogenous shocks to the system that could have undermined sea otter populations either directly or through another trophic cascade.

5.4 Conclusion

The invasive species scenario demonstrated the BGE model's ability to simulate bird species declines from a novel, invasive predator in a parametric fashion. With additional information on the Norway rat, we could include a full characterization of its bioenergetics in the model to examine its impact on the ecosystem. The introduction of its predation as a shock generated a trophic cascade of its own as outlined by Kurle and co-authors (Kurle et al., 2008). Bird populations declined substantially, their prey increased significantly, and other proximal "ripple effects" of the cascade were identified. The trophic cascade scenario examined a more extended network of effects driven by harvesting activity. The model was able to mimic much of the hy-

pothesized and observed behavior in a relative sense, though magnitudes were more muted. This helped to demonstrate how different parameterizations of the model can produce predictable differences in population outcomes consistent with foraging theory on switching behavior. Last, the trophic cascade scenario echoed the mantra that a ‘model is only as good as its data.’ The species resolution was too low to test hypotheses on lower-trophic responses to otter population dynamics and data aggregation may have contributed to the more muted responses observed earlier in the cascade.

Overall the BGE model has performed well in mimicking observed phenomena in direction if not entirely in level. This limited but successful test of model validity lends support to further investigations with the BGE model, perhaps including more highly-resolved data or more detailed characterizations of observed phenomena. The value of the model hinges critically on its ability to generate outcomes consistent with observed ecosystem realities. Having cleared this admittedly low but critical bar, it is worth the additional effort to identify the next-highest bar of validity and test the BGE model’s capacity for clearing it.

CHAPTER 6: CONCLUSION

6.1 Summary

This work has demonstrated how the input-output foundation and analytical structure of general equilibrium modeling is well-suited to analyzing both ecosystems and economies. Modeling these systems requires careful accounting and analysis of participants' behavior. Chapter 2 showed how exploiting accounting identities can enable integrating highly-detailed representations of energy and abatement technology into the CGE framework to represent both engineering and economic activity.

Chapter 3 provided a careful review of the biology literature needed to construct the theoretical basis for a general equilibrium model of an ecosystem. Resource scarcity, fundamental to economics, was shown to be a key driving factor in optimal foraging. The micro-behavioral features of optimal foraging were given an explicit metric of energy expenditure and benefit, forging a linkage with bioenergetic optimization. Functional representations of this measured, micro-behavioral activity was then assembled into a coherent model of aggregate ecosystem behavior.

Chapters 4 and 5 drew on empirical data to demonstrate the stability and the internal and external validity of the BGE model. Model responses to the various shocks imposed by the test scenarios in Chapter 4 made evident the damped nature of the ecosystem as represented in the BGE model. Results in Chapter 5 showed the BGE model's ability to mimic observed "real-world" phenomena as highlighted in the ecology literature. This critical test of the BGE model offered a modicum of external validity to encourage further investment in developing and testing the model for other applications.

Ecosystems and economies bear many similarities. These biological and technological systems carry a set of adaptive and interacting biologies or technologies that

combine inputs to produce distinct outputs. Beyond physical conservation of mass and energy, the participants in each system are constrained in their ability to make substitutions by the biology or technology available to them. Changes in these biologies and technologies over time are possible and indeed integral to the evolution of the system as a whole. In an abstract, and perhaps real, sense, technological systems represent an evolved part of biological systems. The capacity for one species to manipulate tools and rapidly generate new technologies spawned an entire technological system in itself - a clear punctuation in a continuum of biological and technological processes.

6.2 Future work

Ecosystems and economies are both complex adaptive systems that require sophisticated methods to represent their behavior. These systems interact in critical ways that influence the outcomes prevailing in each. Climate change has generated considerable interest in the economics community in the “integrated assessment” of climate and economics. That is, research to model the interactions between physical and technological systems has been underway for over two decades, but less work has been completed on the integrated assessment of biological and technological systems *as complex adaptive systems*.

This work is well-positioned to help complete the triangle of linkages among complex physical, biological, and technological systems. The BGE model can simulate the effects of shocks from both the climate and the economy. For example, the bioenergetic costs of increased temperature and ocean acidification could be imposed on the model and the population outcomes used to shock harvesting effort and yield in an economic model. Moreover, employing a common general equilibrium framework for both the ecosystem and economy models may enable deeper integration of the models

than is currently available to climate and economy models, opening opportunities for modeling resource management more dynamically.

In all this has been an interdisciplinary work. Using a common framework, I've demonstrated how much of the logic employed in ecology carries helpful analogues in economics. Given these analogues and the well-developed tool of economic general equilibrium, adapting that tool for biological applications is a natural extension. Seeing these systems through a common frame holds promise for casting new light on the structure and dynamics of each.

CHAPTER 7: APPENDICES

7.1 Data Construction

7.1.1 The PAGE Dataset

The Pollution, Abatement, and Generation of Electricity (PAGE) dataset is built on Energy Information Administration (EIA) and Environmental Protection Agency (EPA) data sources. All sources are for 2010 where applicable. Forms EIA-860 and EIA-923 provide a boiler- and abatement-equipment- level summary of 96% of electric generation on the US grid.

Operating Costs

Form EIA-923 data provide generation output and fuel use quantities for each technology installation in the data. Fuel use and electric output quantities are first summarized at the plant-fuel-generator level (approx. 9,300 obs.). Installations of abatement equipment are summarized at the installation-boiler level. The mapping is many-to-many. Some boilers have multiple abatement equipment installations and some installations service multiple boilers.

Cost estimates are capacity-specific. Generating units are categorized on nameplate (NP) capacity as small ($NP < 300$ MW), medium ($300 \leq NP < 700$ MW), and large ($NP \geq 700$ MW). Nameplate data are incomplete. Missing observations are estimated based on prime mover and net generation.

Abatement equipment operating costs are sourced from EPA's IPM (ICF Resources, LLC, 2010, Ch. 5). Fixed capital and O&M costs are specific to the nameplate capacity that the installation services. Variable O&M costs are independent of nameplate. O&M costs are allocated entirely to labor, though likely comprise some materials. Heat-rate penalties are valued at a wholesale fuel price and allocated to

fuel inputs. Capacity penalties are valued at a wholesale electric price and allocated to electric inputs.

Generation equipment operating costs are sourced from EIA's Annual Energy Outlook (Energy Information Administration, 2010, Table 8.2). O&M costs are allocated to labor. AEO technologies are matched to extant grid technologies to assign cost estimates. Cost estimates are adjusted for the "extraordinary rate" of increase in construction costs during the aughts (Kaplan, 2008, p. 18). All capital values are amortized at 6.15% over a 20-year life as in IPM (ICF Resources, LLC, 2010, Ch. 8).

Fuel price-per-BTU data are provided for fuel purchases made by a subset of installations. Fuel-region quantity-weighted averages are used to estimate the value of the heat-rate penalties of abatement equipment. National averages are used where fuel-region averages are unavailable.

Electricity wholesale prices are provided by trading hub by EIA (*Electricity, Wholesale Market Data*, 2013). Trading hubs are mapped to North American Electric Reliability Corporation (NERC) regions and region-specific volume-weighted average wholesale electricity prices are used to value the capacity penalties imposed by abatement equipment. Missing data for certain regions are approximated from neighboring regions.

All values are adjusted to 2010 dollars using the Bureau of Economic Analysis "GDPDEF" series (*Gross domestic product: Implicit price deflator (GDPDEF)*, 2015) for the final PAGE dataset. For the purposes of the model, only relative values enter the bottom-up – top-down reconciliation process.

Emissions

Emissions for oxides of nitrogen and sulfur, particulate matter, mercury, carbon dioxide, nitrous oxide, and methane are estimated. A variety of additional pollutants can be included based on data given in the AP-42 compilation (*AP 42, Fifth Edition*,

Compilation of Air Pollutant Emission Factors, Vol. 1, 1995). Carbon dioxide, nitrous oxide, and methane are combined into a single greenhouse-gas equivalent (GHGe) measure based on common global warming potential multipliers. Emissions are driven by a combination of fuel-specific, uncontrolled emissions factors (*AP 42, Fifth Edition, Compilation of Air Pollutant Emission Factors, Vol. 1*, 1995) and abatement equipment removal efficiencies (Form EIA-860).

Emissions factors rely on fuel sulfur and ash contents, whose empirical averages are taken from Form EIA-923 fuel-use data. These data are given at the boiler level but do not cover all installations. Fuel-specific sulfur content estimates given by Form EIA-923 documentation are modified by the empirical averages in the Form EIA-923 fuel-use data to generate fuel-region-specific averages (using census regions).

Mercury emissions are particularly sensitive to installations of non-mercury abatement equipment. Mercury emissions are estimated as the product of uncontrolled emissions rates from the EPA AP-42 compilation (*AP 42, Fifth Edition, Compilation of Air Pollutant Emission Factors, Vol. 1*, 1995) and emissions modification factors from EPA's Integrated Planning Model (ICF Resources, LLC, 2010, Table 5-13). The modification factors are a function of burner and fuel types plus NO_x, SO_x, and particulate controls. All other uncontrolled emissions rates are taken directly from the EPA AP-42 compilation (*AP 42, Fifth Edition, Compilation of Air Pollutant Emission Factors, Vol. 1*, 1995, Ch. 1) based on fuel type.

Emissions removal efficiencies of the installed equipment are given in the Form EIA-860 data. Where data are missing, abatement-technology averages are applied. These removal efficiencies are used to estimate total abatement and emissions for each installation.

Summary & aggregation

The final dataset then contains capital, labor, fuel, and electricity costs along with electricity and pollution output quantities for each generation and abatement equipment installation on the US grid that is represented in Forms EIA-860 and EIA-923 data – approximately 9,700 installations. The final step in preparing the data for the model is to summarize these values and quantities at a technological resolution sufficiently low for model feasibility.

Collapsing the installations on all technological attributes contained in the dataset produces 173 distinct technologies. To further collapse the data for feasibility, technologies accounting for less than one tenth of one percent of net generation on the grid are collapsed on fuel type, reducing the number of technologies to the final 72 incorporated in the model.

Emissions estimates are accurate to the order of magnitude of independent estimates, though are not exact. For applications where an exact matching is necessary, a balancing procedure that minimally revises the emissions factors ex-post of the value-share revision could be performed in a straightforward way. All model technologies are summarized in Appendix 7.3.

7.1.2 Social Accounting Matrix

Social Accounting Matrix (SAM) data are from the Bureau of Labor Statistics (BLS) Input-Output data (Bureau of Labor Statistics, 2012). Standard matrix manipulations are used to generate a SAM from the nominal 2010 I-O accounts. SAM column-row residuals, which are on the order of \$100,000, are distributed away by a least-squares minimization. Value-add components are allocated based on Bureau of Economic Analysis (BEA) GDP-by-industry data (Bureau of Economic Analysis, 2012).

7.2 Model Elasticities

Elasticities used in the model are adapted from the MIT EPPA (Paltsev et al., 2005) model and are summarized in Figure 7.1.

Model Elasticities			
Production, Consumption, Trade		Energy	
Elasticities	Value	Elasticities	Value
Energy -- value-add		Fixed-factor -- energy-materials	
Generation technologies	0.1	Agriculture	0.6
Nuclear & renewable technologies	0.2		
Energy-intensive sectors	0.3	Energy -- Materials	
All other	0.5	Agriculture	0.3
Capital -- labor		Electricity -- fuel	
All other	1.0	All except generation tech.	0.5
<i>Consumption elasticities</i>		<i>Fixed Factors</i>	
Transportation -- other cons.	1.0	Fixed-factor -- all-other (fuels)	0.6
Energy -- materials-services	0.7	Fixed-factor -- energy-matls (agr.)	0.7
Materials -- services	0.3		
Electricity -- fuels	0.3	Fuels	
Fuels	0.4	All prod. except generation	1.0
<i>Trade elasticities</i>		<i>Electric-specific elasticities</i>	
Imports -- domestic prod.	3.0	Electric loads	0.3
Local -- exports (output)	2.0	Baseload technologies	1.2
		Mid-load technologies	1.0
		Peak-load technologies	0.8

Notes: Indented descriptions indicate the elasticity for a subset of sectors.
Sources: MIT EPPA model (Paltsev et al., 2005).

Figure 7.1: Elasticities used in CGE model

Technology code legend			
<u>Model technology</u>	<u>Code</u>	<u>Model technology</u>	<u>Code</u>
<i>Fuels</i>		<i>Fuels (cont.)</i>	
Bituminous coal	BIT	Oil	OIL
Sub-bituminous coal	SUB	Nuclear	NUC
Lignite coal	LIG	Renewables	RNW
Gas	GAS	Hydro	WAT
<i>NOx Controls</i>		<i>Particulate Controls</i>	
Low NOx burner	LN	Cold side	CS
Catalytic reduction	SR	Fabric filter	FF
Overfire air	OFA	Hot side	HS
Noncatalytic reduction	SN	Other methods	OT
Other change in process	OM		
Fuel reburning	FU		
<i>SOx Controls</i>		<i>Mercury Controls</i>	
Wet scrubber	WET	Activated carbon injection	ACJ
Dry scrubber	DRY		
Sources: PAGE dataset.			

Figure 7-2: Legend of fuel & technology codes

7.3 Model Technologies

This appendix provides a full list of the 72 technologies that operate within the model. Figure 7-3 lists each technology with a description of the attributes that define it and a summary of its net generation and GHGe emissions.

Model Technologies										
Fuel							Small	Net	GHGe	
No.	Type	PM	SOx	NOx	Hg	Net Gen.	Generation (GWh)	Total Cost (\$2010 MM)	Emissions (MMT)	
1.	BIT	CS	WET	SR			374,000	\$ 26,748	463	
2.	SUB	CS	WET	LN			227,000	15,728	328	
3.	BIT	CS	WET	LN			190,000	13,968	247	
4.	SUB	CS	WET	OFA			79,100	5,526	116	
5.	SUB	CS	WET	SR			68,600	5,439	93	
6.	BIT	CS	WET	SN			43,300	3,529	57	
7.	BIT	HS	WET	SR			42,900	2,620	56	
8.	BIT	FF	WET	LN			40,000	2,349	55	
9.	SUB	CS	WET	LN	ACJ		37,600	2,626	53	
10.	SUB					•	36,100	2,568	57	
11.	SUB	HS	WET	LN			35,800	2,271	53	
12.	BIT	HS	WET	LN			35,600	2,257	48	
13.	SUB	FF	WET	LN			35,400	2,052	50	
14.	BIT					•	35,400	2,895	44	
15.	SUB	FF	DRY	SR	ACJ		31,800	2,085	45	
16.	LIG	CS	WET	LN			27,600	1,568	54	
17.	SUB	FF	WET	SR			21,500	1,328	33	
18.	LIG					•	19,600	1,122	40	
19.	SUB	FF	DRY	LN			18,900	1,073	26	
20.	SUB	CS	WET	SR	ACJ		16,900	1,276	24	
21.	SUB	FF	WET	OFA			15,400	865	22	
22.	SUB	CS	WET	OM			14,000	1,082	21	
23.	BIT	FF	DRY	LN			13,800	804	18	
24.	BIT	OT	WET	SR			13,600	817	16	
25.	SUB	CS	DRY	LN			13,600	870	22	
26.	SUB	OT	WET	LN			13,200	795	20	
27.	BIT	FF	WET	SN			12,700	802	17	
28.	LIG	CS	WET	LN	ACJ		12,600	794	24	
29.	SUB	CS	WET	OFA	ACJ		11,500	813	17	
30.	SUB	HS	WET	OFA	ACJ		11,500	754	17	
31.	BIT	HS	WET	OFA			11,100	520	15	
32.	SUB	OT	WET	LN	ACJ		10,700	580	16	
33.	BIT	CS	WET	SR	ACJ		10,100	813	12	
34.	SUB	CS	WET				10,100	911	16	
35.	BIT	FF	WET	SR			9,639	729	12	
36.	BIT	CS	WET	OFA			9,304	842	12	
37.	BIT	HS	DRY	SR			7,748	473	10	
38.	SUB	FF	DRY	SR			7,411	438	11	
39.	SUB	HS	WET	OFA			7,247	453	10	
40.	SUB	FF	DRY	LN	ACJ		7,183	425	10	
41.	LIG	FF	DRY	LN			6,360	244	12	
42.	LIG	CSFF	WET	SN	ACJ		6,087	553	11	

Model Technologies										
No.	Fuel		SOx	NOx	Hg	Small	Net	Total Cost (\$2010 MM)	GHGe Emissions (MMT)	
	Type	PM				Gen.	Generation (GWh)			
43.	SUB	CS	WET	SN				6,039	505	9
44.	BIT	HS	WET	SR	ACJ			6,036	482	8
45.	BIT		WET	LN				5,855	335	7
46.	BIT	FF	DRY	SN				5,729	380	7
47.	SUB	OT	WET	OFA	ACJ			5,548	300	8
48.	BIT	CS	WET	OM				5,340	602	8
49.	SUB	FF	WET	OM				5,319	355	13
50.	BIT	HS	WET	SN				4,954	377	6
51.	SUB	OT	WET	OFA				4,852	294	7
52.	BIT	FF	WET	OM				4,643	303	7
53.	BIT	CS	WET					4,639	594	7
54.	BIT	CS	WET	SN	ACJ			4,531	454	6
55.	LIG	CS	WET	OFA				4,518	207	9
56.	SUB	HS	DRY	LN				4,287	237	6
57.	SUB	CS	DRY	LN	ACJ			4,254	282	6
58.	SUB	FF	DRY	SN				3,956	133	9
59.	SUB	FF	WET	SN				3,913	265	7
60.	LIG	FF	WET	SR	ACJ			3,907	220	7
61.	GAS		WET					749,000	71,892	422
62.	GAS		WET	SR				147,000	9,175	17
63.	GAS		WET	LN				40,700	3,909	14
64.	GAS		WET	OM				22,200	3,105	14
65.	GAS		WET	OFA				8,829	1,159	6
66.	GAS	CS	WET	OFA				3,894	536	3
67.	GAS					•		1,339	261	1
68.	NUC							807,000	22,200	0
69.	OIL		WET					10,800	5,439	213
70.	OIL					•		6,625	3,761	136
71.	RNW							174,000	3,057	0
72.	WAT							<u>255,000</u>	<u>12,239</u>	<u>0</u>
Count:		57	64	60	15					
Total:								3,966,687	\$ 257,461	3,247

Notes: Small net generation technologies is a sum of all technologies producing less than a tenth of one percent of net generation. These technology aggregates operate a variety of abatement equipment.

Source: PAGE dataset.

Figure 7-3: Full list of model technologies

REFERENCES

- Abrams, P. A. (2010, February). Implications of flexible foraging for interspecific interactions: Lessons from simple models. *Functional Ecology*, *24*(1), 7–17. Retrieved from <http://doi.wiley.com/10.1111/j.1365-2435.2009.01621.x> doi: 10.1111/j.1365-2435.2009.01621.x
- Abrams, P. A., & Ludwig, D. (1995). Optimality theory, Gompertz' Law, and the disposable soma theory of senescence. *Evolution*, *49*(6), 1055–1066.
- Agrawal, A. A. (2001, October). Phenotypic plasticity in the interactions and evolution of species. *Science*, *294*(5541), 321–326. Retrieved from <http://www.ncbi.nlm.nih.gov/pubmed/11598291> doi: 10.1126/science.1060701
- AP 42, Fifth Edition, Compilation of Air Pollutant Emission Factors, Vol. 1* (Tech. Rep.). (1995). Research Triangle Park, NC: Office of Air Quality Planning and Standards, Environmental Protection Agency. Retrieved from <http://www.epa.gov/ttn/chief/ap42/>
- Armington, P. S. (1969). A Theory of Demand for Products Distinguished by Place of Production. *Staff Papers - International Monetary Fund*, *16*(1), 159–178.
- Arrow, K. J. (1968). Economic equilibrium. In *International encyclopedia of the social sciences, vol. 4*. New York, NY: McMillan Company.
- Arrow, K. J., Chenery, H. B., Minhas, B. S., & Solow, R. M. (1961). Capital-labor substitution and economic efficiency. *The Review of Economics and Statistics*, *43*(3), 225–250. Retrieved from <http://www.jstor.org/stable/10.2307/1927286>
- Beckerman, A., Petchey, O. L., & Morin, P. J. (2010, February). Adaptive foragers and community ecology: linking individuals to communities and ecosystems. *Functional Ecology*, *24*(1), 1–6. Retrieved from <http://doi.wiley.com/10.1111/j.1365-2435.2009.01673.x> doi: 10.1111/j.1365-2435.2009.01673.x
- Beckerman, A. P., Petchey, O. L., & Warren, P. H. (2006, September). Foraging biology predicts food web complexity. *Proceedings of the National Academy of Sciences of the United States of America*, *103*(37), 13745–9. doi: 10.1073/pnas.0603039103
- Bélisle, C., & Cresswell, J. (1997, August). The effects of a limited memory capacity on foraging behavior. *Theoretical Population Biology*, *52*(1), 78–90. Retrieved from <http://www.ncbi.nlm.nih.gov/pubmed/9356325>

- Berryman, A. A., Michalski, J., Gutierrez, A. P., & Arditi, R. (1995). Logistic theory of food web dynamics. *Ecology*, *76*(2), 336–343.
- Böhringer, C., & Rutherford, T. F. (2008, March). Combining Bottom-up and Top-down. *Energy Economics*, *30*(2), 574–596. Retrieved from <http://linkinghub.elsevier.com/retrieve/pii/S014098830700059X> doi: 10.1016/j.eneco.2007.03.004
- Böhringer, C., & Rutherford, T. F. (2009, September). Integrated Assessment of Energy Policies: Decomposing Top-down and Bottom-up. *Journal of Economic Dynamics and Control*, *33*(9), 1648–1661. Retrieved from <http://linkinghub.elsevier.com/retrieve/pii/S0165188909000529> doi: 10.1016/j.jedc.2008.12.007
- Bond, A. B. (2007, December). The evolution of color polymorphism: Crypticity, searching images, and apostatic selection. *Annual Review of Ecology, Evolution, and Systematics*, *38*(1), 489–514. Retrieved from <http://dx.doi.org/10.1146/annurev.ecolsys.38.091206.095728> doi: 10.1146/annurev.ecolsys.38.091206.095728
- Brose, U. (2010, February). Body-mass constraints on foraging behaviour determine population and food-web dynamics. *Functional Ecology*, *24*(1), 28–34. Retrieved from <http://doi.wiley.com/10.1111/j.1365-2435.2009.01618.x> doi: 10.1111/j.1365-2435.2009.01618.x
- Bureau of Economic Analysis. (2012). *Gross-Domestic-Product-(GDP)-by-Industry Data*. Retrieved from http://www.bea.gov/industry/gdpbyind_data.htm
- Bureau of Labor Statistics. (2012). *Inter-industry relationships (Input/Output matrix)*. Retrieved from http://www.bls.gov/emp/ep_data_input_output_matrix.htm
- Burtraw, D., Krupnick, A., Palmer, K., Paul, A., Toman, M., & Bloyd, C. (2003, May). Ancillary benefits of reduced air pollution in the US from moderate greenhouse gas mitigation policies in the electricity sector. *Journal of Environmental Economics and Management*, *45*(3), 650–673. Retrieved from <http://linkinghub.elsevier.com/retrieve/pii/S0095069602000220> doi: 10.1016/S0095-0696(02)00022-0
- Christensen, V., & Walters, C. J. (2004, March). Ecopath with Ecosim: Methods, capabilities and limitations. *Ecological Modelling*, *172*(2-4), 109–139. Retrieved from <http://linkinghub.elsevier.com/retrieve/pii/S030438000300365X> doi: 10.1016/j.ecolmodel.2003.09.003

- Cohen, J. E., & Newman, C. M. (1985). A stochastic theory of community food webs: I. Models and aggregated data. *Proceedings of the Royal Society of London. Series B. Biological Sciences*, 224(1237), 421–448.
- Dawkins, R. (1989). *The Selfish Gene* (Second ed.). New York, NY: Oxford University Press.
- Dellink, R., Hofkes, M., van Ierland, E., & Verbruggen, H. (2004, December). Dynamic Modelling of Pollution Abatement in a CGE Framework. *Economic Modelling*, 21(6), 965–989. Retrieved from <http://linkinghub.elsevier.com/retrieve/pii/S0264999303000877> doi: 10.1016/j.econmod.2003.10.009
- Dewar, R. C. (2010, May). Maximum Entropy Production and Plant Optimization Theories. *Philosophical Transactions of the Royal Society of London. Series B, Biological Sciences*, 365, 1429–35. doi: 10.1098/rstb.2009.0293
- Diekmann, O., & Metz, J. A. J. (2010, November). How to lift a model for individual behaviour to the population level? *Philosophical Transactions of the Royal Society of London. Series B, Biological Sciences*, 365(1557), 3523–30. doi: 10.1098/rstb.2010.0100
- Drossel, B. (2001, March). Biological evolution and statistical physics. *Advances in Physics*, 50(2), 209–295. Retrieved from <http://www.tandfonline.com/doi/abs/10.1080/00018730110041365> doi: 10.1080/00018730110041365
- Dukas, R. (2002). Behavioural and ecological consequences of limited attention. *Philosophical Transactions of the Royal Society of London. Series B: Biological Sciences*, 357(1427), 1539–1547.
- Dukas, R., & Kamil, A. C. (2001). Limited attention: The constraint underlying search image. *Behavioral Ecology*, 12(2), 192–199.
- Eichner, T., & Pethig, R. (2006, July). An analytical foundation of the ratio-dependent predator-prey model. *Journal of Bioeconomics*, 8(2), 121–132. Retrieved from <http://link.springer.com/10.1007/s10818-006-0005-8> doi: 10.1007/s10818-006-0005-8
- Ejmond, M. J., Czarnoński, M., Kapustka, F., & Kozłowski, J. (2010, May). How to time growth and reproduction during the vegetative season: An evolutionary choice for indeterminate growers in seasonal environments. *The American Naturalist*, 175(5), 551–63. Retrieved from <http://www.ncbi.nlm.nih.gov/pubmed/20331361> doi: 10.1086/651589
- Electricity, Wholesale Market Data* (Tech. Rep.). (2013). Washington, D.C.: Energy Information Administration, Intercontinental Exchange. Retrieved from <http://www.eia.gov/electricity/wholesale/index.cfm>

- Elliott, J. M. (2004, June). Prey switching in four species of carnivorous stoneflies. *Freshwater Biology*, 49(6), 709–720. Retrieved from <http://doi.wiley.com/10.1111/j.1365-2427.2004.01222.x> doi: 10.1111/j.1365-2427.2004.01222.x
- Elliott, J. M. (2006). Prey switching in *Rhyacophila Dorsalis* (Trichoptera) alters with larval instar. *Freshwater Biology*, 51, 913–924. doi: 10.1111/j.1365-2427.2006.01549.x
- Elton, R. A., & Greenwood, J. J. D. (1970). Exploring apostatic selection. *Heredity*, 25(4), 629.
- Emlen, J. M. (1966). The role of time and energy in food preference. *The American Naturalist*, 100(916), 611–617.
- Energy Information Administration. (2010). *Assumptions to the Annual Energy Outlook 2010 - Electricity Market Module, Report No. DOE/EIA-0554(2010)* (Tech. Rep.). Washington, D.C.: Department of Energy. Retrieved from <http://www.eia.gov/oiaf/aec/assumption/electricity.html>
- EPA. (2014). *Clean Power Plan Proposed Rule*. Retrieved 2014-12-01, from www2.epa.gov/carbon-pollution-standards/clean-power-plan-proposed-rule
- Estes, J., Tinker, M., Williams, T., & Doak, D. (1998). Killer whale predation on sea otters linking oceanic and nearshore ecosystems. *Science*, 282(October 16), 473–6.
- Fann, N., Fulcher, C. M., & Hubbell, B. J. (2009, September). The influence of location, source, and emission type in estimates of the human health benefits of reducing a ton of air pollution. *Air Quality, Atmosphere, & Health*, 2(3), 169–176. Retrieved from <http://www.pubmedcentral.nih.gov/articlerender.fcgi?artid=2770129&tool=pmcentrez&rendertype=abstract> doi: 10.1007/s11869-009-0044-0
- Finnoff, D., & Tschirhart, J. (2003). Protecting an endangered species while harvesting its prey in a general equilibrium ecosystem model. *Land Economics*, 79(2), 160–180.
- Finnoff, D., & Tschirhart, J. (2005, February). Identifying, preventing and controlling invasive plant species using their physiological traits. *Ecological Economics*, 52(3), 397–416. Retrieved from <http://linkinghub.elsevier.com/retrieve/pii/S0921800904003118> doi: 10.1016/j.ecolecon.2004.06.021
- Finnoff, D., & Tschirhart, J. (2008, May). Linking dynamic economic and ecological general equilibrium models. *Resource and Energy Economics*, 30(2), 91–114. doi: 10.1016/j.reseneeco.2007.08.005

- Form EIA-860* (Tech. Rep.). (2010). Washington, D.C.: Energy Information Administration. Retrieved from <http://www.eia.gov/electricity/data/eia860/>
- Form EIA-923* (Tech. Rep.). (2010). Washington, D.C.: Energy Information Administration. Retrieved from <http://www.eia.gov/electricity/data/eia923/>
- Garcia-Domingo, J. L., & Saldaña, J. (2007, August). Food-web complexity emerging from ecological dynamics on adaptive networks. *Journal of Theoretical Biology*, *247*(4), 819–26. Retrieved from <http://www.ncbi.nlm.nih.gov/pubmed/17512552> doi: 10.1016/j.jtbi.2007.04.011
- Gerlagh, R., Dellink, R., Hofkes, M., & Verbruggen, H. (2002). A Measure of Sustainable National Income for the Netherlands. *Ecological Economics*, *41*, 157–174.
- Giacomini, H. C., & Shuter, B. J. (2013, August). Adaptive responses of energy storage and fish life histories to climatic gradients. *Journal of Theoretical Biology*, *339*, 1–12. Retrieved from <http://www.ncbi.nlm.nih.gov/pubmed/23999284>
- Giacomini, H. C., Shuter, B. J., & Lester, N. P. (2013, September). Predator bioenergetics and the prey size spectrum: Do foraging costs determine fish production? *Journal of Theoretical Biology*, *332*, 249–60. Retrieved from <http://www.ncbi.nlm.nih.gov/pubmed/23685066> doi: 10.1016/j.jtbi.2013.05.004
- Greenwood, J. J. D., & Elton, R. A. (1979). Analysing experiments on frequency-dependent selection by predators. *Journal of Animal Ecology*, *48*(3), 721–737.
- Gross domestic product: Implicit price deflator (GDPDEF)* (Tech. Rep.). (2015). Washington, D.C.: Bureau of Economic Analysis. Retrieved from <http://research.stlouisfed.org/fred2/series/GDPDEF/>
- Guénette, S., & Christensen, V. (2005). *Food web models and data for studying fisheries and environmental impacts on Eastern Pacific ecosystems* (Tech. Rep.). Fisheries Centre, University of British Columbia. Retrieved from <http://www.ecopath.org/model/109>
- Hannon, B. (1985). Linear dynamic ecosystems. *Journal of Theoretical Biology*(116), 89–110. Retrieved from <http://www.sciencedirect.com/science/article/pii/S0022519385801326>
- Hannon, B. (1986). Ecosystem Control Theory. *Journal of Theoretical Biology*, *121*, 417–437.
- Holland, S. P. (2010). *Spillovers from climate policy*. Cambridge, MA. Retrieved from <http://www.nber.org/papers/w16158>

- Holling, C. S. (1959, May). The components of predation as revealed by a study of small-mammal predation of the European Pine Sawfly. *The Canadian Entomologist*, 91(5), 293–320. Retrieved from http://journals.cambridge.org/abstract_S0008347X00072564 doi: 10.4039/Ent91293-5
- ICF Resources, LLC. (2010). *Standalone Documentation for EPA Base Case 2010 (V.4.10), Using the Integrated Planning Model* (Tech. Rep.). Environmental Protection Agency. Retrieved from <http://www.epa.gov/airmarkets/progsregs/epa-ipm/BaseCasev410.html>
- Jones, H. P., Tershy, B. R., Zavaleta, E. S., Croll, D. a., Keitt, B. S., Finkelstein, M. E., & Howald, G. R. (2008). Severity of the effects of invasive rats on seabirds: A global review. *Conservation Biology*, 22(1), 16–26. doi: 10.1111/j.1523-1739.2007.00859.x
- Kaplan, S. (2008). *Power plants: Characteristics and costs, Order code RL34746* (Tech. Rep.). Washington, D.C.: Congressional Research Service.
- Katsukawa, Y., Katsukawa, T., & Matsuda, H. (2002). Indeterminate growth is selected by a trade-off between high fecundity and risk avoidance in stochastic environments. *Population Ecology*, 44, 265–272.
- Kavanagh, P., Newlands, N., Christensen, V., & Pauly, D. (2004, March). Automated parameter optimization for Ecopath ecosystem models. *Ecological Modelling*, 172(2-4), 141–149. Retrieved from <http://linkinghub.elsevier.com/retrieve/pii/S0304380003003661> doi: 10.1016/j.ecolmodel.2003.09.004
- Kean-Howie, J. C., Pearre, S., & Dickie, L. M. (1988, December). Experimental predation by sticklebacks on larval mackerel and protection of fish larvae by zooplankton alternative prey. *Journal of Experimental Marine Biology and Ecology*, 124(3), 239–259. Retrieved from <http://linkinghub.elsevier.com/retrieve/pii/0022098188901748> doi: 10.1016/0022-0981(88)90174-8
- Kirkwood, T. B. L. (1981). Repair and its evolution: Survival versus reproduction. In C. R. Townsend & P. Calow (Eds.), *An evolutionary approach to resource use* (pp. 165–189). Oxford, UK: Blackwell Scientific.
- Kiula, O., & Rutherford, T. F. (2013, March). The Cost of Reducing CO2 Emissions: Integrating Abatement Technologies into Economic Modeling. *Ecological Economics*, 87, 62–71. Retrieved from <http://linkinghub.elsevier.com/retrieve/pii/S0921800912004892> doi: 10.1016/j.ecolecon.2012.12.006
- Křivan, V., & Diehl, S. (2005, March). Adaptive omnivory and species coexistence in tri-trophic food webs. *Theoretical Population Biology*, 67(2), 85–99. Retrieved from <http://www.ncbi.nlm.nih.gov/pubmed/15713322> doi: 10.1016/j.tpb.2004.09.003

- Křivan, V., & Schmitz, O. J. (2003). Adaptive foraging and flexible food web topology. *Evolutionary Ecology Research*, 5, 623–652.
- Kleidon, A., & Lorenz, R. D. (Eds.). (2005). *Non-Equilibrium Thermodynamics and The Production of Entropy: Life, Earth, and Beyond*. New York, NY: Springer Verlag.
- Kondoh, M. (2003, February). Foraging adaptation and the relationship between food-web complexity and stability. *Science*, 299(5611), 1388–91. Retrieved from <http://www.ncbi.nlm.nih.gov/pubmed/12610303> doi: 10.1126/science.1079154
- Kooijman, S. A. L. M. (2000). *Dynamic energy and mass budgets in biological systems* (2nd ed.). Cambridge, U.K.: Cambridge University Press.
- Kozłowski, J., & Teriokhin, A. T. (1999). Allocation of energy between growth and reproduction: The Pontryagin Maximum Principle solution for the case of age- and season-dependent mortality. *Evolutionary Ecology Research*, 1, 423–441.
- Kozłowski, J., & Uchmański, J. (1987). Optimal individual growth and reproduction in perennial species with indeterminate growth. *Evolutionary Ecology*, 1(3), 214–230.
- Kurle, C. M., Croll, D. a., & Tershy, B. R. (2008, March). Introduced rats indirectly change marine rocky intertidal communities from algae- to invertebrate-dominated. *Proceedings of the National Academy of Sciences of the United States of America*, 105(10), 3800–4. doi: 10.1073/pnas.0800570105
- Lorenz, R. D. (2002). Planets, life and the production of entropy. *International Journal of Astrobiology*, 1(01), 3–13.
- MacArthur, R. H., & Pianka, E. R. (1966). On optimal use of a patchy environment. *The American Naturalist*, 100(916), 603–609.
- May, R. M. (1972). Will a large complex system be stable? *Nature*, 238, 413–414.
- Morris, J., Paltsev, S., & Reilly, J. (2012, November). Marginal abatement costs and marginal welfare costs for greenhouse gas emissions reductions: Results from the EPPA model. *Environmental Modeling & Assessment*, 17(4), 325–336.
- Mullon, C., Shin, Y., & Cury, P. (2009, November). NEATS: A Network Economics Approach to Trophic Systems. *Ecological Modelling*, 220(21), 3033–3045. Retrieved from <http://linkinghub.elsevier.com/retrieve/pii/S0304380009000891> doi: 10.1016/j.ecolmodel.2009.02.008

- Murdoch, W. W. (1969). Switching in general predators: Experiments on predator specificity and stability of prey populations. *Ecological Monographs*, 39(4), 335–354.
- Murdoch, W. W., & Oaten, A. (1975). Switching, functional response, and stability in predator-prey systems. *The American Naturalist*, 109(967), 299–318.
- Nagurney, A. (1998). *Network economics: A variational inequality approach* (Second ed., Vol. 10). Boston, MA: Kluwer Academic.
- Nagurney, A., & Nagurney, L. S. (2011, May). Spatial price equilibrium and food webs: The economics of predator-prey networks. *2011 International Conference on Business Management and Electronic Information*, 1–6. Retrieved from <http://ieeexplore.ieee.org/lpdocs/epic03/wrapper.htm?arnumber=5914417> doi: 10.1109/ICBMEI.2011.5914417
- Nam, K.-M., Waugh, C. J., Paltsev, S., Reilly, J. M., & Karplus, V. J. (2014, November). Synergy between pollution and carbon emissions control: Comparing China and the United States. *Energy Economics*, 46, 186–201. Retrieved from <http://linkinghub.elsevier.com/retrieve/pii/S0140988314001947> doi: 10.1016/j.eneco.2014.08.013
- Nemet, G. F., Holloway, T., & Meier, P. (2010, January). Implications of incorporating air-quality co-benefits into climate change policymaking. *Environmental Research Letters*, 5(1), 014007. doi: 10.1088/1748-9326/5/1/014007
- Nestor, D. V., & Pasurka, C. A. (1995). Environment-Economic Accounting and Indicators of the Economic Importance of Environmental Protection Activities. *Review of Income and Wealth*, 41(3), 265–287.
- The NewERA Model*. (2013). New York, NY: NERA Economic Consulting. Retrieved from http://www.nera.com/67_7658.htm
- NOAA. (2015). *Annual Landings*. Retrieved 2014-12-14, from <http://www.st.nmfs.noaa.gov/commercial-fisheries/commercial-landings/annual-landings>
- OECD. (2000, October). *Ancillary Benefits and Costs of Greenhouse Gas Mitigation* (Tech. Rep.). Paris, France: Author. doi: 10.1787/9789264188129-en
- Paltsev, S., Reilly, J. M., Jacoby, H. D., Eckaus, R. S., McFarland, J., Sarofim, M., . . . Babiker, M. (2005). *The MIT Emissions Prediction and Policy Analysis (EPPA) model: Version 4* (Tech. Rep. No. 125). Cambridge, MA.: MIT Joint Program on the Science and Policy of Global Change.
- Paul, A., & Burtraw, D. (2002). *The RFF Haiku Electricity Market Model* (No. June). Retrieved from <http://www.rff.org/rff/Documents/RFF-RPT-haiku.pdf>

- Perrin, N., Sibly, R. M., & Nichols, N. K. (1993). Optimal growth strategies when mortality and production rates are size-dependent. *Evolutionary Ecology*, 7(6), 576–592.
- Phelps, E. S. (1963). Substitution, fixed proportions, growth and distribution. *International Economic Review*, 4(3), 265–288.
- Pizer, W. A., & Kopp, R. (2003). *Calculating the Costs of Environmental Regulation* (No. March). Washington, D.C. Retrieved from <http://www.rff.org/documents/RFF-DP-03-06.pdf>
- Plitzko, S. J., Drossel, B., & Guill, C. (2012, August). Complexity-stability relations in generalized food-web models with realistic parameters. *Journal of Theoretical Biology*, 306, 7–14. Retrieved from <http://www.ncbi.nlm.nih.gov/pubmed/22575485> doi: 10.1016/j.jtbi.2012.04.008
- Quince, C., Abrams, P. A., Shuter, B. J., & Lester, N. P. (2008, September). Biphasic growth in fish I: Theoretical foundations. *Journal of Theoretical Biology*, 254(2), 197–206. Retrieved from <http://www.ncbi.nlm.nih.gov/pubmed/18606423> doi: 10.1016/j.jtbi.2008.05.029
- Reader, S. M., & Laland, K. N. (Eds.). (2003). *Animal Innovation*. Oxford, UK: Oxford University Press.
- Rindorf, A., Gislason, H., & Lewy, P. (2006, November). Prey switching of cod and whiting in the North Sea. *Marine Ecology Progress Series*, 325, 243–253. Retrieved from <http://www.int-res.com/abstracts/meps/v325/p243-253/> doi: 10.3354/meps325243
- Robinson, S., Cattaneo, A., & El-said, M. (2001). Updating and Estimating a Social Accounting Matrix Using Cross Entropy Methods. *Economic Systems Research*, Vol. 13(1), 47–64.
- Roff, D. A. (1983). An allocation model of growth and reproduction in fish. *Canadian Journal of Fisheries and Aquatic Sciences*, 40(9), 1395–1404.
- Ross, M. T. (2008). *Documentation of the Applied Dynamic Analysis of the Global Economy (ADAGE) Model Model*. Durham, NC. Retrieved from <http://www.rti.org/page.cfm?obj=DDC06637-7973-4B0F-AC46B3C69E09ADA9>
- Ruth, M. (1993). *Integrating economics, ecology, and thermodynamics*. Dordrecht; Boston: Kluwer Academic.
- Sato, R. (1967). A Two-Level Constant-Elasticity-of-Substitution Production Function. *The Review of Economic Studies*, 34(2), 201–218.

- Sol, D., Duncan, R. P., Blackburn, T. M., Cassey, P., & Lefebvre, L. (2005). Big brains, enhanced cognition, and response of birds to novel environments. *Proceedings of the National Academy of Sciences of the United States of America*, *102*(15), 5460–5465.
- Sousa, T., Domingos, T., Poggiale, J.-C., & Kooijman, S. A. L. M. (2010, November). Dynamic energy budget theory restores coherence in biology. *Philosophical Transactions of the Royal Society of London. Series B, Biological Sciences*, *365*(1557), 3413–28. Retrieved from <http://www.pubmedcentral.nih.gov/articlerender.fcgi?artid=2981977&tool=pmcentrez&rendertype=abstract> doi: 10.1098/rstb.2010.0166
- State-Level U.S. Data for 2010*. (2012). Minnesota IMPLAN Group, Inc.
- Stephens, D. W., & Krebs, J. R. (1986). *Foraging Theory* (Vol. 1) (No. 10). Princeton, N.J.: Princeton University Press.
- Stouffer, D. B. (2010, February). Scaling from individuals to networks in food webs. *Functional Ecology*, *24*(1), 44–51. Retrieved from <http://doi.wiley.com/10.1111/j.1365-2435.2009.01644.x> doi: 10.1111/j.1365-2435.2009.01644.x
- Stouffer, D. B., Camacho, J., Guimera, R., Ng, C. A., & Amaral, L. A. N. (2005). Quantitative patterns in the structure of model and empirical food webs. *Ecology*, *86*(5), 1301–1311.
- Sue Wing, I. (2008, March). The synthesis of bottom-up and top-down approaches to climate policy modeling: Electric power technology detail in a social accounting framework. *Energy Economics*, *30*(2), 547–573. Retrieved from <http://linkinghub.elsevier.com/retrieve/pii/S014098830600079X> doi: 10.1016/j.eneco.2006.06.004
- Teriokhin, A. T. (1998). Evolutionarily optimal age schedule of repair: Computer modelling of energy partition between current and future survival and reproduction. *Evolutionary Ecology*, *12*, 291–307.
- Thygesen, U. H. g., Farnsworth, K. D., Andersen, K. H., & Beyer, J. E. (2005, July). How optimal life history changes with the community size-spectrum. *Proceedings of the Royal Society B, Biological Sciences*, *272*(1570), 1323–31. doi: 10.1098/rspb.2005.3094
- Tschirhart, J. (2003). Ecological transfers in non-human communities parallel economic markets in a general equilibrium ecosystem model. *Journal of Bioeconomics*, *5*(2), 193–214. Retrieved from <http://www.springerlink.com/index/X336M454NP36778R.pdf>

- Tschirhart, J. (2009, October). Integrated Ecological-Economic Models. *Annual Review of Resource Economics*, 1(1), 381–407. Retrieved from <http://www.annualreviews.org/doi/abs/10.1146/annurev.resource.050708.144113> doi: 10.1146/annurev.resource.050708.144113
- Tschirhart, J. T. (2000, March). General equilibrium of an ecosystem. *Journal of Theoretical Biology*, 203(1), 13–32. Retrieved from <http://www.ncbi.nlm.nih.gov/pubmed/10677274><http://www.sciencedirect.com/science/article/pii/S0022519399910585> doi: 10.1006/jtbi.1999.1058
- Tschirhart, J. T. (2004). A new adaptive system approach to predator – prey modeling. *Ecological Modelling*, 176(March 2003), 255–276. doi: 10.1016/j.ecolmodel.2004.01.009
- Tschirhart, J. T., & Pethig, R. (2001). Microfoundations of population dynamics. *Journal of Bioeconomics*, 3(1), 27–49. Retrieved from <http://www.springerlink.com/index/ERQCCKNEC6ACMQUB.pdf>
- Van Leeuwen, E., Jansen, V. A. A., & Bright, P. W. (2007, June). How population dynamics shape the functional response in a one-predator-two-prey system. *Ecology*, 88(6), 1571–81. Retrieved from <http://www.ncbi.nlm.nih.gov/pubmed/17601148>
- van Baalen, M., Křivan, V., van Rijn, P. C. J., & Sabelis, M. W. (2001, May). Alternative food, switching predators, and the persistence of predator-prey systems. *The American Naturalist*, 157(5), 512–524. Retrieved from <http://www.jstor.org/stable/10.1086/319933> doi: 10.1086/319933
- van Leeuwen, E., Brännström, A., Jansen, V. A. A., Dieckmann, U., & Rossberg, A. G. (2013, July). A generalized functional response for predators that switch between multiple prey species. *Journal of Theoretical Biology*, 328, 89–98. Retrieved from <http://www.ncbi.nlm.nih.gov/pubmed/23422235> doi: 10.1016/j.jtbi.2013.02.003
- Walters, C., Pauly, D., Christensen, V., & Kitchell, J. F. (2000, January). Representing density dependent consequences of life history strategies in aquatic ecosystems: EcoSim II. *Ecosystems*, 3(1), 70–83. Retrieved from <http://link.springer.com/10.1007/s100210000011> doi: 10.1007/s100210000011
- Weale, M. E., Whitwell, D., Raison, H. E., Raymond, D. L., & Allen, J. A. (2000, August). The influence of density on frequency-dependent food selection: A comparison of four experiments with wild birds. *Oecologia*, 124(3), 391–395. Retrieved from <http://link.springer.com/10.1007/s004420000399> doi: 10.1007/s004420000399

- Williams, R. J., & Martinez, N. D. (2000, March). Simple rules yield complex food webs. *Nature*, *404*(6774), 180–3. Retrieved from <http://www.ncbi.nlm.nih.gov/pubmed/10724169> doi: 10.1038/35004572
- Williams, T. M., Estes, J. A., Doak, D. F., & Springer, A. M. (2004). Killer appetites: Assessing the role of predators in ecological communities. *Ecology*, *85*(12), 3373–3384.
- Wissner-Gross, A. D., & Freer, C. E. (2013, April). Causal Entropic Forces. *Physical Review Letters*, *110*(16), 168702. Retrieved from <http://link.aps.org/doi/10.1103/PhysRevLett.110.168702> doi: 10.1103/PhysRevLett.110.168702
- Ziółko, M., & Kozłowski, J. (1983, May). Evolution of body size: an optimization model. *Mathematical Biosciences*, *64*(1), 127–143. Retrieved from <http://www.sciencedirect.com/science/article/pii/0025556483900329> doi: [http://dx.doi.org/10.1016/0025-5564\(83\)90032-9](http://dx.doi.org/10.1016/0025-5564(83)90032-9)

Curriculum Vitae

JARED WOOLLACOTT

Ph.D. Candidate, Department of Earth & Environment, Boston University
685 Commonwealth Ave., Rm. 132, Boston MA 02215
P: 508.330.6578 · E: jcw16@bu.edu · W: LinkedIn

Education

- Ph.D. Boston University Department of Earth & Environment (exp. 2015)
Thesis: *Modeling economies & ecosystems in general equilibrium*
Advisor: Ian Sue Wing
- M.E.M. Duke University Nicholas School of the Environment, 2011
Thesis: *The evolution of energy flows through the US economy*
Advisor: Timothy Johnson
- M.P.P. Duke University Sanford School of Public Policy, 2011
Thesis: *Foreign-aid donors allocation preferences*
Advisor: Sarah Bermeo
- B.S. Bentley University, Economics-Finance *cum laude*, 2004

Professional Experience

- 2014-Pres. Research Economist, RTI International, Durham NC
- 2012-2014 Economist, RTI International, Durham NC
- 2010-2011 Research Analyst, Peterson Institute for International Economics, Washington D.C.
- 2009 Research Intern, World Trade Organization, Geneva Switzerland
- 2004-2008 Research Analyst, Analysis Group, Boston MA

Publications

- Hufbauer, G. C. and **J. Woollacott**. "Trade disputes between China and the United States: Growing pains so far, worse ahead?" In: *European Yearbook of International Economic Law*. Ed. by Herrmann, C. and J. P. Terhechte. Heidelberg: Springer-Verlag, 2012. Chap. 2
- Hufbauer, G. C. and **J. Woollacott**. "Three Tensions in Sino-US Economic Relations". In: *A decade in the WTO: Implications for China and global trade governance*. Ed. by Meléndez-Ortiz, R., C. Bellmann, and S. Cheng. Geneva, Switzerland: International Centre for Trade and Sustainable Development (ICTSD), 2011
- Hufbauer, G. C., J. F. Kirkegaard, W. F. Wong, and **J. Woollacott**. *US protectionist impulses in the wake of the great recession, Report to the International Chamber of Commerce Research Foundation*. Tech. rep. Washington, D.C.: Peterson Institute for International Economics, 2010

Works in Progress

Modeling ecosystems in general equilibrium – theory and demonstration
Representing ecosystem dynamics in a Biological General Equilibrium model
Integrating BGE & CGE models of a marine ecosystem & dependent economy
Bioeconomically optimal inter-temporal tradeoffs in biomass allocations
Costs & ancillary benefits of CO₂ policy in the electric sector
Calibrating SAMs to external forecasts using the dynamic IO framework

Teaching

Teaching fellow	Fundamentals of international economics (IR 292)
Teaching fellow	Environmental policy analysis (GE 420/620)
Instructor	Advanced mathematics preparatory workshop
Instructor	Advanced MS Excel skills workshop
Teaching assistant	Economic analysis and evaluation (PP 200)
Teaching assistant	Policy evaluation with data (PP 264.80, PP 220)

Awards

Boston University Graduate Scholarship, 2014, 2015
Boston University Student Scholarship, 2012-2013
Boston University Dean's fellowship, 2011-2012
Sanford School of Public Policy outstanding dual-degree student 2011
MEM Student Scholarship, 2009-2011
Duke Program in Global Policy & Governance Fellowship, 2009
MPP Student Fellowship, 2008-2010

Presentations

Jun-2015	[Invited] Air & Waste Management Association Annual Conference, Panel speaker: <i>Micro to Macro Decision Making Impacts on Climate & Environment at Nano, Local, Regional and Global Scales</i>
Jun-2015	International Input-Output Association Conference, <i>Exploiting the dynamic input-output framework to calibrate a time-series of social accounting matrices to external forecasts</i>
Jun-2015	[Invited] 32 nd Stanford Energy Modeling Forum, <i>Distributional Impacts of Carbon Taxation</i>
Jun-2015	Association for Environmental and Resource Economists, Summer conference, <i>Modeling ecosystems in general equilibrium</i>
Feb-2015	[Invited] Appalachian State University, Department of Economics Seminar Series, <i>Costs and ancillary benefits of the Clean Power Plan</i>
Nov-2014	Association for Public Policy Analysis & Management Fall Research Conference, <i>Greenhouse gas policy in the electric sector – Measuring the Costs and Ancillary Benefits</i>

-
- Jun-2014 World Congress of Environmental & Resource Economists, *Greenhouse gas policy in the electric sector*
- Apr-2014 Boston University, Earth & Environment department seminars, *Modeling ecosystem dynamics in general equilibrium*
- Apr-2014 RTI International, Center for Environmental, Technology, & Energy Economics, *Modeling economies and ecosystems in general equilibrium*
- Nov-2013 RTI International, Center for Environmental, Technology, & Energy Economics, *Clean air policy in the electricity sector*
- Apr-2013 Boston University, Earth & Environment department seminars, *A national static CGE model of the U.S. electric sector*
- Feb-2013 Boston University, Graduate International Relations Council conference, *Allocation of foreign aid across bilateral and multilateral institutions*
- Aug-2012 RTI International, Economic modeling working group, *A national static CGE model built on U.S. public data*

Professional Activity & Memberships

Participant, Energy Modeling Forum (31, 32)

Ad hoc reviewer, IEEE Transactions on Smart Grid

Member, Association of Environmental and Resource Economists

Member, European Association of Environmental and Resource Economists